8-21-2008

The Design and Evaluation of Boronic Acid Derivatives for the Recognition of Cell Surface Carbohydrates for Medicinal Applications

Sandra Navonne Craig

THE DESIGN AND EVALUATION OF BORONIC ACID DERIVATIVES FOR THE RECOGNITION OF CELL SURFACE CARBOHYDRATES FOR MEDICINAL APPLICATIONS

by

SANDRA NAVONNE CRAIG

Under the Direction of Binghe Wang

ABSTRACT

Carbohydrates in various forms play vital roles in numerous critical biological processes including cell-cell adhesion and communication, embryo development, immune response, etc. Fluorescent sensors for such carbohydrates have a wide range of potential applications including glucose concentration determination, cell labeling and targeting based on carbohydrate biomarkers, as *in vitro* diagnostic tools, and biomarker-directed cellular imaging. Our group has been interested in the design and synthesis of multi-boronic acid compounds with well-defined three-dimensional scaffolding for the specific recognition of selected carbohydrate biomarkers. Aberrant expression of carbohydrate antigens such as sialyl Lewis X (sLex), sialyl Lewis A (sLea), Lewis X (Lex), and Lewis Y (Ley) have been associated with tumor formation and metastasis in various cancer types.[1-4] As such, for our initial design, we have selected sialyl Lewis X (sLex) as our potential target due to implication in the development of liver and colon cancer.[5, 6] Herein, we describe the design, synthesis and evaluation of four such compounds, each having about ten linear steps in its synthesis. In addition to the design of fluorescent probes for cell surface carbohydrates, we also have designed lipophilic

boronic acid derivatives as potential fusogenic agents. Due to boronic acid's ability to bind to 1,2 and 1,3 cis diols, we hypothesize that the aliphatic chain should be able to insert into lipid cellular membrane and the boronic acid units should allow for the "attachment to neighboring cells" through complexation with cell surface glycans. Such interactions should allow the boronic acid compounds to bring two or more cells together for fusion. Herein, we have described the methodologies of the design of such compounds.

INDEX WORDS: Boronic acid, sialyl Lewis X probe, boronolectin, fluorescence, sensor, cell-cell fusion, fusogen, immunotherapy.

The Design and Evaluation of Boronic Acid Derivatives for the Recognition of Cell Surface Carbohydrates for Medicinal Applications

by

Sandra Navonne Craig

A Dissertation Submitted in Partial Fulfillment of the Requirements for the Degree of

Doctor of Philosophy

in the College of Arts and Sciences

Georgia State University

2007

The Design and Evaluation of Boronic Acid Derivatives for the Recognition of Cell Surface Carbohydrates for Medicinal Applications

by

Sandra Navonne Craig

Advisor: Dr. Binghe Wang
Committee: Dr. Alfons Baumstark,
Dr. Kathryn Grant

Electronic Version Approved:

Office of Graduate Studies
College of Arts and Sciences
Georgia State University
December 2007

Dedication

In Loving Memory of My Grandmother 'Doretha A. Craig'

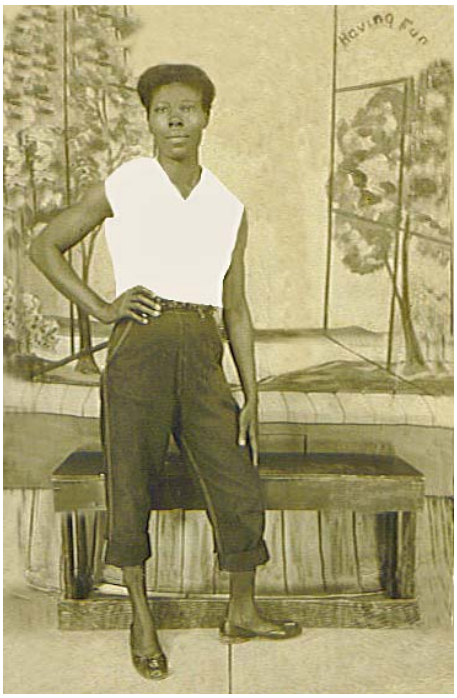

The Elements of Essence

Once I reflected on everything that was good and wanted to thank him for all his creations. Kneeling suddenly appeared this revelation.
I envisioned His hands reaching down on a ball of clay molding and shaping a man in just one day. He reveled at the finished product and knew this accomplishment was grand,
But wanted to add perfection to his great land and decided to create woman.
An easy task he knew this would not be
for this creature would reign as Queen and from her would be born all posterity.
The Creator took his time and shaped a form that was sophisticated and added loyalty for she was going to be dedicated.
He made her audacious and autonomous to convey her strength.
Delightful, admirable, graceful so her company will be good when you are in it. He formed her lips ever so that the words will be genuine, authentic as she flows.
This woman had to possess an attitude, not simple, but complex. He made her positive, attentive, distinctive, aggressive, all that, and nothing less. Determined, charming, and daring, elegant, independent, strong, and bold
With all these divine traits this ruby is not matched with the wealth of gold.
The Creator's masterpiece was finally completed and today she still walks the Earth in you and me. You called her Mother, Sister, Friend, and Granny.
Now, she stands proud in her white robe and boasts her crown upon her head. Having planted seeds into her legacy through which love will be fed.
Long she lived until the Creator called her back home
She is now His angel of fortitude and her spirit lives on.
She watches over us from her mansion on high
Soaring through her garden naming each lily for us and blowing kisses through the sky.
Revere her, she is divine, marvel in her magnificence
And remember that all things in her that were good were
The Elements of Essence.

by

Tanya D. McPhail

Acknowledgements

I would like to thank the Creator of all things, who made it all possible.

Special thanks to my immediate family:

Johnsie Craig

Tanya McPhail

Julia McCauley

Your faith, love, and support help turn a ‘dream’ into reality.

I would like to thank the Jones family, my extended family and friends for all your love and faithful prayers.

I would like to thank Janet Jones, Charmita Burch, and Paulette Dillard for their acts of kindness and support.

I would like to thank my research advisor, Dr. Binghe Wang for the words of encouragement and guidance during my graduate work.

I would like to thank the Wang group; especially Minyong Li, Junfeng Wang, and Shilong Zheng for their words of wisdom.

I would like to thank Dr. Shafiq Khan and his lab members; especially Cecille Millena, at Clark Atlanta University for all their help and support.

I would like to thank Udai Singh at Morehouse School of Medicine for his helpful suggestions and ideas.

I would like to acknowledge Georgia State University, National Institutes of Health (CA88343 and NO1-CO-27184), and the GAANN Fellowship for their financial support.

Table of Contents

Table of Schemes

List of Tables

List of Figures

List of Abbreviations

$((Boc)_2O$	di-tert-butyldicarbonate
CH_3CN	Acetonitrile
ARS	Alizarin Red S.
^{11}B-NMR	Boron nuclear magnetic resonance
^{13}C-NMR	Carbon nuclear magnetic resonance
CCl_4	Carbon tetrachloride
CD	Circular dichorism
$(CH3)_3SI$	trimethylsulfonyl iodide
COS7	monkey kidney epithelial cell line
CT	Charge transfer
° C	degrees Celsius
DMF	Dimethylforamide
DMSO	Dimethylsulfoxide
CH_2Cl_2	Dichloromethane
EDCI	1-(2-dimethylaminopropyl)-3-ethylcarbodiimide hydrochloride
EDG	Electron donating group
E-selectin	Endothelial-selectin
EWG	Electron withdrawing group
FET	Fluorescent electron transfer
H_2O	Water
HCC	Hepatocellular carcinoma
^{1}H-NMR	Proton nuclear magnetic resonance

HEPG2	Hepatocellular carcinoma cell line
HOBt	*N*-hydroxybenzotriazole
K_{trig}	Equilibrium constant of the trigonal boronic acid with the diol
K_{tet}	Equilibrium constant of the tetrahedral boronic acid with the diol
Ley	Lewis Y
Lex	Lewis X
LiBr	Lithium bromide
M	Molarity
MeOH	Methanol
NaH	Sodium hydride
$NaBH_4$	Sodium borohydride
$NaHCO_3$	Sodium bicarbonate
P-selectin	Platelet-selectin
PBA	Phenylboronic acid
PBS	Phosphate buffer saline
PPh_3	Triphenylphoshine
QBA	Quinolineboronic acid
sLea	Sialyl Lewis A
sLex	Sialyl Lewis X
TEA	Triethylamine
TFA	Trifluoroacetic acid
THF	Tetrahydrofuran
DIC	Differential interference contrast

DAPI	(4',6-diamidino-2-phenylindole)
WGA	Wheat germ agglutinin
PS	phosphatidylserine
ADAM12	a disintegrin and metalloprotease
VLA-4	very late antigen
VCAM-1	vascular cell adhesion molecule
PEG	polyethylene glycol
Ig	immunoglobulin
H_2SO_4	sulfuric acid
HNO_3	nitric acid
SOCl2	thionyl chloride
CHO	Chinese hamster ovarian
Hey	human ovarian cancer cell line
Hela	human cervical cancer cell line
Messa	human uterine sarcoma cancer cell line
CMTMR	[5-(and-6)-(((4-chloromethylbenzoyl)amino)tetramethylrhodamine
CMFDA	5-chloromethylfluorescein diacetate
FACS	Fluorescent activated cell sorter
PI	Propidium iodide
RT	Room temperature

1. Introduction

The recognition and detection of particular saccharides in an aqueous environment can be a useful way for monitoring the progression of certain diseases such as cancer and diabetes among others. A key in developing such a system is to design a molecule with the appropriate three-dimensional scaffold that is conducive to a particular carbohydrate only. In addition, the molecule must have strong functional group interactions with the saccharide of interest, and must exhibit some physiochemical property that can trigger a measurable event when bound to an oligosaccharide. With that said, boronic acids in the last decade, due to their ability to bind reversibly to 1,2 and 1,3 cis diols (Scheme 1.1), are an attractive commodity for sensory design in the diagnosis of the detection, and in monitoring of the progression of various diseases.[7-11]

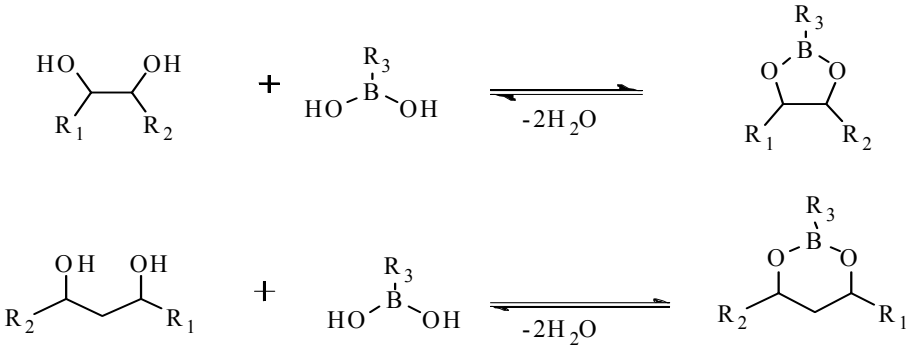

Scheme 1.1 Ester formation of boronic acid and 1, 2 or 1, 3 cis diol.

In developing a sensor for a particular carbohydrate, it is important to select a mode of detection that is conducive to the output desired. There have been many methods used to determine the binding constant for the interaction of boronic acid and a diol such as: pH depression,[12-14] ^{11}B-NMR,[15-17] and other spectroscopic methods[18, 19] to name a few. In addition, there are factors that govern the interaction of a boronic acid and diol that must be considered before devising a receptor with specificity for the carbohydrate of interest. For instance: the boronic acid pK_a, diol pK_a solution pH, solvent, buffer, steric and stereoelectronic effects are all factors that need to be considered. Our group has performed extensive studies in determining the method of detection that is required in designing spectroscopic boronic acid sensors.[20] Also we have studied the factors that govern the interaction between a diol and boronic acid.[21-23] With such understanding of the interactions between a boronic acid and a diol, one has the essentials needed to develop the appropriate sensory device for the saccharide of choice.

1.1. Factors That Influence the Binding Affinity of Boronic Acids and Diols

In designing an artificial receptor for saccharides, one must consider factors that govern relevant intermolecular interactions. Boronic acid acidity is quite uniquely different from the traditional carboxylic acid. With boronic acid in an aqueous environment, it is the reaction of a water molecule with the boron empty *p* orbital of the center and the concomitant release of a proton from the water that accounts for the aciditiy of a boronic acid. Such an ionization reaction also converts the boron from a planar (sp^2) form to a sp^3 tetrahedral (boronate) anionic species (Scheme 1.2). Upon addition of a cis 1,2 or 1,3 diol, the complexation of the boronic acid and corresponding

diol is governed by several factors such as 1) the pK_a of the diol and a boronic acid, 3) pH of solution, 4) properties and sometimes concentration of the buffer system, and 5) steric and stereoelectronic effects.

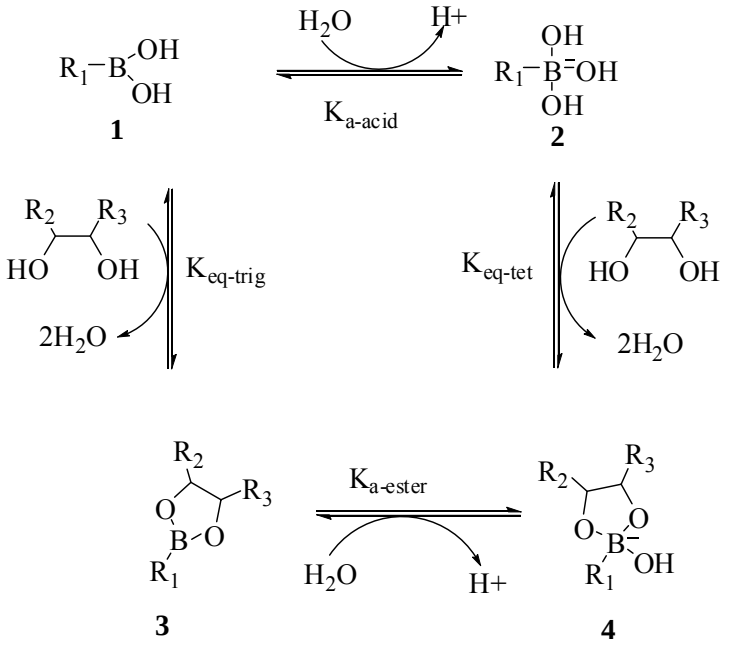

Scheme 1.2 The ionization states of a boronic acid molecule and the complexation with a diol in aqueous buffered medium. [12, 13]

The formation of the complexation between a diol and boronic acid is a function of pH; for example the apparent pK_a of phenylboronic acid (PBA) is 8.8.[20] Theoretically speaking at physiological pH, PBA is approximately 10 times more in its acidic form than basic form. As the pH solution becomes more basic the anionic boronate species **2** becomes predominant. After addition of a diol in Scheme 1.2, the boronate ester **3** is more acidic than the boronic acid, in some cases at physiological pH elucidating species **4**, as the major counterpart.

With most commonly seen sugars, the apparent pK_a of the boronic ester is lower than 7.4. For example, glucose (pK_a ~ 12) lowers the apparent pK_a of PBA by 2 units to 6.8.[20] Generally speaking, the lower the pK_a of the boronic acid, the greater the binding affinity with a given diol. Consequently, electron-withdrawing substituents (-R group) should increase the acidity and thus augment binding affinity. Our group has studied a series substituted PBA and determine the apparent pKa of each boronic acid, and their binding constants at various pH values with commonly seen diols such as glucose, fructose, and catechol.[21] It was found that there were many exceptions to the commonly held beliefs[24, 25] of the pK_a effect on binding.[21] For example, the ester formation between 2,5-difluorophenylboronic acid (pK_a 7.6) and 3,4,5-trifluorophenylboronic acid (pK_a 6.8) with glucose (pK_a 12.5) is not what is expected (Table 1.1).[21] If the common belief is that the lower the pK_a of boronic acid the higher the binding affinity, then theoretically the binding constant of 3,4,5-trifluoroPBA with glucose **8** should be higher than that of 2,5-difluoroPBA-glucose **5** at pH ranging from 6.5-7.5, which is not the case (Table 1.1).

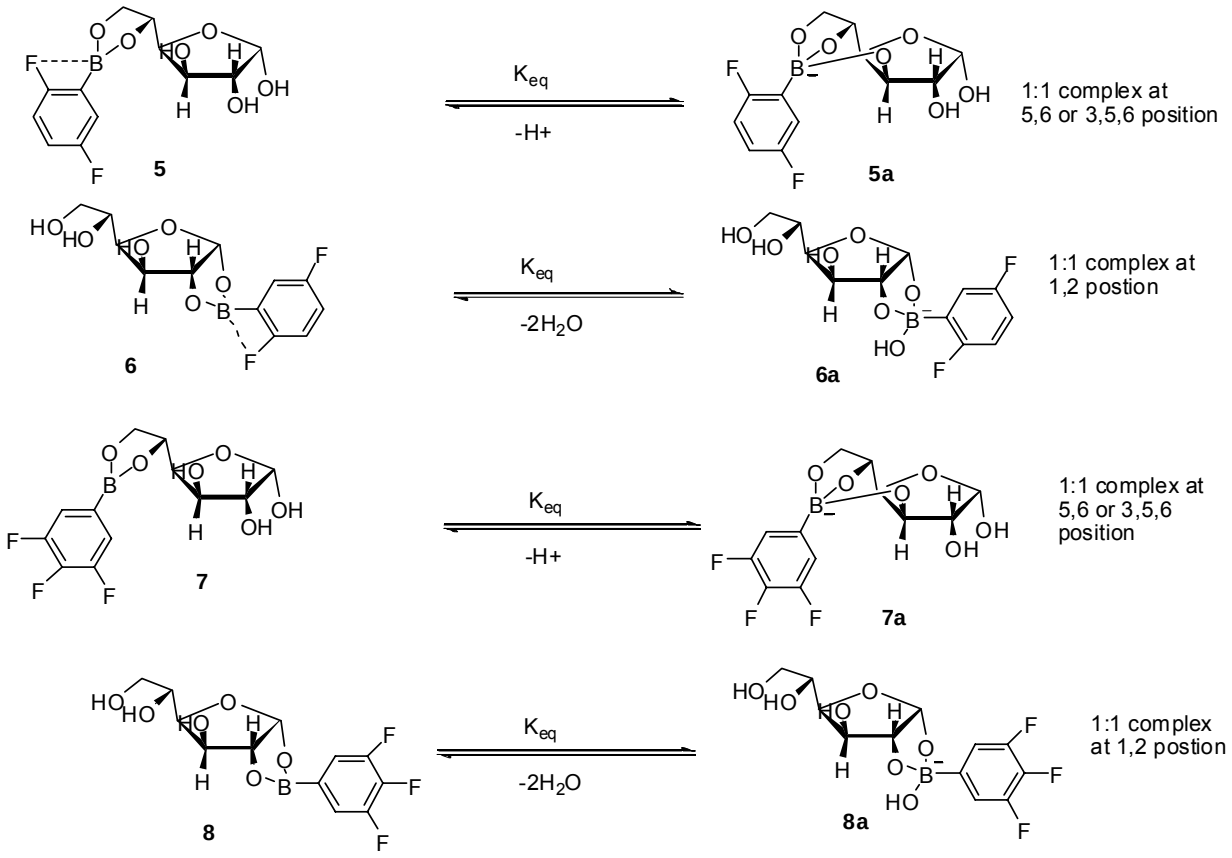

Scheme 1.3 Example of factors that affect binding affinity of the interaction of a boronic acid and a diol.

Table 1.1 Binding constants (M^{-1}) of PBAs and glucose (pKa 12.6).

	2,5-difluoroPBA (pKa 7.6)	3,4,5-trifluoroPBA (pKa 6.8)
pH 6.5	33	17
pH 7.5	47	41
pH 8.5	7.3	53

Along with the pK_a of the two components, the affinity of the boronic acid for a diol is also affected by the dihedral angle O-C-C-O of the carbohydrate. The smaller the angle, the easier it is for the anionic boronate species to adapt to the "ideal" tetrahedral configuration, which increases stability of the boronate complex and enhances the binding affinity.[18]

In conclusion, the factors that govern the stability of the interaction between a boronic acid and a diol include 1) the pK_a of each component, 2) solution pH, 3) dihedral angle of the diol, and 4) other properties such as steric and stereoelectronic factors. These factors must be carefully considered before designing a receptor for the recognition of a carbohydrate of interest.

1.2. Method for Determining Binding Constants

The ability for boronic and boric acids to bind with diols was first recognized over a century ago. In 1842, it was reported that sugars increased the acidity of boric acid.[26] The acquirement of such knowledge led to extensive studies to determine the strength of boronic/boric acid binding with diols. Some of the common methods used were pH depression, ^{11}B-NMR, and spectroscopic methods among others. In determining which method would be most appropriate, one must consider the specific circumstance.

In 1959, Lorand performed the first quantitative assay between a series of diols and phenylboronic acid (PBA).[14] He determined the binding constant by using the pH depression method (Table 1.2). With this method, two assumptions were made: 1) that only the boronate anion complexes (**10**,**12**) were formed and 2) that the change in concentration of the boronic acid (**9**) form due to ionization was negligible. The

formation of the complex between a boronic acid and a diol is pH and pK_a dependent as discussed earlier. Initially with the pH depression method the concentration of boronic

Table 1.2 Association constants with PBA as measured by the pH depression method.[14]

1,3-propanediol	0.88
ethylene glycol	2.8
phenyl-1,2-ethanediol	9.90
glucose	110
fructose	4370
catechol	17500

acid **9** and the boronate ion **10** are at equal quantities, which allows the pH to be equal to the pK_a. After the addition of a diol to an aqueous boronic acid solution, a change in pH occurs and the equilibrium is shifted toward the boronate ester form **12**. The boronic ester form is said to more acidic than boronic acid, which results in a pH decrease with diol addition. The change in pH is directly related to the binding constant. If the concentration of the boronic acid is in essence constant and there is no formation of **11**, then K_{tet} (binding constant of the complex formation boronate and diol) and the change in pH are directly correlated. With such assumptions, Lorand derived *equation* 1 to determine the binding constant with K_c being the formation constant, ΔpH the change in pH after polyol is added to the acid-base equilibrium, and $[P]_f$ the equilibrium polyol concentration.

$$K_c = \frac{10 - \Delta pH - 1}{[P]_f} \qquad (1)$$

This method is generally acceptable when a high concentration of boronic acid is used, but is not very useful when the boronic acid quantity is limited. Furthermore, the central

hypothesis that the boronic ester form does not exist is not correct in a large number of cases. Therefore, the pH depression method only gives an approximation of the K_{tet}, not K_{eq} (Schemes 1.4 and 1.5).[20]

Another method commonly used is that of ^{11}B-NMR spectroscopy. This method is somewhat analogous to the pH depression method in that it relates to the ionization states of the boronic acid-diol complex. When a diol is added to a solution of boronic acid promoting formation of a boronic ester, the ester is consider to be more 'acidic' than the acid, reducing the apparent pK_a. This helps to facilitate a large portion of the boronic ester complex to be converted from a neutral trigonal form to the anionic tetrahedral form. The change from a trigonal ester **11** to tetrahedral ester **12** can be directly detected using ^{11}B-NMR because of the significant change in chemical shift of the boron atom, trigonal ester being around 30 ppm and the tetrahedral form around 10 ppm. This method can be used for studying physiochemical changes that may occurred due to binding, solvolysis, pH, steric and other factors. However, this method also requires a large amount of sample and therefore is not applicable when only a small amount of the boronic acid can be obtained in sensor research.

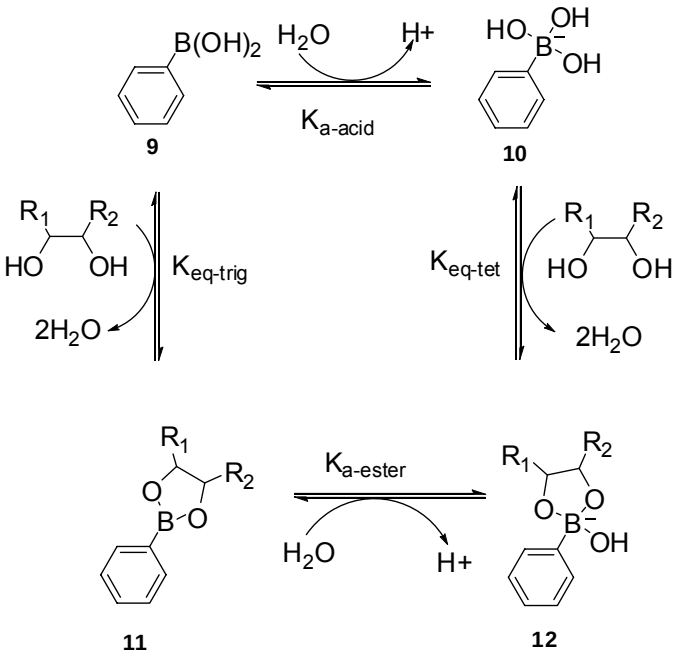

Scheme 1.4 Binding process between phenylboronic acid and a diol.

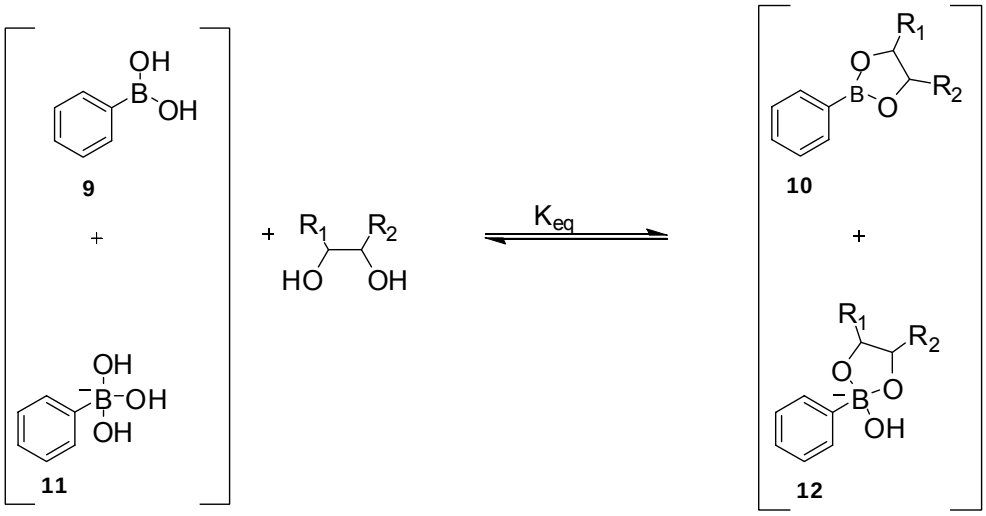

Scheme 1.5 Overall binding process between phenylboronic acid and a diol.

Lastly, spectroscopic methods are commonly used to detect the binding between a boronic acid and diol because this provided sensitivity, rapid detection, and a continuous means of monitoring changes in concentration. In this regard, spectroscopic methods

used for binding constant determination include CD, absorption, and fluorescence approaches. Our group has established a three component- competitive assay containing a fluorescent compound Alizarin Red S. (ARS), phenyl boronic acid (PBA), and a cyclic or acyclic diol. ARS is commercially available and commonly used in the textile industry. It has also been used for fluorometric detection of boric acid[27] and other metals.[28, 29] We have employed it as a fluorophore due to its sensitivity in the detection of boronic acids. ARS **(13)** initially is non-fluorescent due to excited state proton transfer resulting in fluorescence quenching (Scheme 1.6).[30, 31] However, after addition of a boronic acid, the proton on the phenol hydroxyl group is no longer present. Therefore, fluorescence quenching through excited state proton transfer is no longer possible, which leads to a fluorescence intensity increase. A more in depth discussion of how this method works for binding constant determination is as follows: the first equilibrium between the boronic acid and the ARS reporter can be directly measured based on fluorescence intensity changes (Scheme 1.6). The addition of a diol produces a second equilibrium between the boronic acid and diol to give boronate ester **13b**. This perturbs the ARS/boronic acid equilibrium resulting in a change in the fluorescence intensity of the solution. With the establishment of this design, the binding constants of phenyl boronic acid with a series of diols were determined. After carefully obtaining the results, we noticed a discrepancy between our binding constant and the binding constant of Lorand and co-workers determined using pH depression method (Table 1.2). Several reasons led to this discrepancy. First, the assumption that there is no formation of trigonal boronate ester is not true in all cases. Boronic acids and their esters can exist in two different ionization states; there are actually three different "binding constants" to consider. The

first one relates to the conversion of the trigonal boronic acid **(9)** to the trigonal ester **(11)** termed K_{trig}. The second one refers to the conversion of tetrahedral boronate **(10)** to its ester counterpart **(12)** termed K_{tet}. However, neither of these two truly represents the overall binding constant between a diol and boronic acid for the purpose of sensor design. The third binding constant describes the overall binding strength regardless of the ionization state of the boron species, K_{eq} (Scheme 1.5). Lorand's assumption does not consider the nature of diol in question. For example, the pKa of the phenylboronic ester of glucose is determined to be 6.8. At physiological pH, ca. 20% should be in the free boronic ester form. Our group was the first to derive an equation to determined the K_{trig} binding constant within the equilibrium process.[20] In most cases, the trigonal boronic ester is present in substantial proportions and this must be considered when determining binding constants.

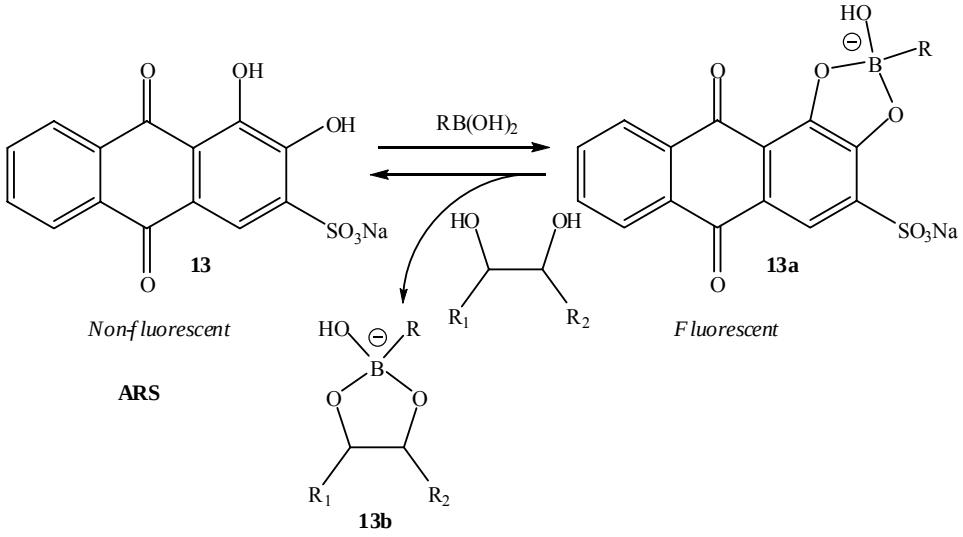

Scheme 1.6 Competitive binding assay with a boronic acid, ARS, and a diol.

Table 1.3 Association constants with PBA.

Diols	[a]K_{tet}	[b]K_{eq}
1,3-propanediol	0.88	
Ethylene glycol	2.8	
Phenyl-1,2-ethanediol	9.90	
catechol	17500	830
sorbitol		370
fructose	4370	160
mannitol	2275	120
galactose	276	15
glucose	110	4.6

[a]measured by the pH depression method[14]

[b]measured by the ARS competitive method at physiological pH[20]

When choosing a method for determining the binding constant of the interaction between a diol and a boronic acid, one must be aware of the limitations of each method. Clearly, with the pH depression method, the binding constant is determine to be between the anionic ionization state of the complex of a diol and boronic acid, K_{tet} , not the overall binding constant K_{eq} regardless of the ionization state of the boron species. ^{11}B-NMR method is only significant in acquiring knowledge of the physical state of the complex and physiochemical properties; in addition both the pH depression method and ^{11}B-NMR require a large amount of sample which is not always appreciable in the preliminary discovery of sensory design. Spectroscopic approaches are the most efficient mode of detection due to: 1) high sensitivity, 2) facile preparatory set-ups, and 3) the requirement

for very little sample. Below is a brief discussion of the progression of fluorescent chemosensors in the detection of saccharides.

1.3. The Development of Fluorescent Chemosensors

In the design of chemosensors for carbohydrates, there must be a method, with high sensitivity in determining the concentration at a low detection limit for medicinal applications; and a physiochemical change that is measurable when the recognition moiety is complexed to an oligosaccharide. Fluorescent boronic acid sensors have been in development since the early 1990's. Much ground work has been laid in developing fluorophores that can act as molecular reporter units. A brief review in the advancement of fluorescent reporters will be briefly presented. More in depth discussions can be found in many excellent reviews on fluorescent boronic acid sensors.[18, 19, 32-34]

Czarnik and co-workers were the first to design a fluorescent chemosensors using an anthracene-boronic based system for the detection of polyol through a photoinduced electron transfer mechanism (Scheme 1.7).[35] In basic aqueous medium, the ionization state of anthrylboronic acid shifts from a trigonal planar boron species, which is fluorescent, to a weakly fluorescent tetrahedral species **14b**. The addition of a diol creates a new equilibrium between the boronate ester form (weakly fluorescent) and the boronic ester form (fluorescent). The quenching process was said to be regulated by the boronate anionic species. This pioneering work signaled the beginning of subsequent extensive work in chemosensory design for the detection of carbohydrates for industrial and medicinal applications. Shinkai and colleagues in the early 90's designed mono and di-boronic acid derivatives using the fluorescent anthracene system.[36]

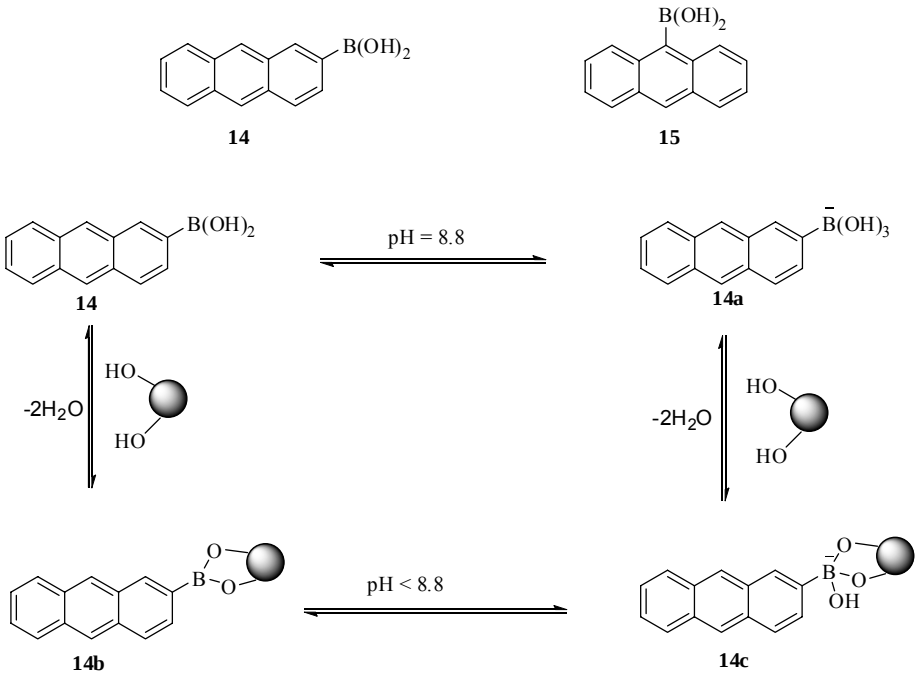

Scheme 1.7 Equilibrium of anthrylboronic acid in aqueous media in the presence and absence of diol.

In hopes of establishing an anthracene-boronic acid based system that can function at physiological pH, Shinkai incorporated a tertiary amine in a 1,5 arrangement based on the concept first introduced by Wulff.[37] In this system it is presumed that, when no sugar is added the lone pair electrons on the amine reduce the intensity of the fluorescence through an exicited state photoinduced electron transfer quenching mechanism (Scheme 1.8). This was considered to be the 'off' state of the sensor. When sugar is added the amine and boron interact and form a B-N bond, stopping the quenching mechanism thus creating an 'on' state of the sensor. It was proposed that the interaction of the boron and amine lowered the pK_a of the boronic acid. This interaction supposedly helped to increase binding affinity between a diol and boronic acid, along with an increase in fluorescent intensity, and enhancement in B-N bond strength. This system has had much success in the selective detection of fructose over glucose, and has prompted others to use

this system as well to develop selective sensors for carbohydrates.[7, 38-40] However, the mechanism, as originally proposed by Shinkai, through which the fluorescent intensity change occurs is somewhat questionable in buffered aqueous medium.[22, 23] The B-N formation has been analyzed by ^{11}B-NMR studies under various experimental conditions. Within these studies, indications of the boronate ester being prone to solvolysis by protic solvent were made, thus eliminating the B-N bond to some extent.[17] Therefore, is the B-N bond strength enough to tie-up the lone pairs of the nitrogen with a competing solvolysis mechanism in place? Wang group has performed several studies to resolve the ambiguity in essentially how the PET mechanism works in the Shinkai system. They believe that there is another plausible hydrolysis mechanism at play, and to test our theory we performed several tests. We: 1) repeated the pH profile of **16** in the presence and absence of sugar, 2) tested the effect of sugars that are capable of trivalent binding to boronic acid, and 3) calculated the B-N bond strength.[22, 23]

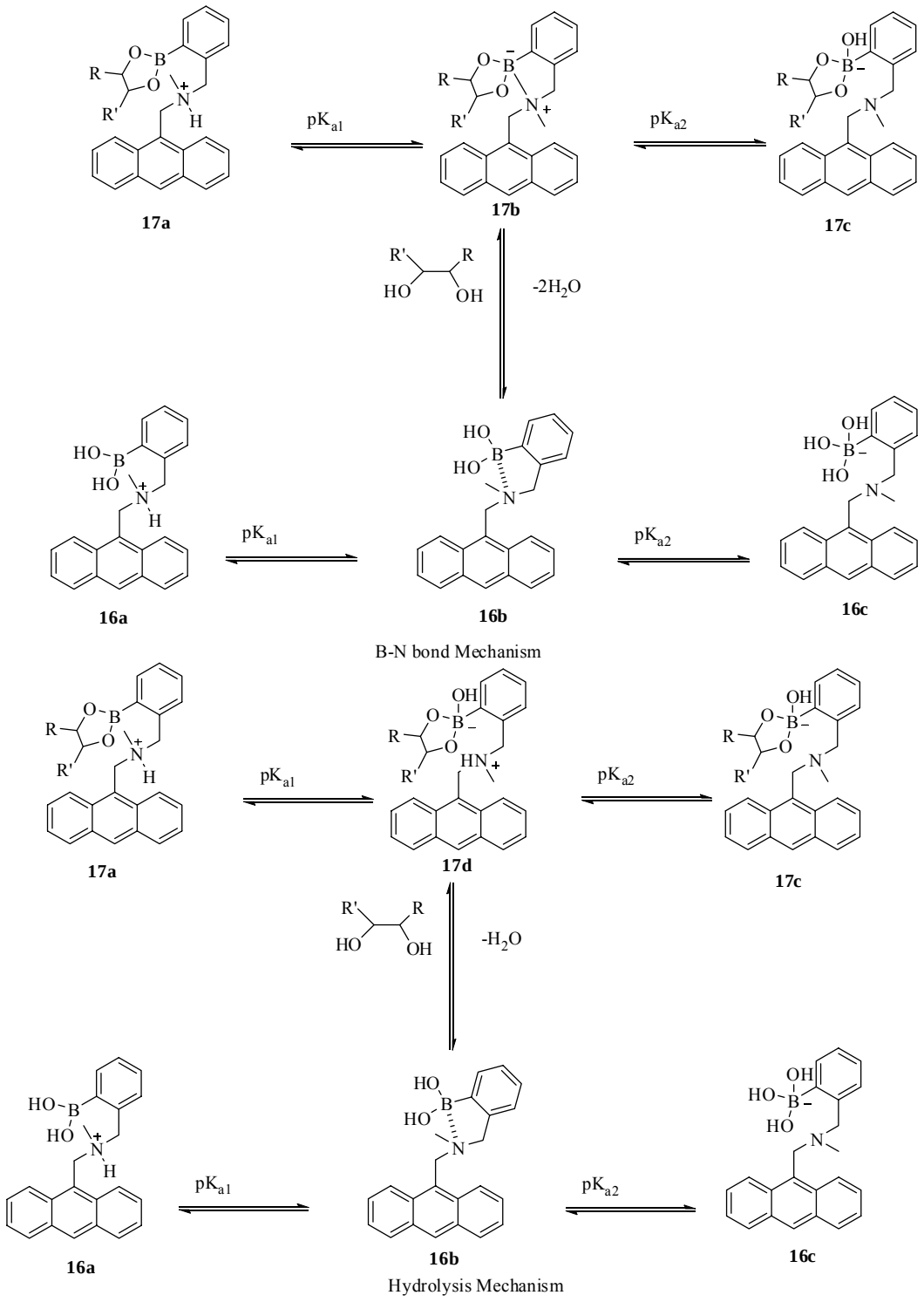

Scheme 1.8 Possible PET mechanisms for the fluorescence intensity changes of the Shinkai system.

Theoretically, in an aqueous pH dependent environment, **(16a)** has two pK_a values to consider, the pK_a of the boron and the pK_a of the amine. It is known in literature that in a 1, 5 relationship between a tertiary amine and boron, the pK_a of the amine is roughly 5[41] The first pK_a is related to the amine which coincides with the reduction of the fluorescence. As the pH increases, **16b** is formed. The addition of a diol promoting formation of a boronic ester **17b** supposedly strengthens the B-N bond in such a way as to 'tie-up' the lone pair on the nitrogen preventing the quenching process, thus augmenting fluorescence, which is contingent upon the 'physiochemical' properties of the carbohydrates (properties in which were discussed earlier in Section 1.2). The apparent pK_a values of boronic esters are different with diverse sugars as it is well known in literature. This would mean B-N bond strength would be different for **17b** which should in turn affect the quenching efficiency by the lone pair electrons and consequently the maximal fluorescent intensity for a particular ester. However, in our studies all esters gave the same maximal fluorescent intensity, which is consistent with the hydrolysis mechanism. The fluorescent species **17d** has the same protonated amine form regardless of which sugar is added. In addition, if the fluorescence change depended upon the B-N formation then with trivalent sugars, fructose[20] and sorbitol[42], there would not be any change in fluorescence intensity, which is not the case. We have also calculated the B-N bond strength to be ca. around 3 kcal/mol, which is essentially the same as a nonlinear hydrogen bond dissociation constant.[22, 23] It was concluded that an alternate hydrolysis mechanism might produce the fluorescent boronate ester form, **17d** in Scheme 1.8. The addition of a diol within the system of **16b** is correlated with a lower intrinsic pK_a of the boron species. As a result the first pK_a becomes the reaction of the boron with the water

molecule to give **17d**. The formation of a zwitterion creates stability, which increases the pK_a of the amine. The conversion of the weak B-N bond form in **16b** to the amine-protonated form **17d** allows for the masking of the lone pairs electrons, which prevents the fluorescence quenching process through PET of the anthracene moiety and results in an increase in fluorescent intensity.[22]

Although the mechanism of **16b** in which the fluorescence intensity is regulated to produce an 'on-off' state sensor for carbohydrates maybe questionable in some cases, it has sparked the initiation in the diversity of molecular reporter units for carbohydrates. There has been continuing development in PET sensory design for in vivo application with various fluorophores. FET (fluorescence resonance energy transfer) and ICT (internal charge transfer) have also been introduced as quenching mechanism in designing 'on-off' sensors for saccharides, among others. In addition to the exploration of other 'on-off' molecular chemosensors, this system has also given a starting point for developing a selective sensor for glucose, a biological carbohydrate, the detection and monitoring of which are essential for the control of diabetes. There have been numerous efforts to design molecular reporting units for carbohydrates,[43-46] briefly below are discussed a few chosen chemosensors to display the progression of sensory design to date.

Tony James and co-workers designed an intramolecular energy transfer saccharide sensor with phenanthrene as the donor with excitation and emission wavelengths of 299 nm and 369 nm and an acceptor pyrene with an excitation and emission at 342 nm and 397 nm.[47] Fluorescence energy transfer (FET) is the transfer of energy from a donor to an acceptor. The emission spectrum of the phenanthrene donor overlaps with the

excitation spectrum of the pyrene acceptor, which gives some indication that internal energy transfer can occur.

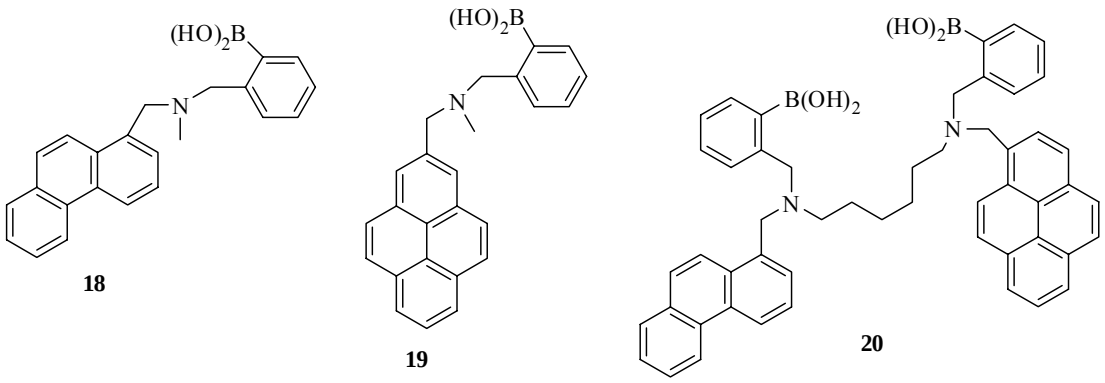

Figure 1.1 Fluorescent energy transfer sensor.

James tethered compounds **18** and **19** to a hexamethylene group to promote selectivity toward glucose since it was known in literature that a bisboronic acid with the appropriate spatial arrangement enhances selectivity toward glucose. When excited at 299 nm and 342 nm, compound **20** displayed an increase in fluorescence 417 nm with the addition of sugar. No emission was observed at the donor emission wavelength (369 nm) in compound **20** when excited at 299 nm, suggesting that the FET mechanism took place. The stability constant K of sensors **18**, **19**, and **20** were also determined for glucose, fructose and others. Bisboronic acid **20** showed selectivity for glucose which complexes in a 1:1 fashion with bisboronic acid as opposed to fructose that binds in a 2:1 complex. In contrast, reporters **18** and **19** favored fructose as presented in literature for monoboronic acids.[36, 42]

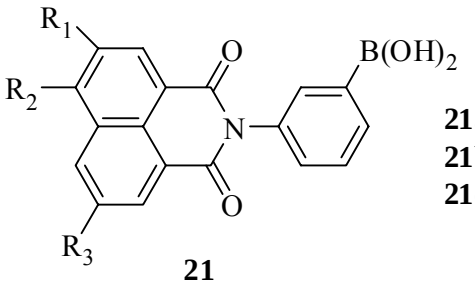

21

21a R_1=H; R_2=H; R_3=H
21b R_1=H; R_2=H; R_3=NO_2
21c R_1=H; R_2=H; R_3=NH_2

Figure 1.2 Fluorescent chelating enhancing reporters.

Thus far there has been many successful chemosensors. However they lack the characteristics of an ideal sensor for *in vivo* biological applications. An 'ideal' sensor must be one that is water soluble, nontoxic, and minimal amount of energy for detection. The Heagy lab synthesized and evaluated a series of water soluble N-phenyl-1,8-naphthalenedicarboimides reporter compounds.[48] They varied functionality at the R_3 position **(21a-c)** H, a strong electrowithdrawing group (–nitro) and an electrodonating group (-amino). The results with **21a-b** demonstrated a decrease in fluorescence intensity upon addition of diol; it was thought that this was due to a chelation enhanced quenching mechanism. Compound **21a** showed the greatest intensity change (ca. 25%) in the presence of fructose with a dissociation constant of 1 mM. Compound **21b** showed pH-dependent selectivity toward glucose over fructose in a ratiometric response. However, the compound exhibited higher binding for fructose over glucose. The fluorescence decreased at an emission wavelength of 430 nm while a small increase was shown at 550 nm. It was proposed that this change may have occurred because of the ability of the *N*-arylnaphthalimides to exhibit a twist angle effect. The amino derivative **21c** showed preferential fluorescence in the order of galactose>glucose>fructose at pH values between 3 and 5. In continuing the efforts to search for more efficient and water-soluble

boronic acid fluorescent reporter compounds, our group discovered that 8-quinoline boronic acid (8-QBA), upon addition of a diol, increased fluorescence intensity over 40-fold at physiological pH.[10, 49] The mechanism through which this compound changes fluorescence is not well understood. Compound **22** is non-fluorescent at pH values above 5 and weakly fluorescent at lower pH in aqueous solutions. However, upon addition of a diol the fluorescent intensity drastically increases providing an 'off-on' state for the detection of a carbohydrate. ^{11}B-NMR studies were conducted to understand the hybridization states of 8-QBA and ester formation with sugars. The results showed that the boron atom in both 8-QBA and the corresponding ester are in their tetrahedral form before reaching physiological pH, indicating that the fluorescence intensity changes are not due to the hybridization state of boron. Lakowicz also used a quinoline system to synthesized a series of 6-methoxyquinoline boronic acid analogs **23** (boronic acid being in the ortho, meta, and para positions) to design a sensor to detect tear glucose concentrations to be placed in a plastic disposable contact lens.[50] Norrild and coworkers synthesized anthracene diboronic acid **24** that was selective for glucose with a binding constant 2512 M^{-1}. This type of scaffold was first reported by Shinkai. However, Norrild introduced a 3-boronic acid pyridinium hydrochloride salt as the receptor to enhance the hydrophilicity needed for *in vivo* design. Although the selectivity showed a substantial decrease compared to Shinkai's system, this provided a starting point for using this particular backbone to improve on the selectivity for glucose as it has displayed binding in a neutral aqueous environment.

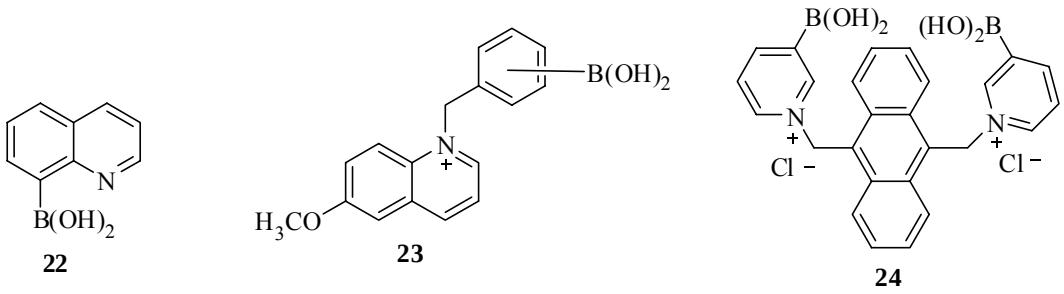

Figure 1.3 Water soluble fluorescent boronic acid sensors.

In addition to PET sensor design and among other reporters, internal charge transfer chemosensors have also been explored. Usually in this system, the donor and acceptor molecule are in conjugation with the fluorophore. At the excited state, there is a charge transfer from the donating group to the empty p orbital of the acceptor group (boron in this case), which quenches the fluorescence. The addition of a diol stops the quenching process by increasing the Lewis acidity of the boron atom, promoting formation of the anionic tetrahedral boronate ester, thus leading to an 'off-on' fluorescence sensor.

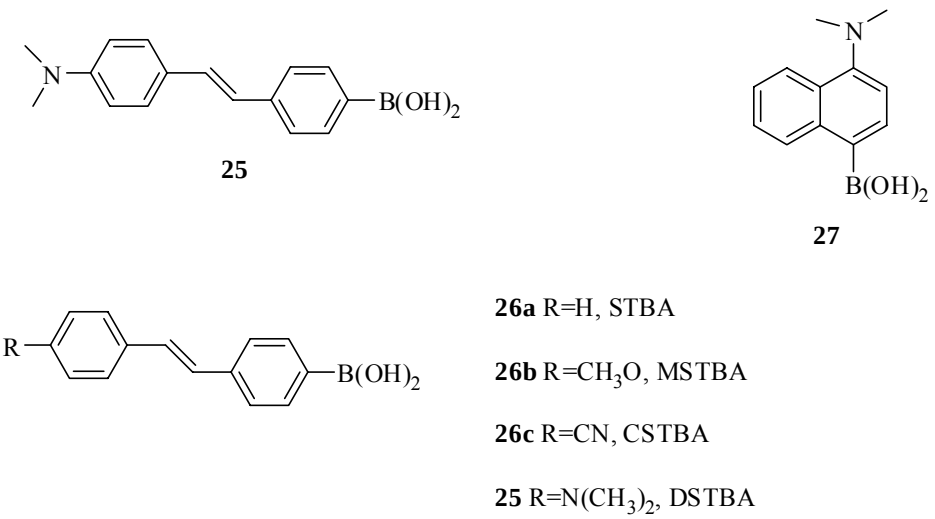

Figure 1.4 Charge transfer fluorescent boronic acid reporters.

There have been several internal charge transfer fluorescent reporter compounds within the realm of sensory design which includes Wang group, and the groups of Shinkai, and Lakowicz as well as others. Shinkai's lab introduced a stilbene boronic acid system that was selective for fructose under basic aqueous conditions **25**.[51] The Lakowicz group also developed a stilbene system with various donor and electron-withdrawing groups to determine the effects on the fluorescence and binding affinities of several diols. They prepared four stilbene boronic acid derivatives one of which was Shinkai's stilbene system **(25)**, 4'- cyanostilbene -4- boronic acid **(26c)**, 4'- methoxystilbene-4-boronic acid (**26b)**, and lastly a stilbene derivative without the boronic acid attached **(26a)** as a reference to obtain the different spectral changes with each analog.[52] The incorporation of a boronic acid moiety within systems **25** and **26b** in basic media produced a blue shift in the emission spectra compared to **26a** and an increase in fluorescent intensity, whereas

26c displayed a red shift in its emission spectra and a decrease in fluorescent intensity. Lakowicz correlated these spectral changes in **25** and **26b** to the elimination of the charge transfer between the donor methoxy and/or dimethylamine group with the boronic acid acceptor unit. With increasing pH, the boron hybridization changes from sp^2 to sp^3 creating more electron density around the boron center nullifying the charge transfer quenching mechanism under certain conditions. The same type of spectral changes occurred after the addition of sugar.

Lastly, our group has designed water soluble fluorescent naphthalene-based system **27**.[53] This sensor at physiological pH exhibited a 41-fold increase in fluorescence intensity upon addition of fructose in aqueous phosphate buffer. The fluorescence is said to be quenched due to an internal charge transfer process. Upon addition of a diol, the Lewis acidity is enhanced at the boron center inducing sp^3 hybridization of the boron atom, stopping the charge transfer quenching mechanism. A pH profile study was conducted to determine the relationship between the fluorescence intensity changes and the boron ionization states. Increasing pH leads to the conversion of boron from a trigonal planar species (**27a**; emission wavelength, 338 nm) to a tetrahedral hybridization state entity (**27c**; emission wavelength, 445 nm) (Scheme 1.10). The pK_a of the amino and the boronic acid moieties regulate the fluorescent intensity with or without sugar, providing a method for detection of sugars at physiological pH.

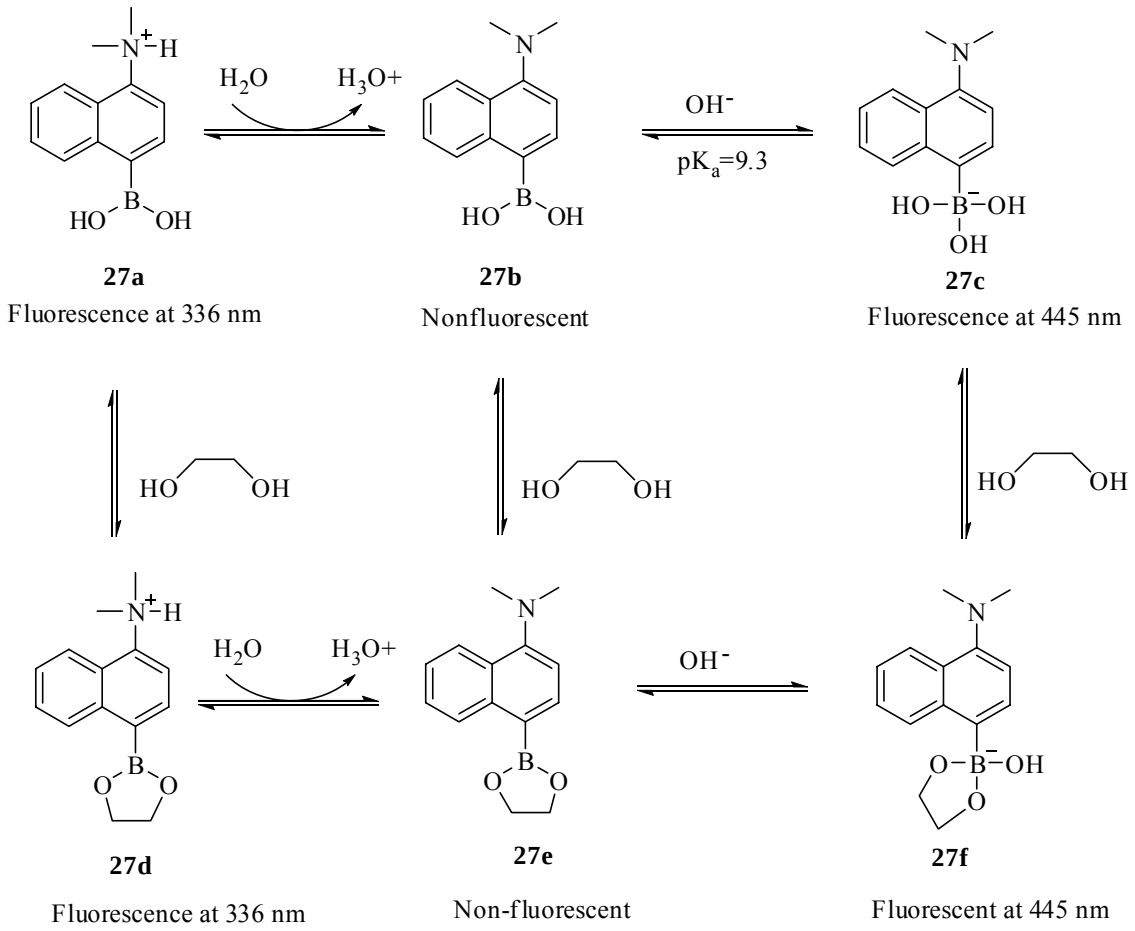

Scheme 1.9 Ionization state of 4-dimethyaminonapthaleneboronic acid in the presence and absence of a sugar.

Tremendous efforts in designing fluorescent boronic acid chemosensors for biological carbohydrates have been made. The first PET chemosensor initiated by Czarnik and co-workers begin the development of 'off-on' sensors. This system has prompted the advancement of incorporating other photodynamic approaches such as FET and ICT, to name a few. The progression of water soluble small fluorescent molecules which exhibits longer wavelength and less energy with the appropriate scaffold to enhance selectivity could lead to the design of continuously monitored chemosensors for glucose. In addition, they could serve as molecular probes for various cell surface carbohydrate

markers present on certain cancer and tumor cell types,[39-41] site specific drug delivery systems, among other possibilities.

2. The Synthesis and Evaluation of Fluorescent Artificial Receptors for sLex

2.1. Importance for the Recognition of Carbohydrates

Carbohydrates are essential for the cell-cell recognition and various biological responses such as inflammation, lymphocyte homing, regulation of metabolic pathways, cell–cell signaling events, pathogenesis of various degenerative diseases,[54-56] autoimmune diseases, bacteria and viral infection,[57, 58] and fertilization to name a few. In addition, the cross-talk between cell surface carbohydrates and receptors of regulatory cells has also been associated with the metastatic behavior of various cancer types.[1, 3, 4]

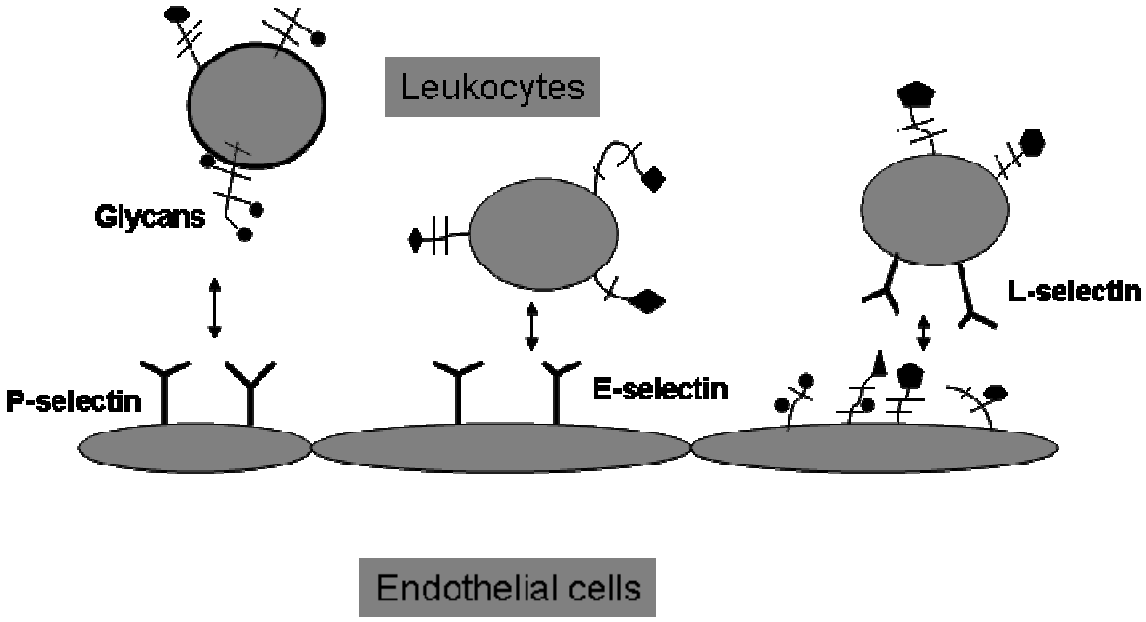

Figure 2.1 Interaction of selectin and ligand during leukocyte recruitment.
The initiation of the recruitment of leukocytes to the inflamed tissue is orchestrated by the interaction of selectins with corresponding carbohydrate ligand. This interaction allows the immune cells to slow down and tether to the endothelium.

For example, in a well studied pathway such as the leukocyte recruitment during an inflammatory response, the overexpression of upstream molecules has been linked to the progression of certain cancer types as well as autoimmune diseases. The first committed step in an acute inflammatory response stimulated by chemical messengers, cytokines (chemokines) as well as other mediators, is the rapid dissociation and association between the carbohydrate sialyl Lewis X (sLex), present on the surface of leukocytes and the adhesion molecule of the lectin family, E-and P-selectins, expressed on the surface of activated endothelial cells. This process allows the immune cells to slow down their movement in the vessels and attach nonspecifically to the infected tissue (Figure 2.1).[59-61] Tumor metastasis mimics this process.[62, 63] Some blood-borne cancer cells expressing sialyl Lewis X (sLex) and sialyl Lewis A (sLea) stimulate the expression of the adhesion molecule E-selectin present on endothelial cells, which promotes adhesion followed by tumor intravasation and metastasis (Figure 2.2).[62] In addition to this aberrant behavior of an inflammatory response, carbohydrate recognition has been implicated in the pathogenesis of such diseases as rheumatoid arthritis (RA), multiple sclerosis, and insulin dependent diabetes, as well as allergies and sepsis.[64, 65]

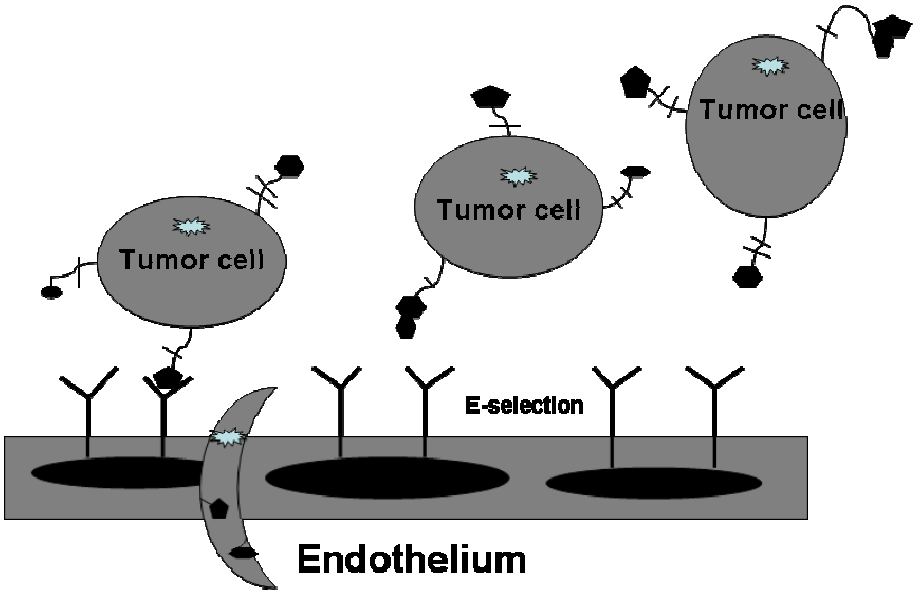

Figure 2.2 Tumor metastasis.
E- selectin mediates the tethering of tumor cells to the vascular endothelium by binding to its glycan ligand, which is followed by tumor intravasation and metastasis.

There is a great need to design small molecules that can aid in the detection of or to block the action of cell surface carbohydrates to combat these aformentioned diseases as well as cancer. Researchers have designed anti-selectin antibodies,[66, 67] synthetic carbohydrates,[68, 69] chemokine-receptor antagonist,[70, 71] as well as bioimaging agents[72, 73] to block the action and/or study the pathways that lead to the abnormalities of this process.

Wang lab is interested in the design and synthesis of small organic molecules with an ability to recognize specific oligosaccharide patterns. With that in mind, boronic acid moieties since the 1940's have been known to form a rapid reversible complex with 1,2 and 1,3 cis diols[14] (Scheme 1.1.) which make boronic acid an ideal system for the detection of a particular biological saccharide of interest and/or blocking of the action of the lectins, among other possibilities. We have adapted the term," boronolectin" to refer to small molecule boronic acid compounds that mimic the action of lectins.

2.2. Design of Potential Sensors for Cancer Carbohydrate Biomarkers

An ideal *in vivo* sensor for carbohydrates consists of: (1) a recognition moiety that is water soluble, (2) a receptor which has strong functional group interaction with the saccharide of interest, (3) a molecule that displays the appropriate three-dimensional scaffold that is conducive to the particular carbohydrate only at physiological pH, and (4) a spectroscopic reporter attached to the receptor which upon binding will change its intrinsic properties and thus allow a measurable event to occur. With that said, the initial design began with the fluorescent anthracene-boronic acid system. This system was first introduced in 1992 by the Czarnik group,[35] and was later used by Shinkai to incorporate a 1,5 relationship between an amine and boron to create more electron density around the boron center. In doing so, they developed monoboronic acid **16**, which is intrinsically selective for fructose, and a diboronic derivative also selective for glucose.[22] Our group has designed successful sensors using this system, and was the first to develop a sLex artificial receptor **(28)**[39] for the hepatocellular carcinoma cell line.

Aberrant expression of carbohydrate antigens such as sialyl Lewis X (sLex), sialyl Lewis A (sLea), Lewis X (Lex), and Lewis Y (Ley) have been associated with tumor formation and metastasis in various cancer types.[1-4] One such cancer hepatocellular carcinoma (HCC)[74] carries a poor prognosis and systemic cytotoxic agents provide marginal benefit.[75] To date, the only detectable marker used in determining the prognosis of HCC is α-fetoprotein. Although the function of this α-1, 3 fucosylated glycoprotein is unknown, it presents itself at increased levels in the sera of patients with HCC. However, the sensitivity and its specificity is not enough for early detection of HCC.[75]

An alternative biomarker is desperately needed along with a method of detection with higher specificity and selectivity in hopes to improve treatment outcome. It is known that sLex present on immune cells is a natural ligand for E- and P- selectin on endothelial cells. The cell-cell adhesion mediated by these macromolecules is the first step in leukocyte recruitment. This step has also been implicated in of colon cancer metastasis to the liver, thus making the detection of sLex an attractive source for the diagnosis and monitoring the progression of liver cancer.[74] In continuing the efforts to produce more successful fluorescent artificial receptors.

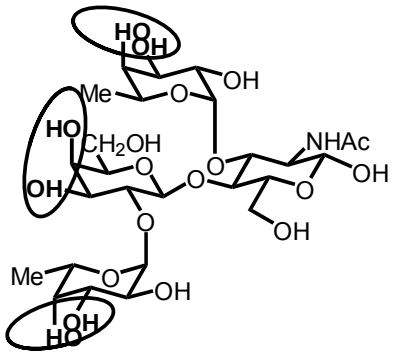

Lewis Y tetrasaccharide

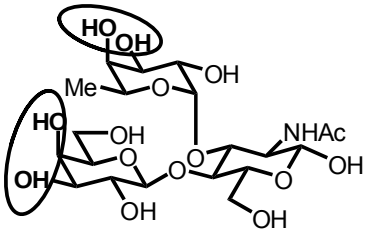

Lewis X trisaccharide

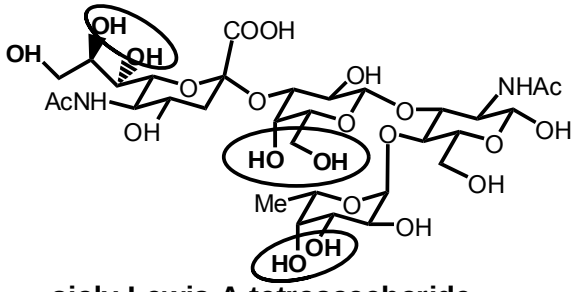

sialy Lewis A tetrasaccharide

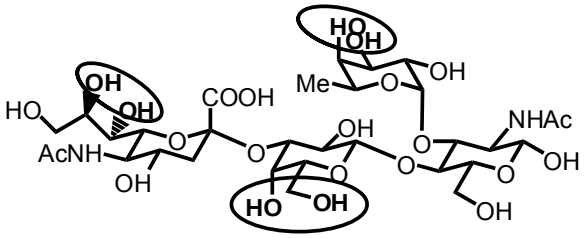

sialy Lewis X tetrasaccharide

Figure 2.3 Structures of sLex, Lex, sLea, and sLex.

Heteroatom(s) were added within the di-carboxylic acid motif in **28,** which has been shown to bind sLex. The tertiary amine attached to the carbonyl group was changed to a

secondary amine to increase the hydrophilicity. The evaluation of how a slight change in electronic properties and reduction of a possible steric effect by the replacement of a methyl group with hydrogen affect the selectivity. Lastly, it is known in literature that the appropriate spatial arrangement is imperative for optimal binding between a boronic acid scaffold[36, 40] and a carbohydrate of choice a such a ring contraction with the use of an imidazole di-carboxylic acid moiety was incorporated to probe the effect of such a change. With that in place, four di-anthracene boronic acids were synthesized and the determination of the selectivity compared with **28** was conducted. As a replica of **28** which labeled HCC cell line selectivity at a concentration of 1 μM, values between 0.5 and 10μM were studied using fluorescence microscopy. This was accomplished with HEPG2 cells possessing the the sLex antigen and COS7 a non-expressing cell line.

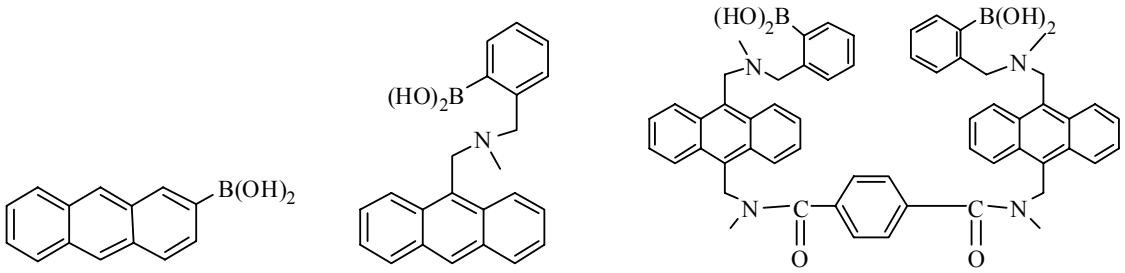

15 **16** **28**

Figure 2.4 Fluorescent chemosensors for saccharides.

2.3. Synthesis of an Artificial Receptor for sLex

The preparation of a dianthracene boronic acid for the development of a fluorescent probe for cell surface oligosaccharide sLex, began with commercially available

anthraquinone **29**[76] which was treated with trimethylsulfonyl iodide $(CH_3)_3SI$ in the

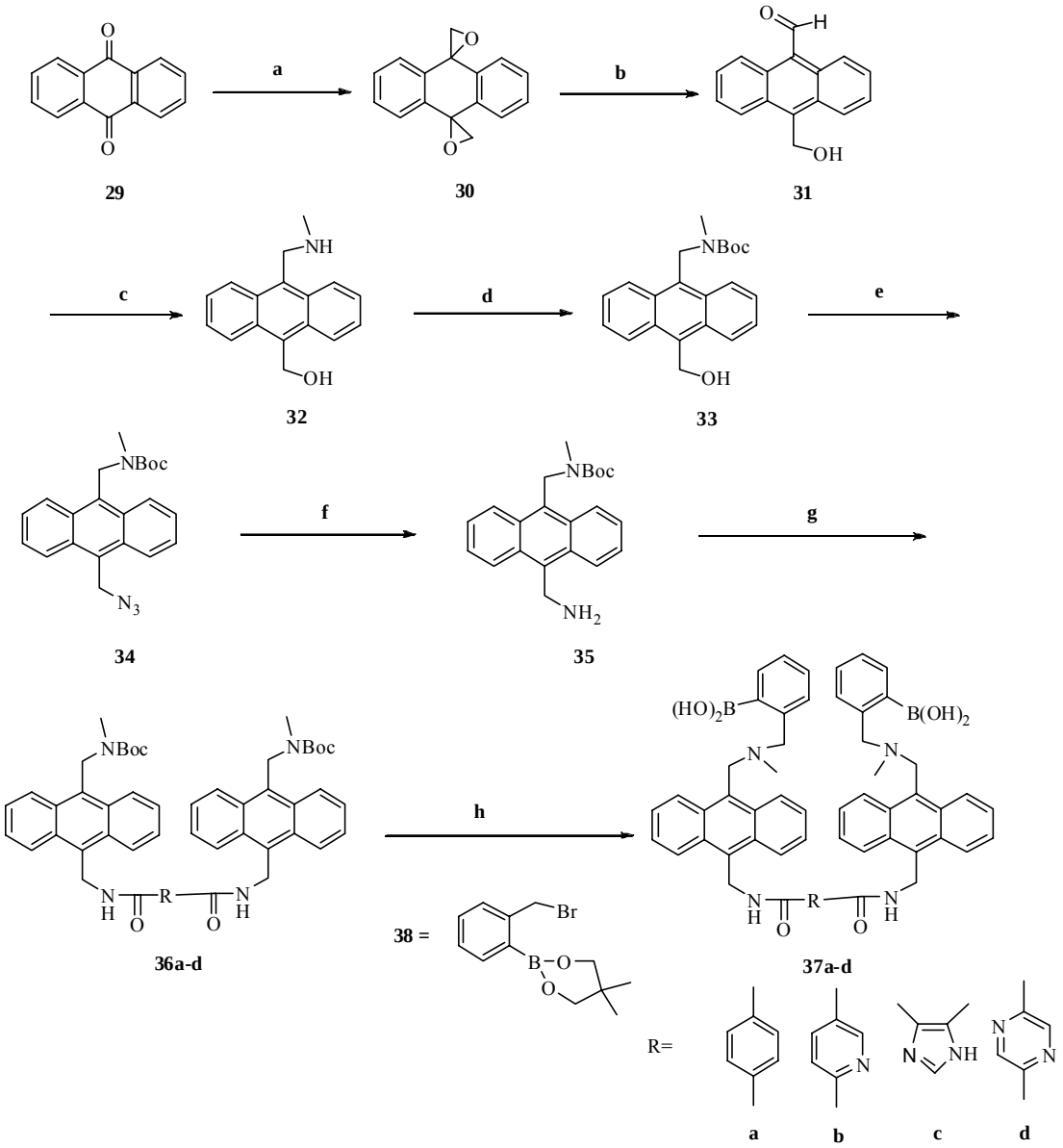

Scheme 2.1 Synthesis of bis-anthracene boronic acid derivatives.

(a) DMSO, Me_3SI, NaH, RT; 86%; (b) CH_3CN, LiBr, 60°C; 85%; (c) i. MeOH, THF, $MeNH_2$ (40% wt), ii.$NaBH_4$, RT; 71%; (d) MeOH, TEA, $(Boc)_2O$, RT; 80%; (e) DMF, PPh_3, CCl_4, NaN_3, RT; 90%; (f) (aq.) THF, PPh_3, RT; 85%; (g) CH_2Cl_2, DMF, EDCI, HOBt, TEA, HOOCRCOOH, 0°C→RT; 50-80%; (h) i. TFA, CH_2Cl_2 , ii. K_2CO_3, cat. KI, CH_3CN, iii.10%$NaHCO_3$, CH_2Cl_2, H_2O, RT; 15-30%.

presence of sodium hydride to afford the bis-epoxide derivative **30**. The rearrangement of **30**[76] in the presence of LiBr led to the aldehyde hydroxyl derivative **31**. Upon reductive amination with methylamine in MeOH/THF along with $NaBH_4$, amine **32** was obtained. After an aqueous acid wash, the protection of **32** was accomplished with di-*tert*-butyldicarbonate ($(Boc)_2O$) in the presence of triethylamine (TEA) in MeOH giving rise to **33** in 60% yield. The hydroxyl moiety of **33** was converted to azide **34** in 90% yield using a mild Mitsunobu type reaction.[76] The reduction of the azide was achieved by the addition of triphenylphosphine in aqueous THF to generate amine **35** in 81% yield. The amidation reaction of **35** with various di-acids was performed by treatment with 1-(2 dimethylaminopropyl)-3-ethylcarbodiimide hydrochloride (EDCI) along with *N*-hydroxybenzotriazole (HOBt) as the activating agents to afford compounds **36a-d** in 50-60% yield. After deprotection of derivatives **36** with trifluoroacetic acid (TFA), the unprotected free amines were then reacted with aryl boronic ester **38**[36] in the presence of potassium carbonate with a catalytic amount of potassium iodide. Then deprotection of the boronate produced compounds **37a-d** in yields of 15-30%.

2.4. Evaluation of Artificial Receptors for sLex

To explore the selectivity for the cell surface carbohydrate sLex with our fluorescent based bis-anthracene boronic acid system, a cell-based assay was conducted. The cell lines of choice were HEPG2 cell line expressing sialyl Lewis X and a non-expressing cell line, (COS7). The procedure was presented in a previous publication.[39] Briefly, cells were cultured in six-well plates with 1×10^6 M per well and incubated at 37 °C in 5% CO_2 for 48 h. The media was then removed and cells were washed with PBS. The cells

then were fixed with methanol/PBS. After fixation, cells were washed twice with PBS. The concentrations between 0.5-10 μM of bis-anthracene boronic acids were added to each well that contained 1 ml of 1:1 MeOH/PBS, and incubated for 45 min at 4 °C. The staining of the biomarkers with the fluorescent probes was observed using a fluorescent microscope with a blue optical filter.

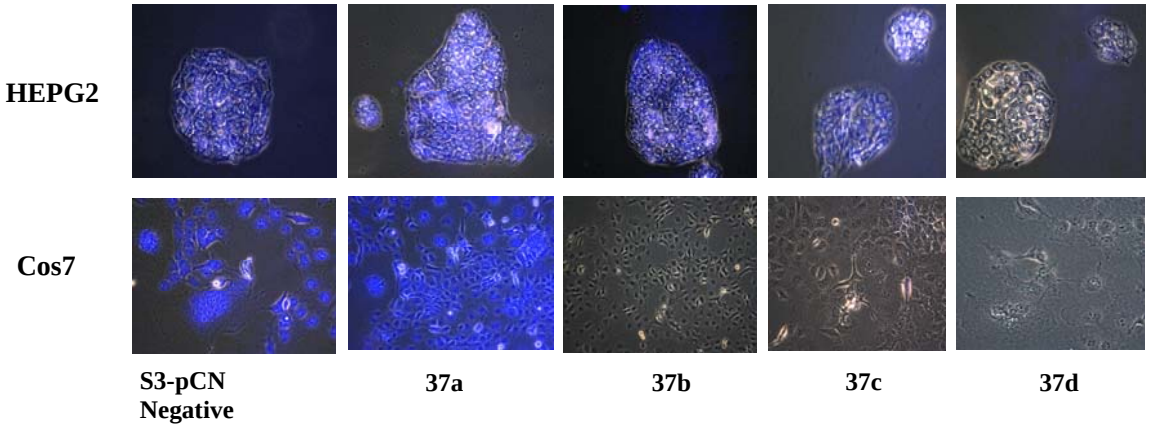

Figure 2.5 Fluorescent labeling studies of the expressing sLex cell line HEPG2 and nonexpressing COS7 with compounds **37a-d**. S3-pCN[77] a sensor selective for glucose was used as a negative control.

2.5. Effects of the Substitution of Phenyl Ring at the Carboxyamide Position

Compound **28** is our lead compound in the development in the design of a fluorescent probe for sLex. It stained the HEPG2 cell selectively at 1 μM. Heteroatoms were added within the dicarboxylic unit to decipher what intermolecular interactions are essential to enhance selectivity toward the cell surface carbohydrate, sLex. S3-pCN , a sensor design for the recognition of glucose was used as the negative control.[77] Results are shown in Figure 2.5. In compound **37a,** the tertiary amine was converted into a secondary amine to increase hydrophilicity. Compound **37a** showed a similar staining concentration as our initial fluorescent probe **28** at (1μM), however showed no selectivity between cell lines. Compound **37b** with a pyridine ring, which is a nonclassical isostere replacement of

benzene, was incorporated to introduce a heteroatom. This introduction of a hereoatom supplies additional hydrogen bonding capability along with the secondary amine. This compound **37b** seemed to display fluorescence labeling behavior that is similar to **28**. Compound **37b** labeled the HEPG2 cell line selectivity also at a concentration of 1 μM. The pyrazine compound **37d** at concentrations between 0.5-10 μM showed no selectivity toward either cell line possibly due to the heteroatom adding electron repulsion, diminishing any selectivity. The imidazole ring of **37c** is also a nonclassical isostere replacement for benzene. This compound has increased selectivity presumably due to its reduced ring size. Compound **37c** labeled the HEPG2 cell line selectively at a concentration as low as 0.5 μM. Thus of all the compounds tested, **37c** showed the most promising results in labeling HEPG2. It is possible that the observed effect with **37c** was due to the ring contraction and additional hydrogen bonding capability. This type of intermolecular interaction is associated with the natural lectin ligand for sLex.[78]

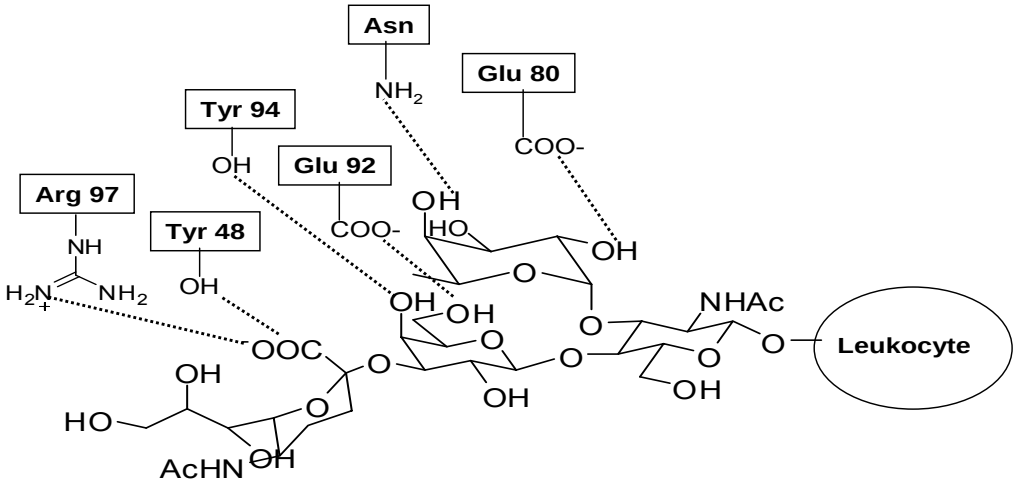

Figure 2.6 sLex and postulated binding of amino acid residues of E-selectin.

In conclusion, there is an obvious need for a recognition moiety as a diagnostic tool to monitor the presence of sialyl Lewis X as it is associated with the progression and the metastatic behavior of certain cancer and tumor cell types. With the appropriate boronic acid scaffold to detect this oligosaccharide one could begin to design selectin inhibitors to block the abnormalities that occur in this particular pathway, possibly aiding in the therapeutic realm of autoimmune diseases and cancer. In addition, it could be used as a diagnostic tool to pursue the effector mechanisms that govern this pathogenesis of cancer and autoinflammatory diseases. With that said, additional exploratory computational and/or molecular modeling design could aid in the discovery of a boronic acid with the appropriate scaffold to serve as lectin antagonists.

3. Cell–Cell Fusion: An Evolving Phenomenon used in "Drug Discovery"

3.1. What is Cell-Cell Fusion?

The human cell is a highly complex unit that contains more than 10 subcellular components that function to regulate and maintain bodily activities. Through the advancement of microscopic technology, scientists are now able to acquire an in depth 'picture' of the anatomy, physiology, and processes of a cell. One particular process of interest is cell to cell fusion also called cell-cell fusion (Figure 3.1).

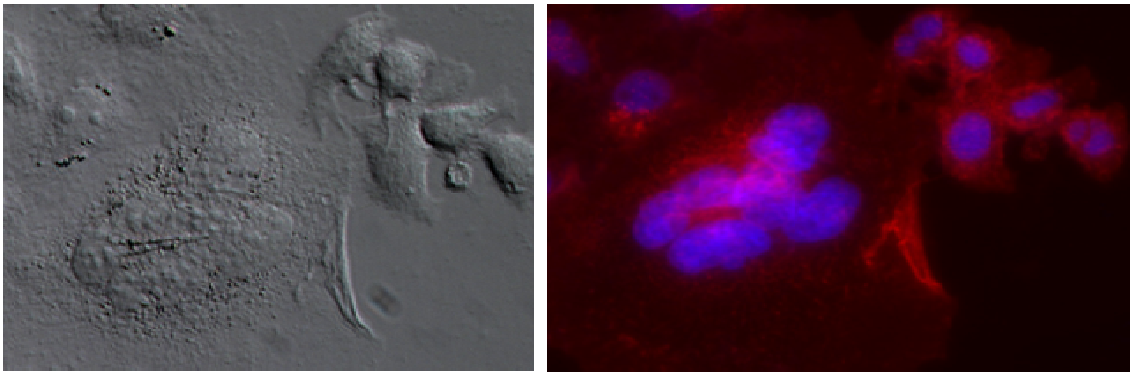

Figure 3.1 Microscopic images of cell-cell fusion of Hela cell line in response to induced fusion.
Differential interference contrast (DIC) images show multinucleated cell. The overlayed fluorescent microscopic image displaying the nuclei and plasma membrane by DAPI (4',6-diamidino-2-phenylindole) and a wheat germ agglutinin protein conjugated to a red dye (alexa fluor 594).

In mammals, cell-cell fusion is a naturally occurring phenomenon that occurs in bone cells, muscle cells, and during fertilization process. There has been a great deal of *in vitro* studies conducted with mammalian cells to determinine what is required for cell-cell fusion to occur and what mediators play a significant role in this process.

There are four stages during the cell-cell fusion that are common irrespective of cell type. The first stage is called the initiation process which begins with cell-cell recognition. The next stage involves cell-cell adhesion (Figure 3.2). The adherence phase is followed by the alignment of the plasma membrane of the adjacent cells. Lastly, destabilization of the lipid bilayers occur. As a result fusion pores develop and membrane union takes place to form a single multinucleated cell (Figure 3.2). There many mediators orchestrated the cell-cell fusion event. The externalization of phosphatidylserine (PS) from the inner to the outer leaflet of the plasma membrane and the activation of caspases have also been associated with the initiation of syncytial (multinucleated) fusion.[79, 80] These processes are also involved in the pathway that leads to apoptosis. In addition, proteases such as ADAM12, calpain and calmodulin, as well as adhesion molecules, VLA4 and VCAM-1 all have been involved in the alignment, adherence phase, cytoskeletal rearrangement, and destabilization of the plasma membrane that lead to cell-cell fusion.[79-81]

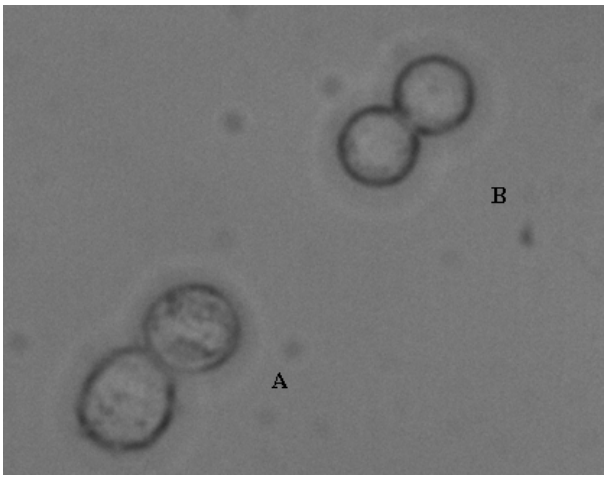

Figure 3.2 Induced cell-cell fusion with PEG of a messa (uterine) sarcoma cell line. **(A)** Cells are beginning to adhere to one another. **(B)** Destabilization of lipid bilayer, creating fusion pores and advancement of cell-cell fusion.

Although the mechanism is not well understood, the process of cell fusion has been used to design monoclonal antibodies for various autoimmune diseases, cancer, and bioimaging, among others.[82-84] The development of a vaccine with the aid of cell fusion is also on the rise as a method to invoke our own immune system to fight against cancer.[85-87] This programmed cell-cell fusion event has also been associated with the development of various defects and diseases. Among them is the metastatic behavior of certain cancer cell types.[88, 89] Devising methods to study the upstream and downstream effectors that play a role in *in vivo* cell-cell fusion may give insight into how the evolution of certain diseases takes place. Below is a brief discussion, non-inclusive, of cell-cell fusion as it relates to disease and preventative drug therapy.

3.2. Cell-Cell Fusion and Human Diseases

With any controlled process, there is always a possibly that abnormalities will occur. Defects in the sperm-egg fusion promote infertility,[80] irregularities of bone cell fusion cause abnormalities such as osteopetrosis,[90] and lastly experimentally evaluated results show tumor cells' ability to spontaneous fuse with each other as well as with normal somatic cells, leading to the formation of metastatic cells.[88, 89, 91] In retrospect, membrane fusion, a process involving in vesicle trafficking, is imitated by HIV as well as by the human influenza virus. HIV-envelope protein gp120/gp41, gp120 binds to the co-receptor CD4 on the surface of T-lymphocytes and macrophages. Subsequently gp41 undergoes a conformational change mediating fusion of the viral membrane with the target cell membrane. In turn, the infected cells expressing gp120/gp41 on the surface can fuse with uninfected cells initiating syncytium formation.[92] This process has been replicated with transfected cell culture experiments to develop fusion inhibitors to block this action.

Sialylated cell surface receptors that line the respiratory tract serve as an entry for the influenza virus via hemagglutinin (HA) binding. The protein HA binds to the surface of the receptor followed by endocytosis and is activated once at endosomal pH by undergoing conformational changes to mediate viral and endosomal targeted membrane fusion.[93] This viral protein has been used to direct liposome drug delivery systems to specific sites for therapeutic purposes.[94]

3.3. Applications of Cell-Cell Fusion

3.3.1. Advances in Monoclonal Antibodies as Therapeutic Agents

Cell fusion is a technique used in traditional hybridoma technology to obtain specific monoclonal antibodies to be used as therapeutic agents for cancer, autoimmune diseases and infections, among others.[82] Production of hybridomas can be formed by injecting a specific antigen into a mouse, collecting antibody-producing cells (plasma or B cells) from the mouse spleen, and then fusing them with long-lived cancerous immune cells with the aid of PEG, electrofusion, or virus. The resulting hybrid cells (hybridomas) become immortal, that is, capable of unlimited cell division (Figure 3.2). Each individual hybridoma (hybrid cell) is cloned and tested to find those that produce the desired antibody.

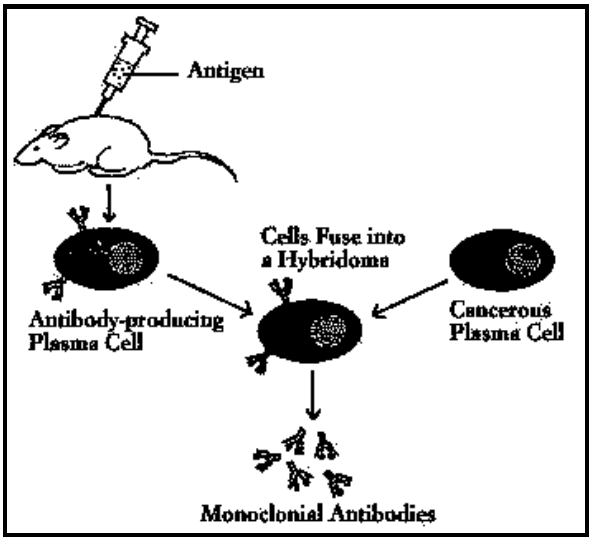

Figure 3.3 Standard hybridoma technology.[95]

The introduction of the mouse hybridoma was first reported in the mid- 1970's by Cesar Milstein and Georges Köhler of the Medical Research Council in Cambridge, England. Their experiments paved the way for the evolution of therapeutic monoclonal antibodies as we know it.

The "first century" monoclonal antibodies (mAb) proved to be unsuccessful in medicinal applications for many reasons. Primarily, these antibodies were produced by mouse cells and encoded by mouse genes. As a result use of these antibodies in therapeutics was limited by their immunogenicity. In recent years, there has been a tremendous amount of progress in genetic engineering techniques to make "mousey" antibodies more humanlike (Figure 3.4).[82] The humanization era of monoclonal antibodies began with the design of chimeric antibodies which are one-third mouse and two-thirds human. They are engineered by grafting the variable regions of the targeted specific antigen from a murine antibody onto the human constant regions (Figure 3.4).[84] Four of the eleven antibodies approved are chimeric antibodies, including Rituxan.

Rituxan is a chimeric antibody used to treat Non-Hodgkin's lymphoma. A more 'humanized' monoclonal antibodies with only 5-10% mouse, was accomplished by CDR (complementarity-determining region) grafting. Only the DNA sequences encoding the actual antigen binding pocket of the original "mousey" antibody, the CDR sequences

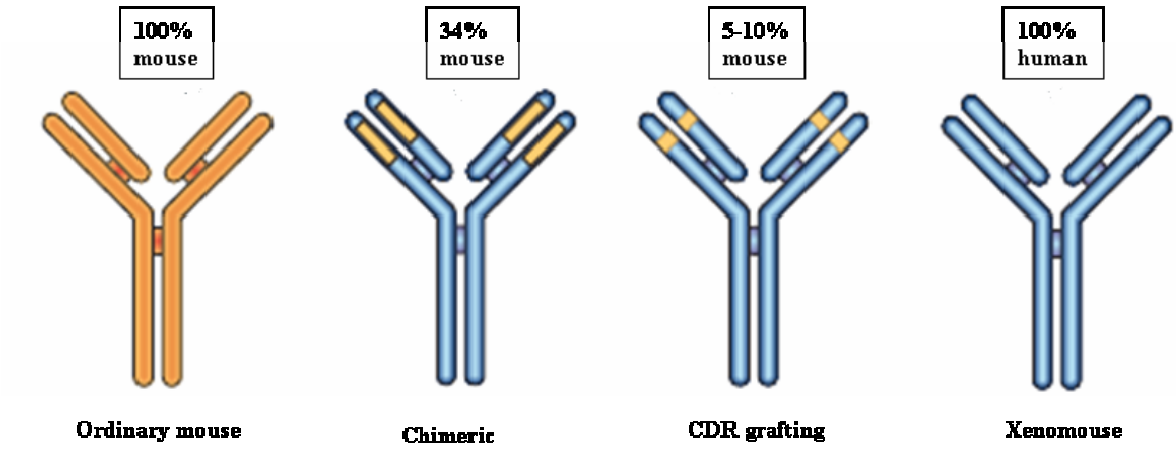

Figure 3.4 The evolution of monoclonal antibody technologies.[82]

remain.[82] The CDR sequences of the mouse are inserted into the genes encoding a selected human antibody of interest. Trastuzumab (Herceptin) is produced in this fashion. Herceptin is directed against the protein HER2 which is the receptor for epidermal growth factor. Epidermal growth factor binds to HER2 protein and stimulates proliferation in breast cancer cells. Herceptin binds to the extracellular domain of the HER2 receptor and thus blocks the triggering event. Clinical trials demonstrate that it is effective as a single entity or in combination with other anticancer drugs, such as Taxol.[84] Further advancement in technology is the fully 'humanized' antibodies, Xenomouse technology. The transgenic mouse are genetically engineered and bred for the human Ig (immunoglobulin) locus. After removal of the B cells (antibody producing cells) from the spleen of the mouse, they are then harvested. After immunization, they are

immortalized by fusion with cancerous cell line, as in traditional hybridoma technology. Hybrid cells are then screened for specific antibodies. [82, 96]

Up to date, there are hundreds of monoclonal antibodies in clinical trials for various diseases. This technology has the great advantages of high throughput and specificity.[82]

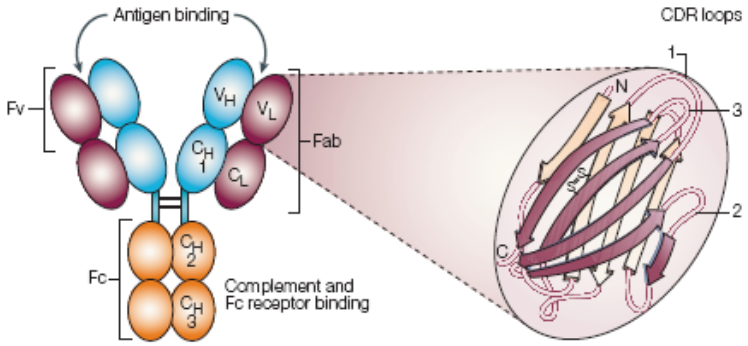

Figure 3.5 Structure of immunoglobulin.
The molecule contains two identical light chains and heavy chains. They both are composed of a variable region and a constant region. The variable region of both heavy and light chains is the antigen binding part of the molecule. Within the variable region, the complementarity determining region (CDR) defines the specificity of the antibody. Fc is glycosylated and contains three sites for interactions with effector molecule and complement.[82]

3.3.2. New Evolution of "Cell – Fused Vaccines"

Vaccines were first discovered in 1796 by an English doctor Edward Jenner. Jenner performed a courageous experiment. First he infected a patient with cowpox and gave him time to recovery. After some time, he injected the smallpox virus into the same patient. The patient showed no signs of smallpox. This process of vaccination saved thousands of lives.[97] Most modern day vaccines are B cell vaccines.[97] They contain attenuated pathogens, which are capable of stimulating immunity, but have been genetically "disabled" so that they cannot cause disease. In the late 1990's, a new innovative way of developing vaccines was introduced by a group of German physicians

and scientists for renal cell carcinoma.[87] Standard vaccines are used to prevent infections such as tetanus, small pox, and polio, where these vaccines actually treat the disease. The concept involves fusing tumor cells with immune system cells and using these hybrids cells as a vaccine to stimulate the immune system to eliminate the tumor. Dr. David Kufe and colleagues were the first to illustrate this type of vaccine therapy. They fused dendritic cells (APC's) from an unrelated donor with cancerous cells from a patient. These hybrid cells were then treated with radiation and finally injected with and without interleukin 12 (used to activate cell-mediated immunity). The results showed that interleukin 12 induces an immune response. Seventeen patients were administered this vaccine. Seven of the seventeen responded to hybrid cell vaccination with four complete tumor remission and three partial responses. All of the complete responses were ongoing after 10-19 months. Among the partial responders, one patient relapsed after six months, but two others were still in remission after 9 and 21 months. The results seem to be promising, although it is too soon to draw conclusions at the initial pre-clinical stage.[86, 98] This study introduced a new therapeutic method which uses 'nature' to fight off cancer instead of xenobiotics.

3.3.3. Stem Cell Research

Stem cells are self-renewing cells. They are not terminally differentiated. Upon division the daughter cells have a choice of two fates: 1) they can remain an undifferentiated stem cells or 2) they can terminally differentiate into specialized cells such as epidermal stem cells for the epidermis, intestinal stem cells for intestinal epithelium, hemopoietic stem cells for the blood, and so forth. Undifferentiated stem cells are in place for the (re)generation and/or repair of corresponding damaged tissue. Cell

culture studies have shown that mouse embryonic stem (ES) cells can differentiate into any linage of cell types and all tissue in the body, allowing an avenue for facilitating tissue repair.[99] Although the mechanism of how this process takes place is still under scrutiny, one of the proposed evaluated mechanisms is spontaneous cell-cell fusion.[99, 100] Some tissues seem to be incapable of repairing because no competent stem cells are present. Therefore, stem cells could be very useful for tissue repair and regeneration for patients with various diseases such as muscular dystrophy, Parkinson's disease, diabetes and so on.

3.3.4. Conclusion

Cell fusion has been a powerful tool for antibody production and other applications. Recent developments in the treatment of various cancers by the use of monoclonal antibodies have shown much success as well. There are hundreds of mAb (monoclonal antibodies) in clinical trials for the treatment of inflammatory and other autoimmune diseases.[82] In addition, the new "wave" vaccine therapy has shown promising results with minor side effects.[98]

As of now, cell-cell fusion is accomplished by 'nature' spontaneously and by, viruses, PEG, or electrofusion. To continue to use the attributes of cell-cell or cell-membrane fusion in creating versatility for drug design. In such a case as in the development of *in vivo* site specific drug vehicles or the design of small fusogenic molecules that can aid in monitoring the pathogenic behavior of various diseases related to cell fusion for the development of drugs, and immunotherapeutic applications, among other possibilities. One must use a vector (fusogenic agent) that does not provoke immunogenicity and that possess minimum toxic effect. Taking advantages of the properties of arylboronic acids'

ability to bind to 1,2 and 1,3 cis diols in aqueous media,[14] Wang group, among others, have designed various chemosensors to detect biological carbohydrates for medicinal applications. We are interested in expanding the application of boronic acids into the design and synthesis of boronic acids with long aliphatic chains as potential fusogens. We hypothesize that the aliphatic chain should be able to insert into lipid cellular membranes and then the boronic acid units should allow for the "attachment to neighboring cells" through complexation with cell surface glycans. Such interactions should allow the boronic acid compounds to bring two or more cells together for fusion. The next chapter discusses the details of our work along this line.

4. Phenylboronic Acid Derivatives as Potential Fusogen

4.1. Boronic Acids as Recognition Moiety for Cell-Cell Fusion

Cell fusion is a technique used in traditional hybridoma technology to obtain monoclonal antibodies for medicinal, diagnostic, and other biomedical purposes (Figure 3.2).[82] The process involves fusion of two different cells or two cells of different species. Upon cell-cell fusion, the plasma membranes adhere to one another and a single continuous cytoplasm forms producing one cell. Currently, cells are induced to fuse by the aid of PEG (polyethylene glycol), viruses, or by a mild electric shock. Although the mechanism is not well understood, *in vivo* and *in vitro* systems involving cell fusion have been studied extensively.[80, 81, 92, 101] In the course of cell-cell fusion, there is a destabilization of the lipid bilayer, which leads to aggregation; subsequently fusion is triggered. In the enveloped virus systems, it is proposed that the congruity of the bilayer is caused by a conformational change of the fusogenic peptide establishing membrane fusion.[88] On the other hand, PEG's mechanism is based on: 1) PEG's adsorption on the cell surface brings cells together, and 2) PEG's depletion from cell surface resulting in cells being induced together by osmotic pressure.[102] It is noteworthy to mention that pH sensitive PEG-COOH derivatives are used in drug delivery systems.[94] The acidity of the PEG-COOH derivative causes membrane destabilization and fusion occurs with the plasma membrane of the target cell.

In our group, we are designing molecules that could be a potential asset to this field. It was discovered in the 1940's that boronic acid moieties reversibly bind to 1, 2 or 1, 3

cis diol in aqueous media.[14] There has been much success in the design various fluorescent chemosensors for the recognition of biological carbohydrates.[103-105] With the knowledge of success in the recognition of cell surface carbohydrate,[39, 106] boronic acid was incorporated as a potential fusogen. Boronic acid derivatives with a fatty aliphatic side chain were designed to investigate the potential application of fusogenic properties. The hypothesis is that the boronic acid will serve as a receptor for a carbohydrate substituent on one cell and the fatty aliphatic side chain will migrate in the bilayer of the adjacent cell merging the cells together provoking a cascade of events that lead to the fusion process (Figure 4.1).

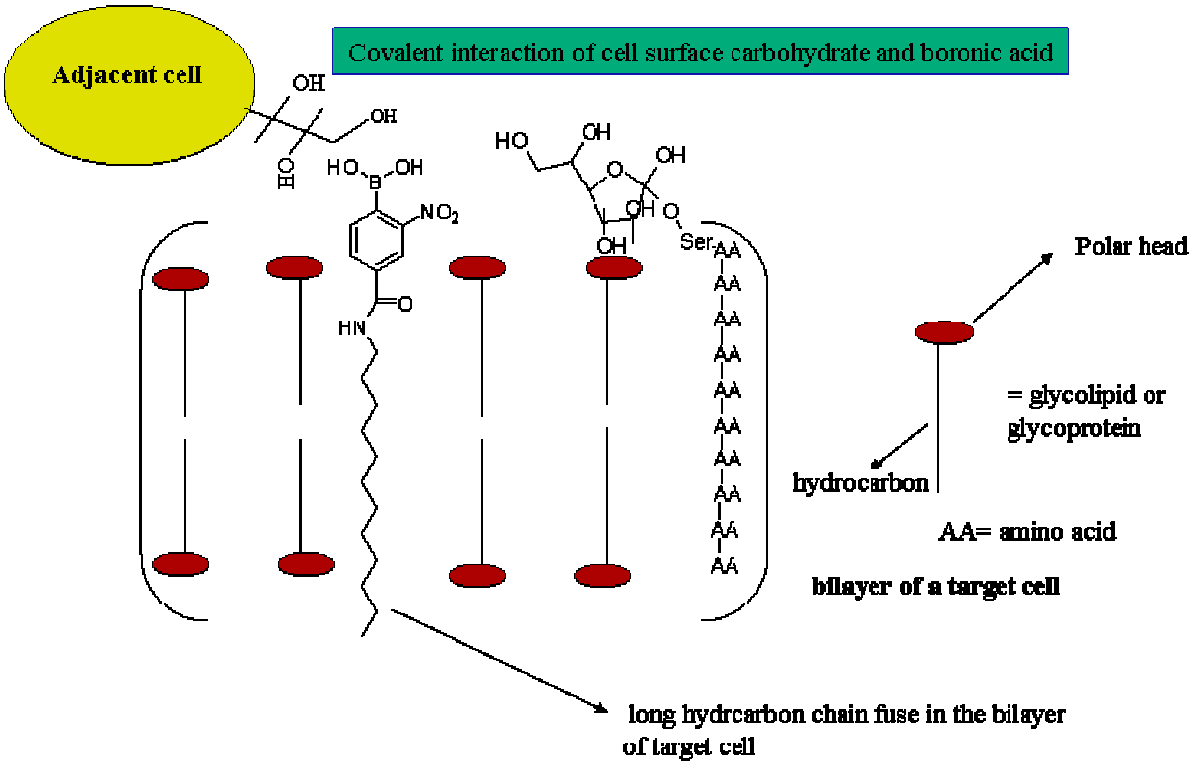

Figure 4.1 Plausible mechanism of boronic acid derivatives as a potential fusogen.

Cancer cells are known to be fusogenic in nature, although the mechanism is not well understood.[89] For the initial design, cancer cells were chosen to validate the potential fusogenic properties of the boronic acid derivatives. Can they increase cell fusion above basal activity of various human cancer cell lines. With that in mind, four [4–caboxyamide,2-nitro(phenyl boronic acid)] derivatives have synthesized to test the fusogenicity with the use of cancer cells.

4.2. Synthesis of 4-Carboxyamide Phenyl Boronic Acid Derivatives

The synthesis of each compound was accomplished in three-step process. We begin with the commercially available 4-carboxy phenyl boronic acid **39**, which was treated with fuming nitric acid in sulfuric acid to afford the nitro derivative **40** in a 65% yield. The next step involved the formation of an acid chloride, **41** with the use of thionyl chloride. Finally, the carboxyamide **42** was obtained in 25-39% yields through the amidation of an alkyl amine derivative in tetrahydrofuran. The very nature of boronic acid being a Lewis acid makes it acceptable to the attack of polar protic solvent. As a result, for further ^{1}H-NMR spectral characterization, boronic acid derivatives were oxidized with 30% hydrogen peroxide in the presence of sodium hydroxide to yield phenol compounds.

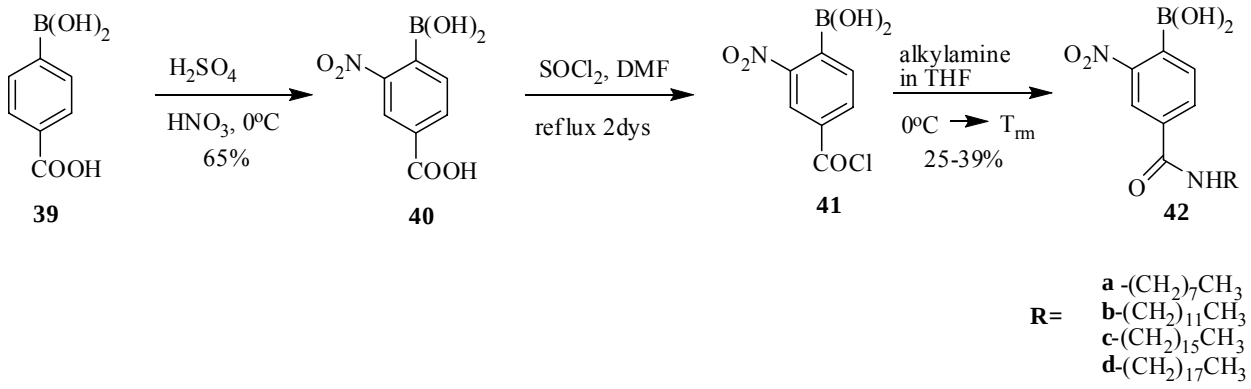

Scheme 4.1 Synthesis of boronic acid derivatives as potential fusogens.

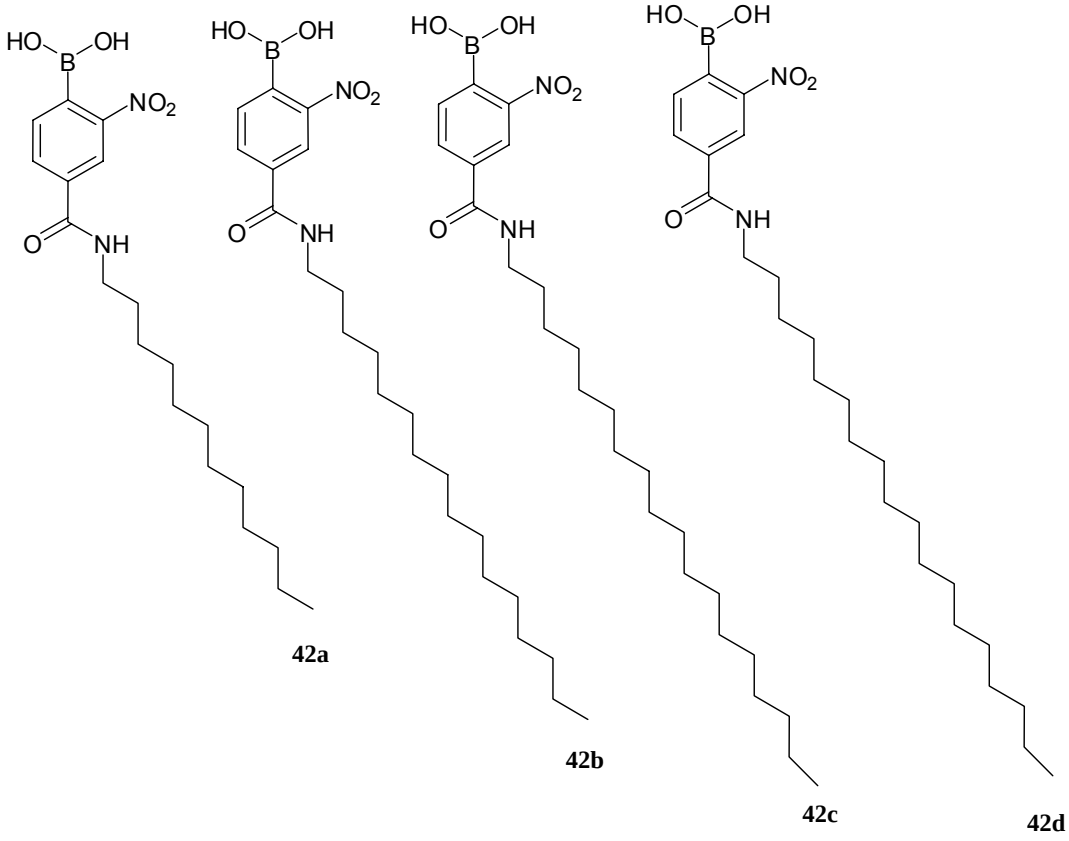

Figure 4.2 Structures of potential fusogens.

4.3. Applicable Procedures in Determining Fusogenic Properties of Phenylboronic Acid Derivatives

For our initial studies, we chose three human cancer cell lines: two epithelial cell lines Hey (ovarian) and Hela (cervical) and one fibroblast cell line Messa (uterine sarcoma). Cell- cell fusion is a process in which plasma membrane and cytoplasm of two adjacent cells become incessant. A discrete assay to monitor this process is needed. We chose DAPI [4',6-diamidino-2-phenylindole] to stain the amount of nuclei present in a given cell boundary, and next cytoplasmic dyes[107] (rhodamine and fluorescein derivatives) to determined merger of the cell cytoplasms, and lastly an artificial lectin to stain the plasma membrane.[108]

4.3.1. Nuclear staining.

Cells were stained with DAPI to demonstrate the amount of nuclei or the presence of gigantic nuclei per cell. Cell-cell fusion index and syncytium formation were analyzed using Zeiss microscope particle fluorescent counting program, which allows one to measure the size of each cell. Compound **42a** displayed poor activity compared to control at basal level, an increase in compound concentration caused salt formation to occur during the fusion process in all cell lines. Compounds **42c** and **42d** both had solubility problems and exhibited toxic effect in Hey and Messa cell lines. Compound **42b** (Figures 4.3, 4.4, 4.5) was the most effective (Table 4.1.), predominantly in the Messa cell line.

Table 4.1 Results from fluorescent staining counting software of each cell line and control.

% Fusion	**Hela**	**Hey**	**Messa**
Control	47.4±0.32	35.0±5.54	40.5±3.5
42a (76 μM)	37±2.5	26.5±0.03	41.7±0.42
42b (47 μM)	43.6±1.45	36.7±1.97	49.7±5.3
[a]**42c** (40 μM)	28±4.2		
[a]**42d** (29 μM)	37±2.5		

Each experiment was performed in triplicate; statistical analysis (mean ± s.e.m.)
[a]No results were obtained due to solubility problems and toxic effect of **42c** and **42d** with Hey and Messa cell lines.

Cell aggregation brings difficulty in distinguishing cell fusion events from cell adhesion with using this assay alone, especially with the Messa cell line. After careful evaluations, before continuing the remaining protocols several issues were addressed: 1) solubility of phenylboronic acid derivatives; 2) concentration of phenylboronic acid derivatives, preventing toxicity issues; 3) volume of medium used during the cell fusion process; 4) time and temperature during process and lastly; 5) cell density.

As far as we know, we are the first group to use cell base assays to indicate fusogenic properties of phenylboronic acid derivatives. We initially begin by adapting a procedure used for PEG, with the exception of the use of growth medium instead of phosphate buffer. The protocol was finally adjusted after evaluating each parameter listed above.

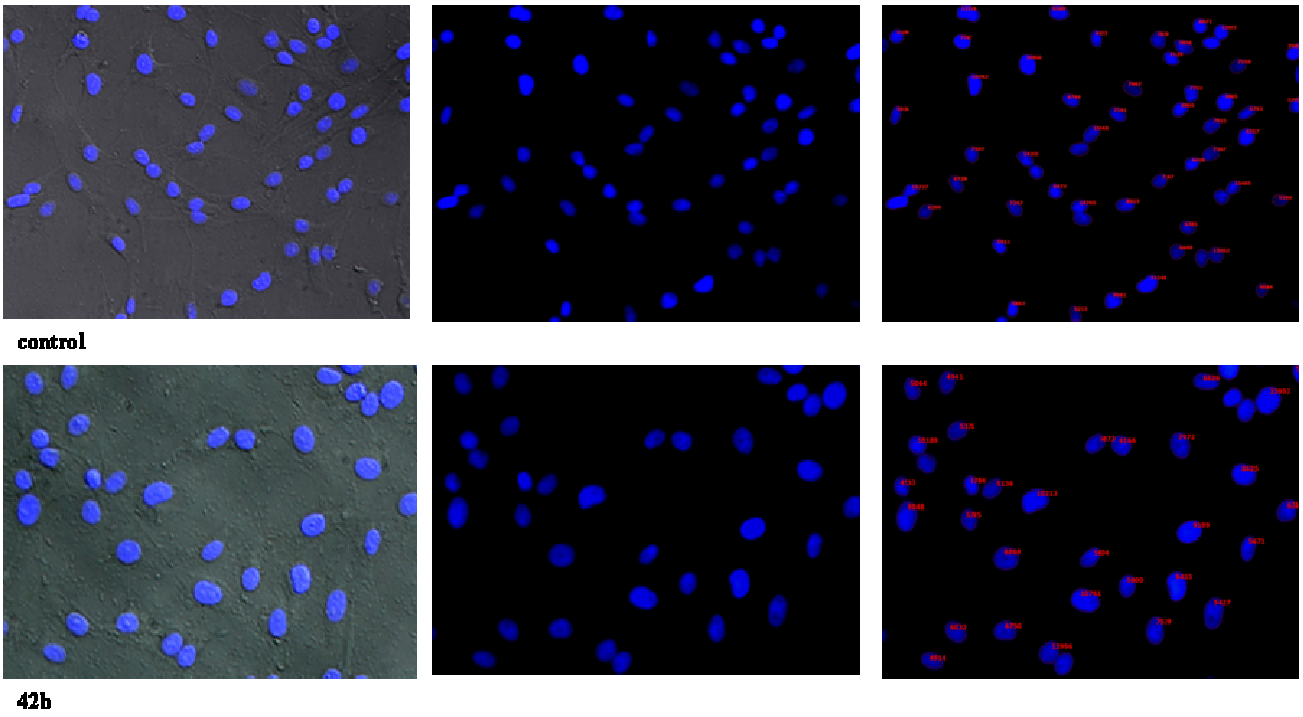

Figure 4.3 Cell fusion assay of Hey cell line.
Images are displayed as DIC overlays, DAPI, and numbers in red indicating size of each cell. A cell line without PBA derivative was used as a negative control. Compound **42b** is at a concentration of 47 μM.

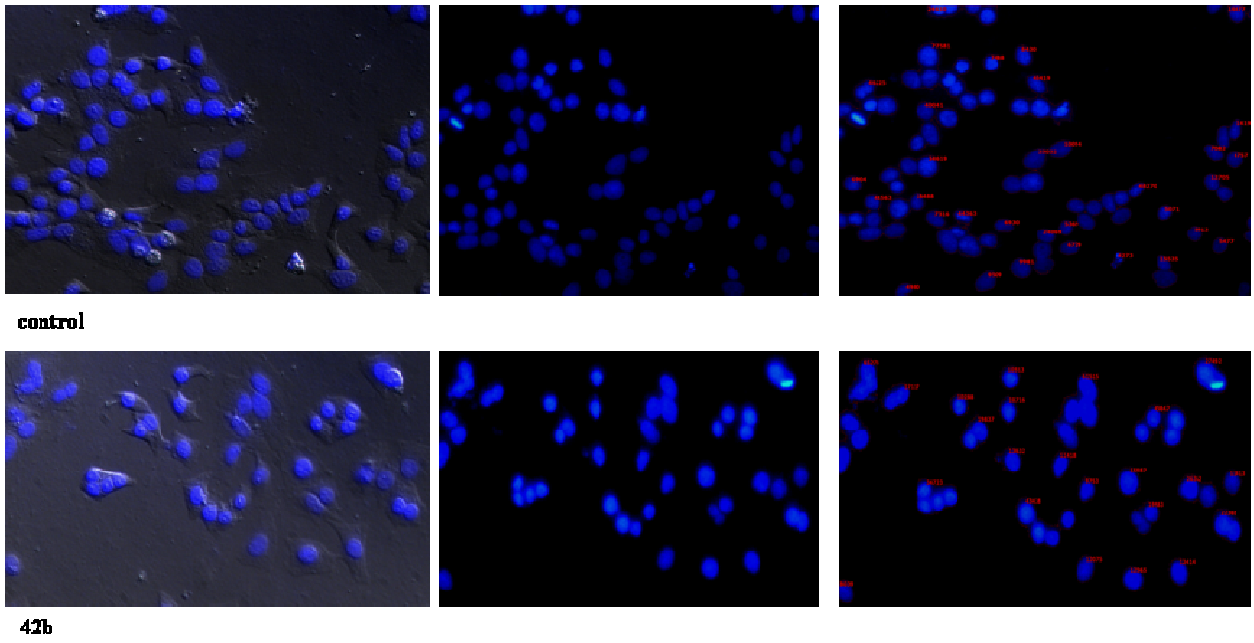

Figure 4.4 Cell fusion assay of Hela cell line.
Images are displayed as DIC overlays, DAPI, and numbers in red indicating size of each cell. A cell line without PBA derivative was used as a negative control. Compound **42b** is at a concentration of 47 μM.

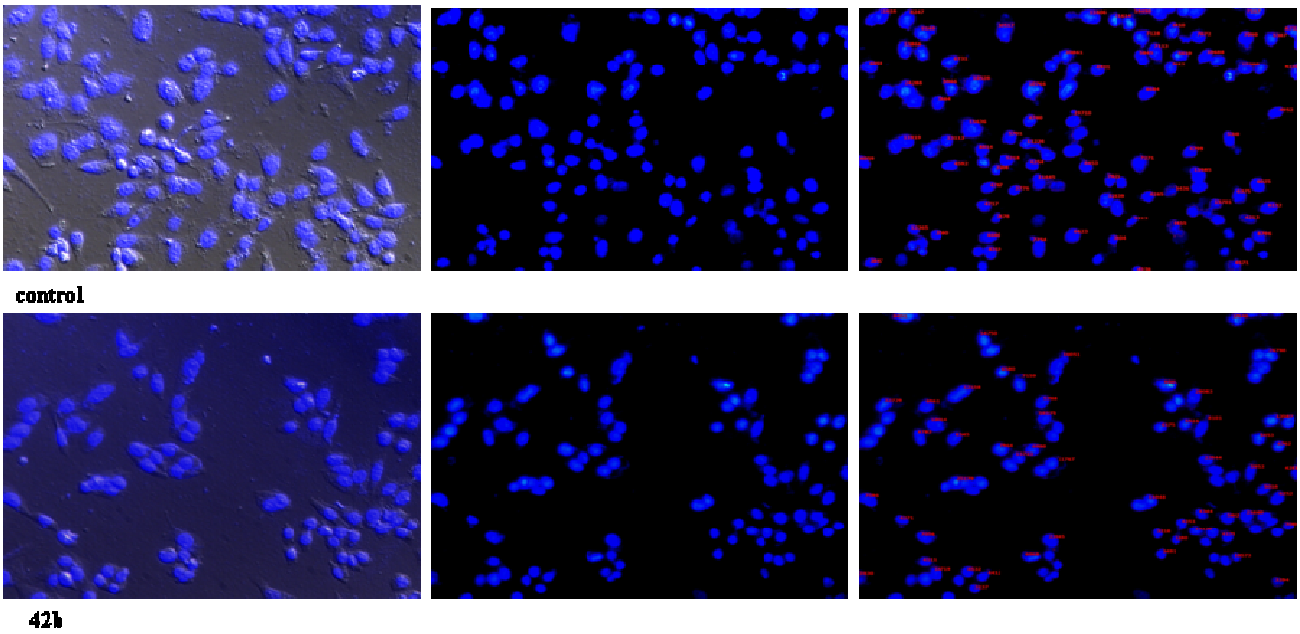

Figure 4.5 Cell fusion assay of Messa cell line.
Images are displayed as DIC overlays, DAPI, and numbers in red indicating size of each cell. A cell line without PBA derivative was used a as negative control. Compound **42b** is at a concentration of 47 μM.

The experimental conditions among cell lines consisted of a reduction in volume to 2.5 ml of growth medium, an increase in time to 15 min to allow cell-cell fusion to occur, and a cell density of 0.5-1 $\times 10^6$ M/cell before seeding. After seeding cells were allowed to fused for three days before evaluations (a density per well was determine by the cell size of each line) and lastly upon the addition of PBA derivative, which was dissolved in DMSO (a stock solution of (5-11 mg/ml) before addition to medium. The temperature played a factor as well as the amount in salt formation of boronic acid derivatives. The temperature was maintained at room temperature during addition of boronic acid and increased to 37 °C during fusion process. The concentration of each PBA derivative was adjusted according to their toxicity to cells and the solubility in the growth medium in each cell line. The finding suggested that the added volume amount of boronic acid to

the medium before aliquoting to the cells should not exceed 10 µl to prevent salt formation. These final parameters were accessed by the use of fluorescent microscopy with DAPI and the plasma membrane dyes in combination (data not shown). This procedure was used in remaining assays.

Hey cell line was eliminated due to lack of cell fusion events, and because the cells seemed to acquire a lot of space to grow and adhere to the flask. This could hinder cell-cell contact, a process needed for cell fusion to occur. A CHO (Chinese hamster ovarian) cell line was introduced as a non-human cell base assay, and because the cells grew in a nice monolayer in close proximity to each other and the diameter of the cell allowed visibility of organelles with the inverted microscope.

4.3.2. Plasma Membrane Staining

A wheat germ agglutinin protein conjugate to dye, alexa fluor 594, selectively binds to *N*-acetylglucosamine and *N*-acetylneuraminic (sialic) acid residues allowing labeling of the plasma membrane along with Hoechst for nuclear staining. The combination of the two dyes provides a precise measurement of cell-cell fusion events, and reduces the uncertainty between cell-cell adhesion. Generally speaking, in the Hela and CHO cell lines, there was no evidence of cell fusion events with boronic acid or any spontaneous events (Table 4.2). However in the Messa cell line, there was some indication of cell fusion. Compound **42d** showed the most promising results, displaying over 2-fold increases compared to cells without boronic acid, which indicates that cell-cell fusion

initiated by boronic acid derivatives is possibly a function of chain length (Figure 4.6, Table 4.3).

Table 4.2 Results of % cell fusion from the plasma and nuclear membrane assay of CHO and Hela cell lines.

Concentration (μM)	CHO (%)	Hela (%)
Control (0)	1	3
42a (100)	2	5
42b (75)	1	4
42c (20)	2	4
42d (20)	2	2

Experiments performed in triplicate

Images of each cell line were displayed below (Figures 4.7, 4.8, 4.9). The Messa cell line seemed to grow in clusters and in monolayers. To aid in the visibility of the nuclei; cells were permeabilized with 70% methanol (MeOH). The cells at this time were not labeled with the plasma membrane dye, because of the distortion of membrane that occurs with the use of methanol (Figure 4.10). The results were similar to the plasma and nuclear membrane results (data not shown). In order to validate these results flow cytometry was conducted with the Messa cell line. CHO and Hela cell line were used to test the fusogenic properties of the PBA derivatives between two different cell types.

Table 4.3 Results of % cell fusion from plasma and nuclear membrane assay of the Messa cell line.

Concentration (μM)	Messa
Control (0)	8.7±2.31
42a (100)	9.7±1.53
42b (60)	14±3.6
42c (10)	11.7±2.08
42d (10)	20±4

Each experiment was performed in triplicate; statistical analysis (mean ± stdev.)

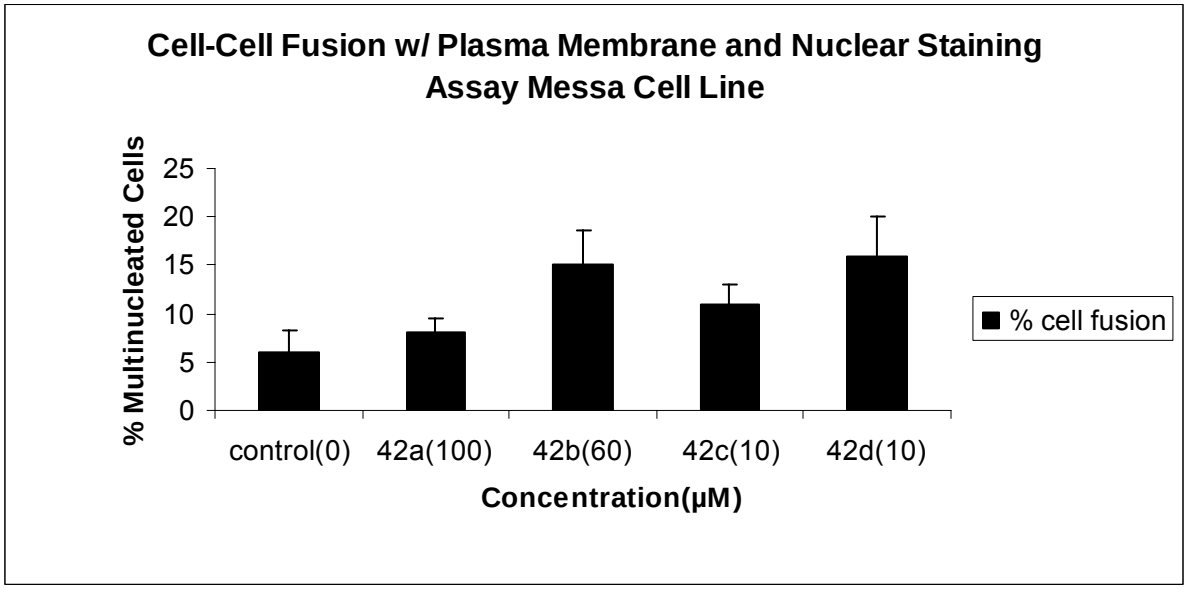

Figure 4.6 Cell fusion assay of the Messa cell line with plasma and nuclear membrane staining.
WGA-alexafluor594 was used to display the plasma membrane and DAPI stains the nucleus. A cell line without addition of boronic acid was used as the negative control. PBA derivatives were displayed as a function of concentration.

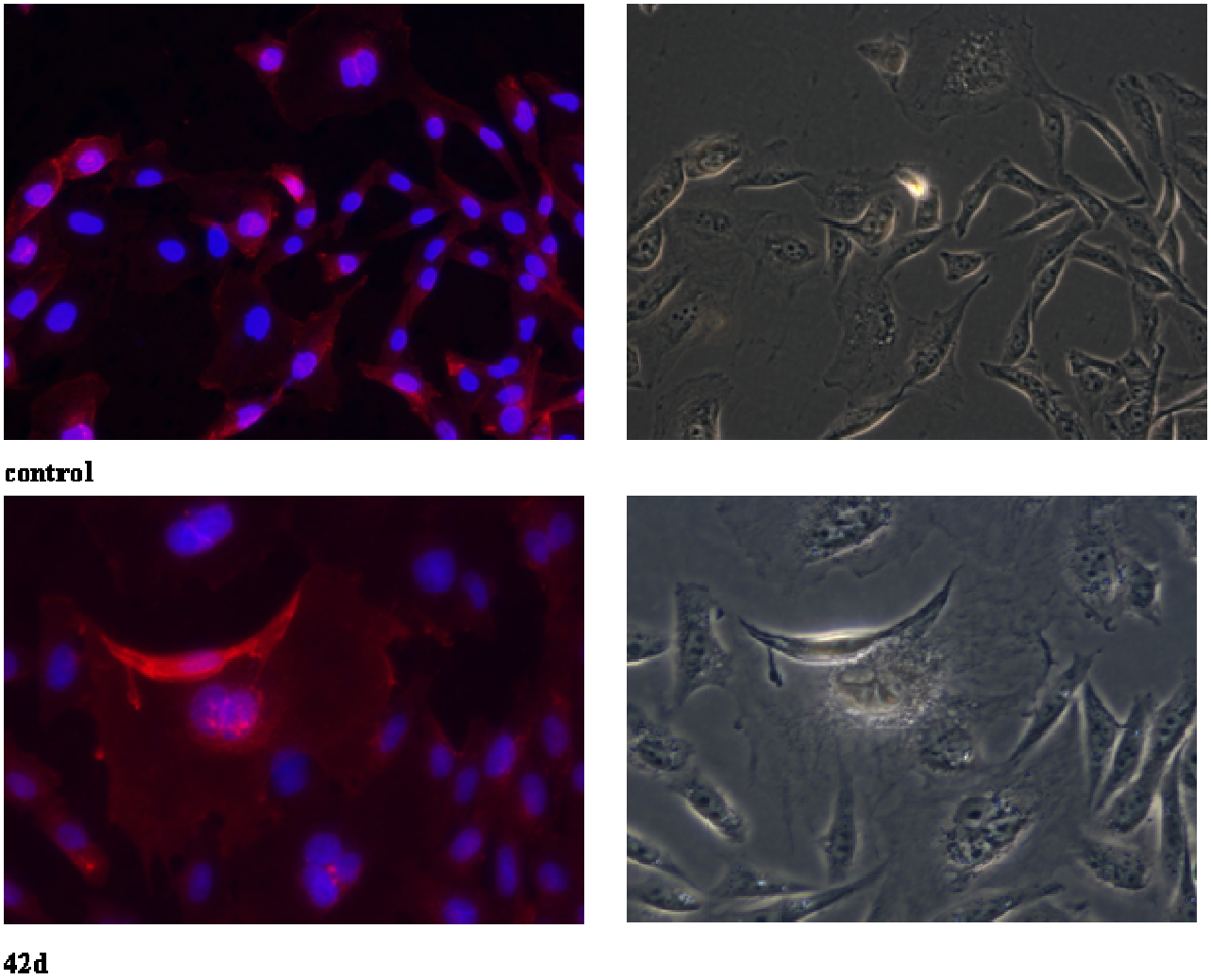

Figure 4.7 Cell fusion images of the CHO cell line.
WGA-alexafluor594 was used to display the plasma membrane and Hoescht stains the nucleus. A cell assay without the addition of boronic acid was used as the negative control. Compound **42d** is at a concentration of 20 μM. Phase contrast is also shown.

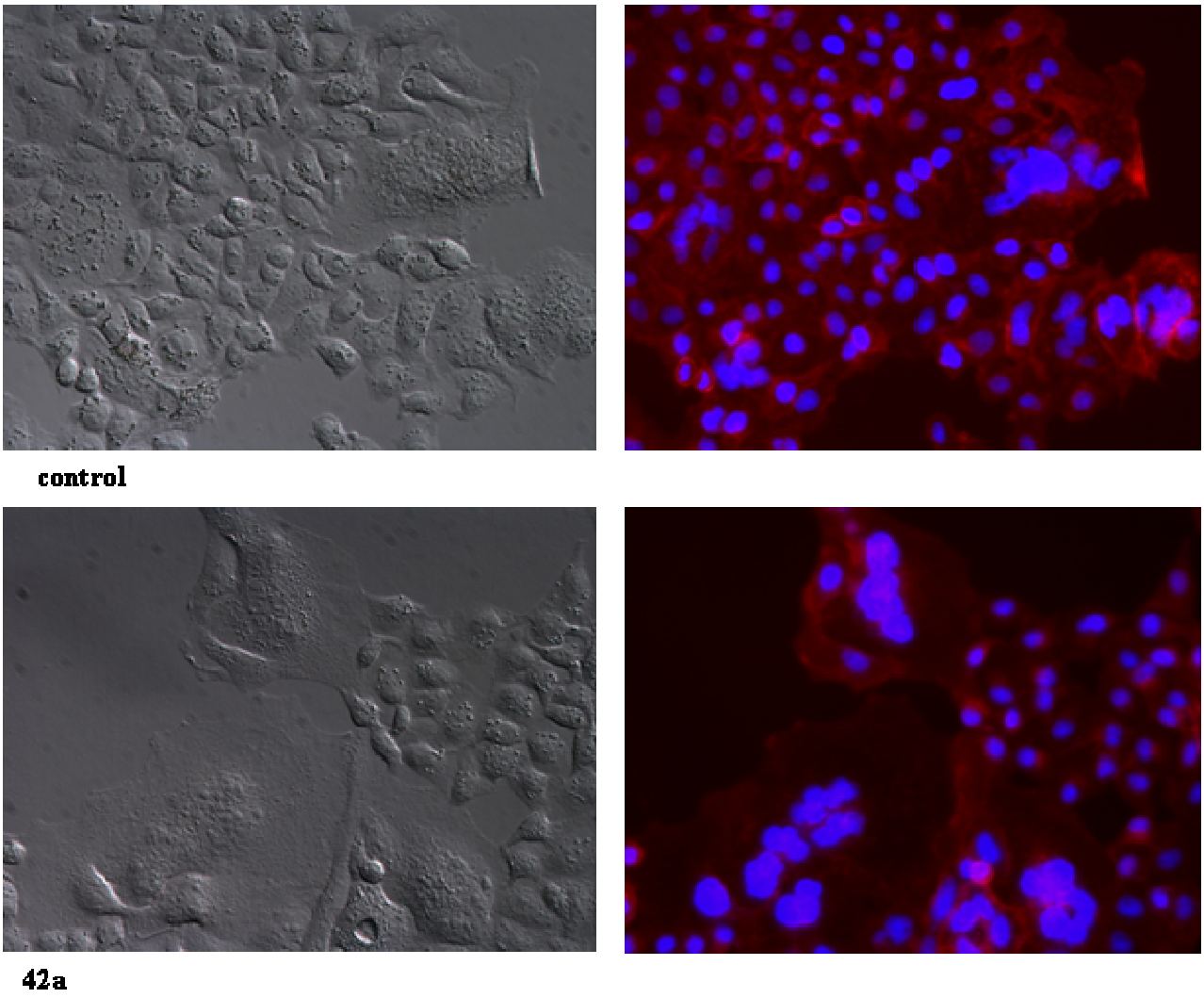

Figure 4.8 Cell fusion images of the Hela cell line.
WGA-alexafluor594 was used to display the plasma membrane and Hoescht stains the nucleus. A cell assay without the addition of boronic acid was used as the negative control. Compound **42a** is shown at a concentration of 100 μM. DIC images are also shown.

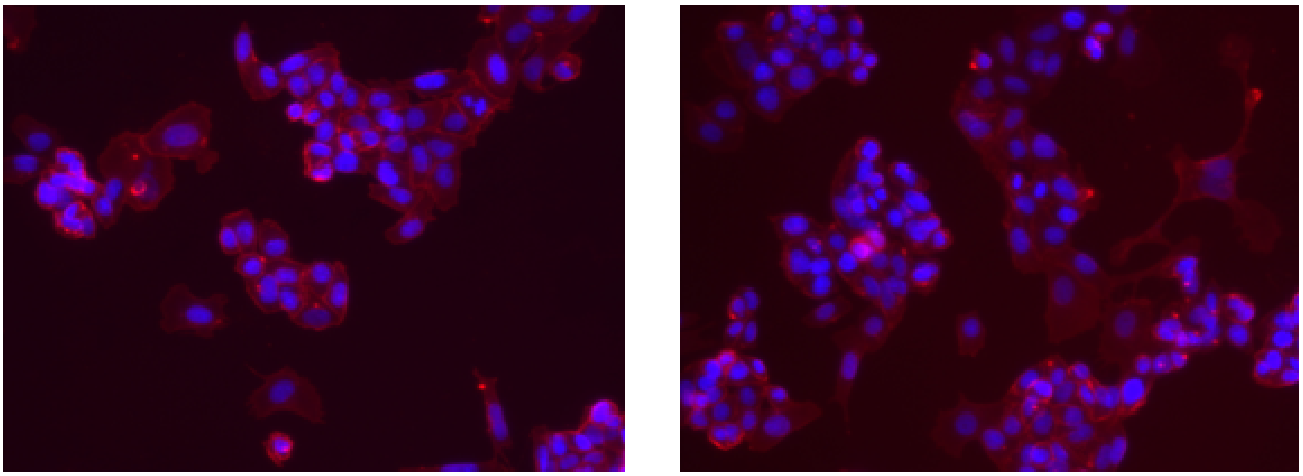

Figure 4.9 Cell fusion images of the Messa cell line.
WGA-alexafluor594 was used to display the plasma membrane and Hoescht stains the nucleus. A cell assay without the addition of boronic acid was used as the negative control. Compound **42d** is at a concentration of 10 μM.

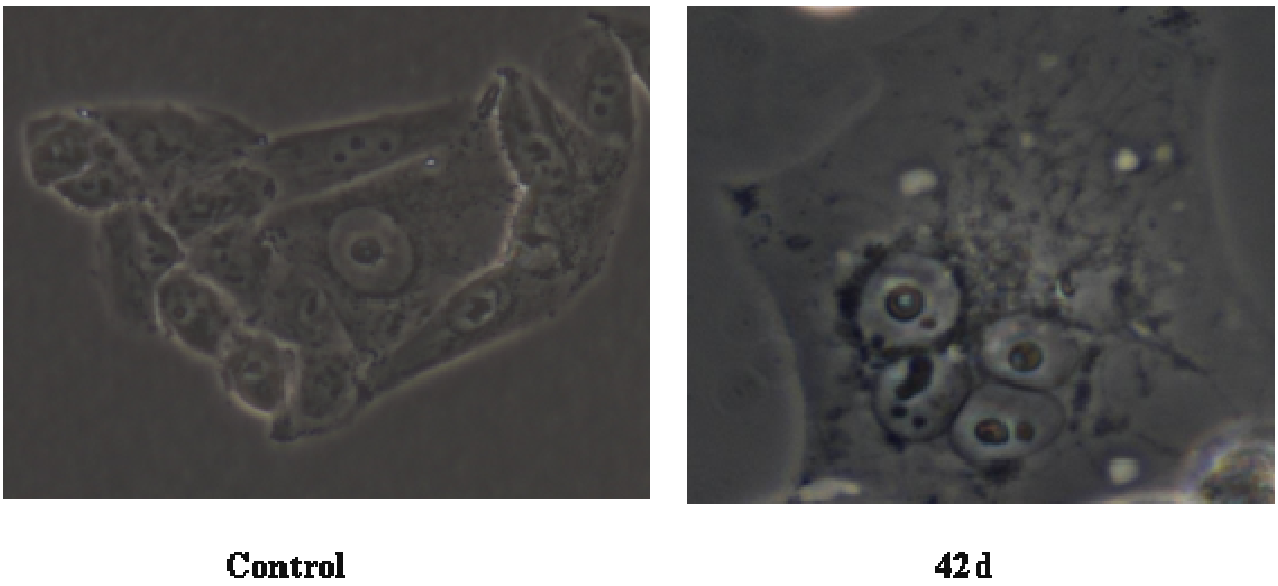

Figure 4.10 Cell fusion phase contrast images of the Messa cell line.
Cells have been impermeabilize with 70% MeOH to help in displaying the nucleus. A cell assay without the addition of boronic acid was used as the negative control. Compound **42d** is at a concentration of 10 μM.

4.3.3. Cytoplasmic Staining

Dual dye assays of homogeneous and heterogeneous cell types were performed to help differentiate between cell division or endomitosis of cell fusion events. Once stained with the cytoplasmic dyes upon fusing of the cytoplasms a change in color from the combination of red [(5-(and-6)-(((4-chloromethyl) benzoyl)amino) tetramethylrhodamine (CMTMR)] isomers and green (5-chloromethylfluorescein diacetate (CMFDA)) dyes appears as a yellow to orange color. Before performing flow cytometry experiments (FACS), the dual dye assay was assessed using fluorescent microscopy with compound **42b**. Hey was re-introduced as a possible human cell line to fuse with cell of different origins. The orange color after fusion between cells appears randomly if at all (Figs. 4.11, 4.12) with each homogeneous cell type. Green cells seem to aggregate and then fuse with each other and vice versa. However as seen with phase contrast microscopy multinucleated cells are present (Figs. 4.11, 4.12). Interestingly enough, in the Hela cell line, the control appeared to have two gigantic nuclei and cytoplasms where as with addition of the **42b,** multiple nuclei and cytoplasms co-existed within the plasma membrane (Figure 4.11). The Hey and Hela cell lines were used to test for fusion events with **42b**. There seemed to be some fusion activity as the day progressed. Fusion events slightly increased, however the event was not enough to be significant. At this time, flow cytometry was introduced for quantitative and validation of cell fusion events.

The Messa cell line showed inconsistent results with the plasma and nuclear membrane data. Possibly cell aggregation contributed to false positive/negative results (Figure 4.14, Table 4.4).

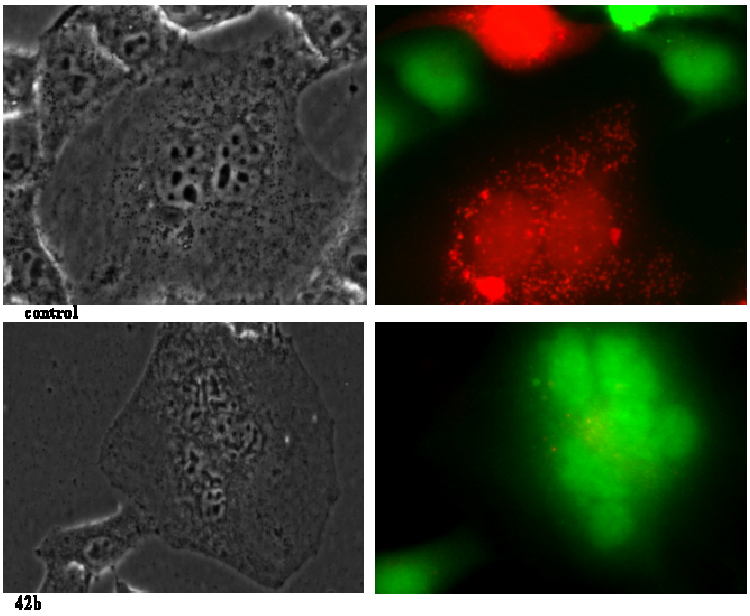

Figure 4.11 Dual dye assay for the Hela cell line in response to **42b**. The cell line without **42b** was used as the control.

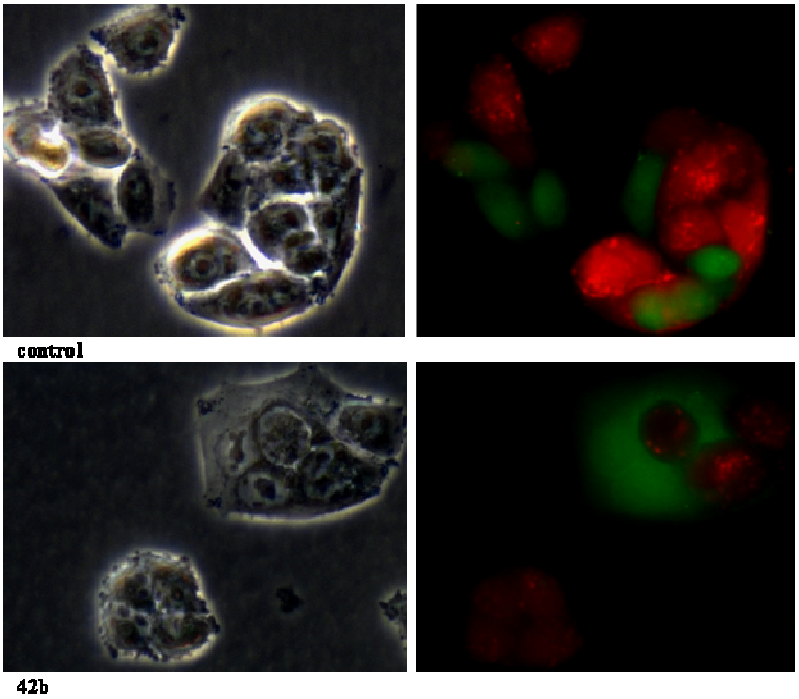

Figure 4.12 Dual dye assay for the Messa cell line in response to **42b**. The cell line without **42b** was used as the control.

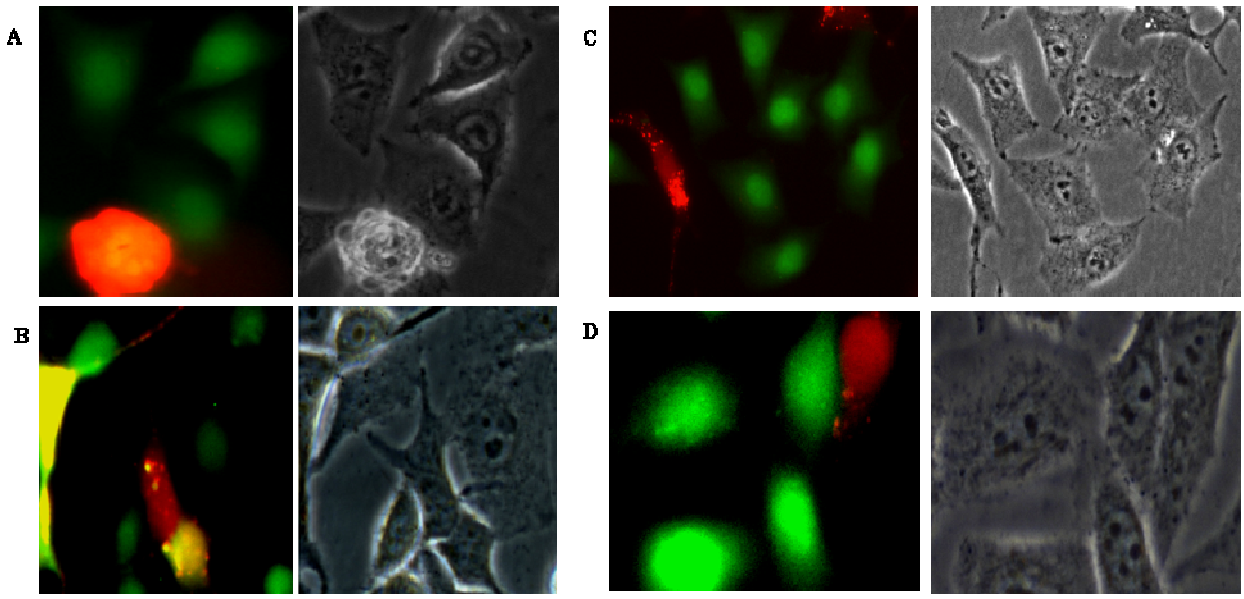

Figure 4.13 Fluorescence and phase contrast microscopy.
The fusion of Hey (green) and Hela (red) cell lines in response to addition of **42b**. **A,** is a 3 day process with **42b**; **B**, is a 4 day process with **42b**; **C**,**D** are 3 and 4 day process used as the controls without **42b**.

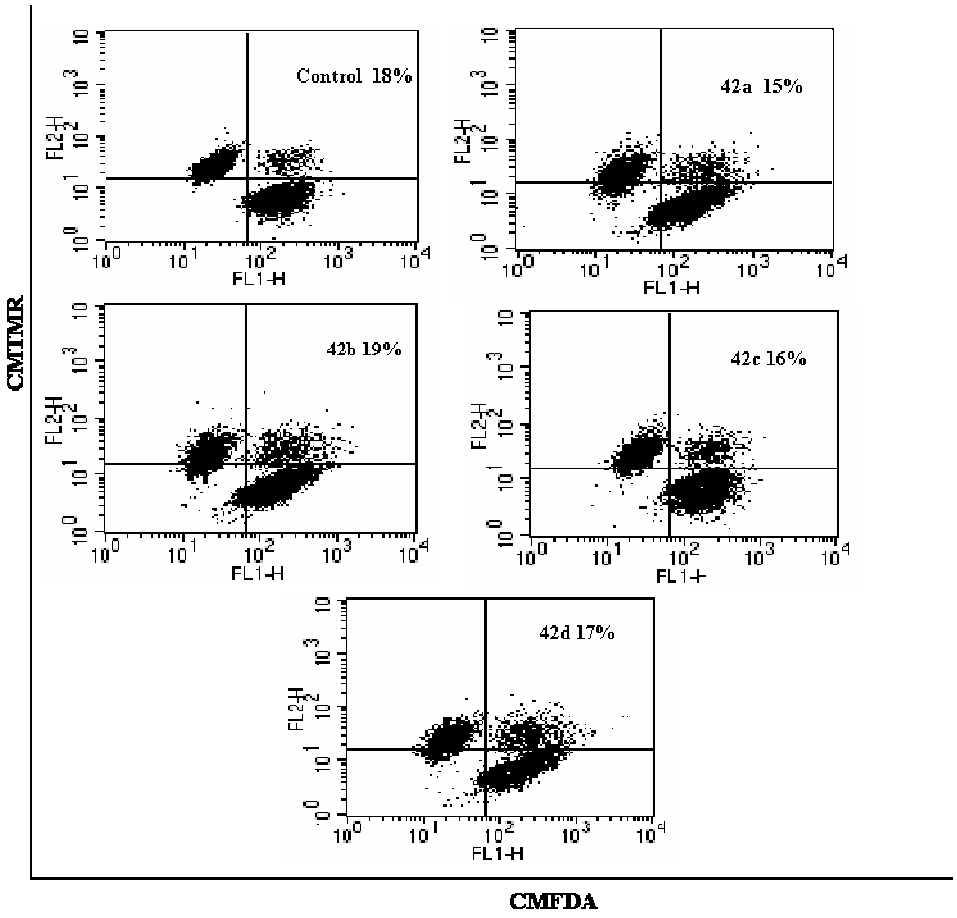

Figure 4.14 Cell-cell fusion assay with the Messa cell line using FACS analysis.
Cell density was divided into two equal halves before fusion. They were dye with CMTMR and/or CMFDA. Following seeding overnight, the cells of different dyes were allowed to fuse for 3 days after which the flow cytometry assay was conducted. The upper right quadrant represents dual staining, a indication of cell-cell fusion occurred between different cells of different dyes.

Table 4.4 FACS data of the Messa cell line for cell fusion events.
Each experiment was performed in triplicate; statistical analysis
(mean ± stdev.)

Concentration (μM)	Trial 1	Trial 2	Trial 3	Avg.
control (0)	21.3	16.1	17.2	18.2±2.7
42a (100)	17.4	17	11.2	15.2±3.45
42b (60)	25.7	13.4	16.9	18.7±6.31
42c (10)	16.4	19.9	11.2	15.8±4.31
42d (10)	11.9	20.4	19.5	17.3±4.69

An assay that displays DNA content (ploidy) and cell cycle information (Figure 4.15) would perhaps give a better assessment of cell fusion events for the Messa cell line. DNA ploidy is defined as DNA diploid, a single G0/G1 peak corresponding to the same channel of the biological control, and a DNA aneuploid, a separate distinct G0/G1 peak from the diploid G0/G1.[109] RNA was removed and propidium iodide (PI), a dye that binds to DNA, was used to acquire chromosomal content to validate cell fusion event in the Messa cell line.

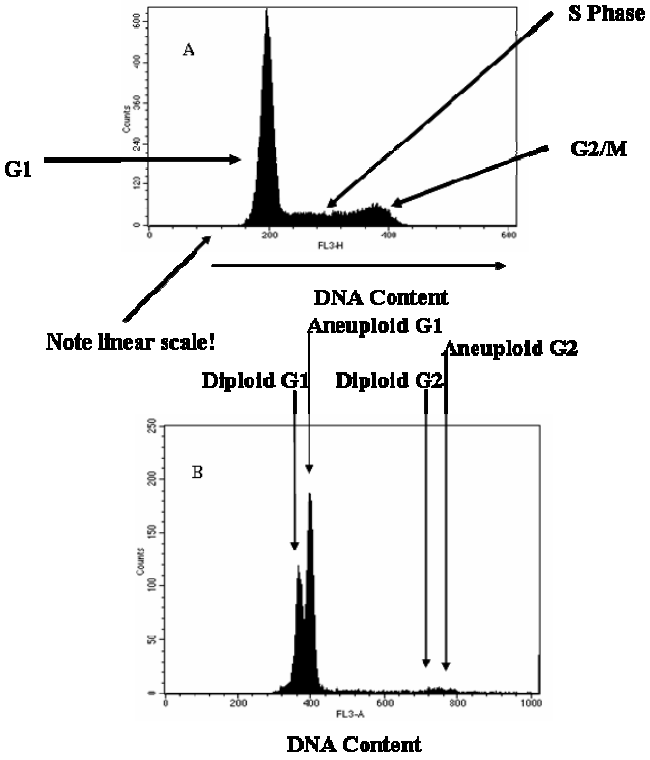

Figure 4.15 FACS of cellular DNA content.
A, display of cell cycle analysis; **B**, DNA analysis in tumor near diploid fibrosarcoma.

The results are somewhat identical to results from the unfused control (Figure 4.17), validating that the phenylboronic acid derivatives did not increase fusion above basal activity in the Messa cell line. The single cell fusion approach was abandoned and focus was geared toward fusion analysis between two different types of cells.

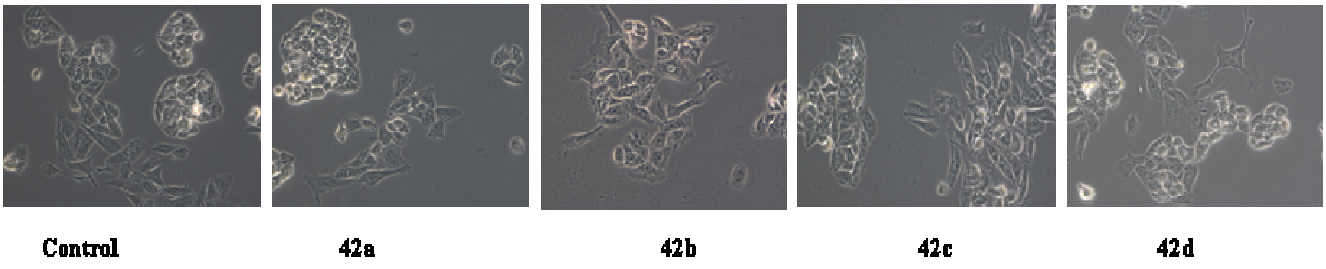

Figure 4.16 Phase contrast images of Messa cell line in response to PBA derivatives.

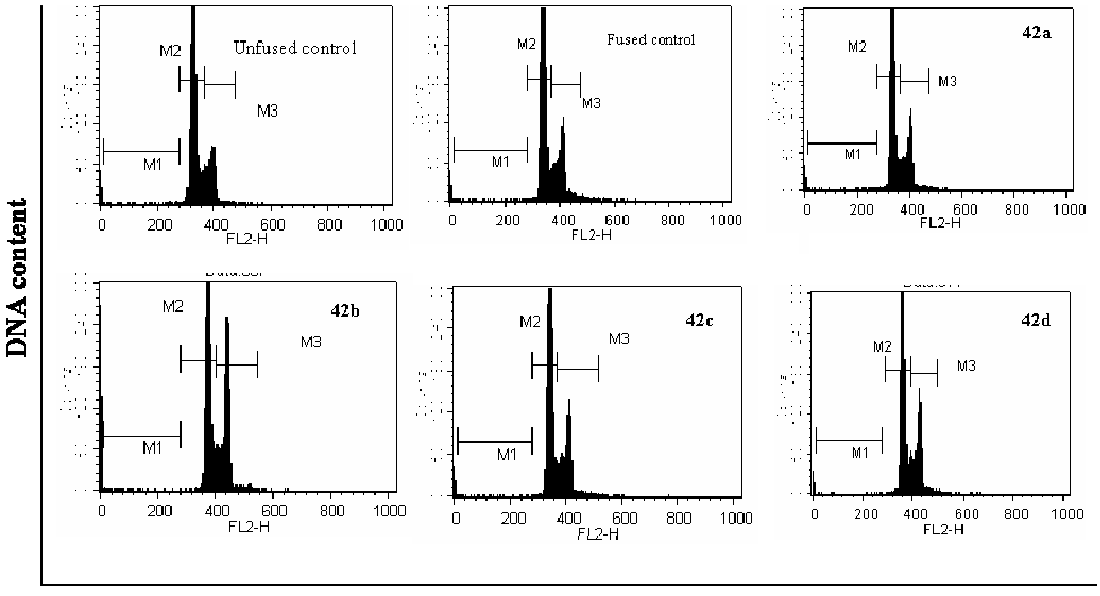

Figure 4.17 Cellular DNA content of Messa cell line in response PBA derivatives.

Hela and CHO cell lines were used to demonstrate cell fusion between two different types of cells. Before fusion between the chosen cell line, each cell line was fused as a

separated entity and cell survival assays were conducted to determine the most effective concentration of each compound without creating toxicity.

In normal live cells phosphatidylserine (PS) is located on the cytoplasmic surface of the cell membrane. However in apoptotic cells PS is flipped from the inner leaflet of the plasma membrane to outer leaflet of plasma membrane exposing it to the external cellular environment. Annexin, the human anticoagulant has a high affinity for PS. The Annexin conjugate use in this case AlexaFluro488 (green dye) can be used to label PS and can be detected by a fluorescent activated cell sorter (FACS). Propidium iodide (PI) a red nucleus binding dye can be used simultaneously to label dead cells only, because it can not permeant in live or apoptotic cells. In this particular assay, we have dead cells staining red and green, apoptotic cells staining green and live cells showing little or no fluorescence.

Table 4.5 Cell survival assays of CHO cell line.

CHO	control (0 µM)	**42a** (100 µM)	**42b** (100 µM)	**42c** (30 µM)	**42d** (30 µM)
Live	81.7	83.7	74.8	85.5	82.8
	86.9	78.6	68.3	80.6	78.6
Dead	13	5.6	10.4	6.8	7
	6.5	8	16	7.5	10.0
Apoptosis	4.6	11	14.9	7.6	10.6
	5.7	13.4	15.5	12	11.8

Experiments performed in duplicates

Raw data from CHO and Hela cell line were analyzed (Table 4.5, 4.6) and concentration for cell fusion assay was in some cases reduced in **42b** (75 μM), **42c** and **42d** to (20 μM); whereas **42a** remained constant.

Table 4.6 Cell survival assays of Hela cell line.

Hela	control (0 μM)	**42a** (100 μM)	**42b** (100 μM)	**42c** (30 μM)	**42d** (30 μM)
Live	86.7	87.9	81.9	87.6	48.0
	90.7	93.1	72.6	84	57.4
Dead	5.1	6.3	10.7	5.1	22
	6.0	4.8	17.3	3.8	25.5
Apoptosis	6.0	4.7	5.7	6	26.4
	1.3	1.3	8	10.5	14.1

Experiments were performed in duplicates

Cell fusion experiments were performed, and each PBA derivative showed fusogenic properties with compound **42c** displaying the highest percentage of cell-cell fusion activity (Figure 4.18, 4.19, and Table 4.7).

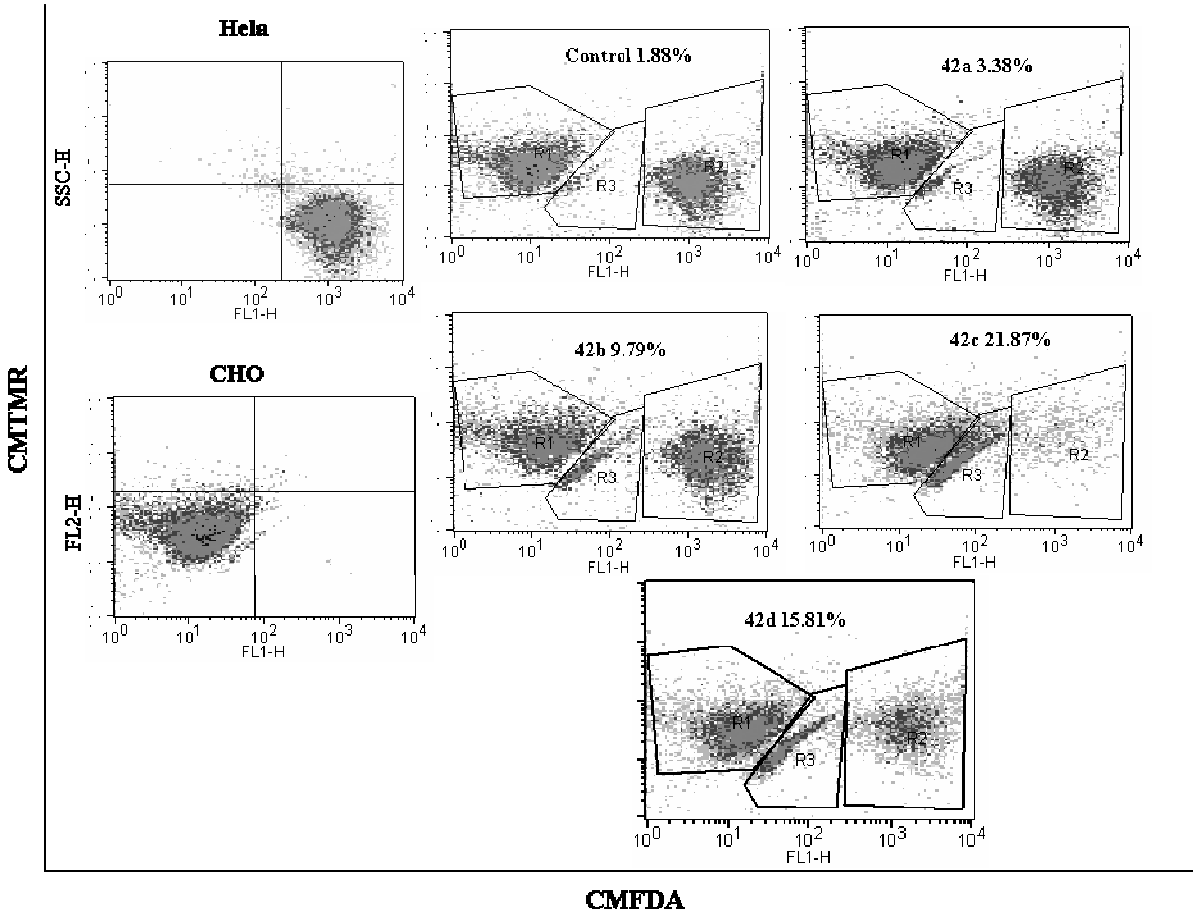

Figure 4.18 Cell-cell fusion assay with Hela and CHO cell line.
Cell were seeded in Petri dishes for two days then stained with the corresponding dye. The cells were then detached and with equal density were allowed to fuse for 3 days after which flow cytometry assay was conducted. The upper R3 represents dual staining, an indication of cell-cell fusion occurred between different cells of different dyes. Hela cells are stain with (green dye (CMFDA)) and CHO stain with (red dye (CMTMR)).

Table 4.7 Extrapolated data of cell-cell fusion experiment of Hela and CHO cell lines.

Conc. (μM)	Trial 1	Trial 2	Trial 3	%Cell Fusion
Control (0)	1.2	1.9	2.5	1.9±0.66
42a (100)	2.9	3.6	3.7	3.4±0.45
42b (75)	12	8.2	9.2	9.8±1.98
42c (20)	17.6	20.8	27.2	21.9±4.92
42d(20)	19.4	12.4	15.7	15.8±3.53

Each experiment was performed in triplicates; statistical analysis (mean ± stdev.)

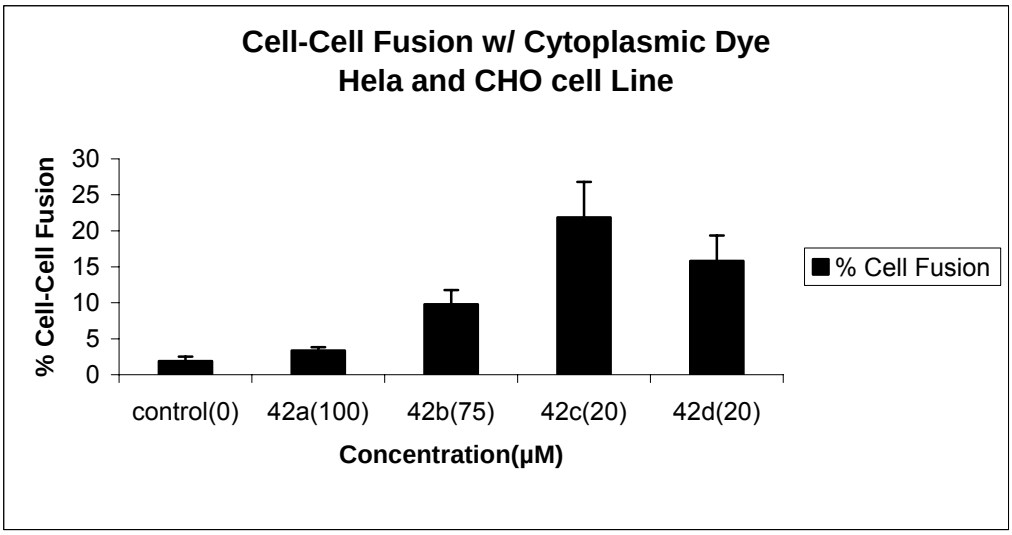

Figure 4.19 A plot of cell fusion data of Hela and CHO cell line using cytoplasmic dye.

4.3.4. Conclusion

A series of boronic acids were synthesized as potential fusogens for medicinal purposes such as drug delivery, immunotherapy, hybridoma technology, and among other possibilities. All compounds exhibited fusogenic activities between the CHO, a mammalian ovarian cell line and Hela, a human cervical cancer cell line. Among them compound **42c** has a greatest potential in aiding in induction of cell-cell fusion.

Next endeavors in this project will be geared toward actually implementing boronic acid derivatives in immunotherapeutic applications. In addition, to increase our knowledge in the mechanism at which the PBA derivatives induces cell fusion; the design of fluorescent boronic acid dyes are in route, which will be monitored by Time Lapse Video Microscopy.

5. Experimental Section.

5.1. Biology

5.1.1. Cell Culture

Cell lines were purchased from ATCC. HEPG2 and COS7 cells were maintained in RPMI with 10% FBS (fetal bovine serum), 1% L-glutamine, and 0.5% gentamicin sulfate (50mg/ml) (MediaTech). Hela, CHO, and Hey were cultured in DMEM/F12 media containing 5% FBS, 1% penicillin/streptomycin. Messa cell line was seeded in McCoy's media comprising of 10% FBS, 1% penicillin/streptomycin. All cells were maintained at 37 °C in a 5% CO_2 incubator. Remaining materials were purchased from Media-Tech unless otherwise noted.

5.1.2. Fluorescent Labeling Studies

HEPG2 and COS7 cells were harvest in six well plates in growth medium until ca. 50% confluency. Cells were then washed with PBS following fixation with 4% paraformaldehyde at 4 °C for 25 min or in 1:1 solution of MeOH/PBS for 25 min. After fixation the cells were washed with PBS twice. Next, 1 ml of 1:1 MeOH/PBS was placed in each well, followed by the desired concentration of anthracene boronic acid derivative (0.5-10 μM). The six well plates were placed at 4°C for 45 min. The cells were viewed with a blue emission filter.

5.1.3. Images

Phase contrast, DIC (Differential Interference Contrast), and fluorescence overlay images were taken with Carl Zeiss Axiovert 200M by the process imaging software Axiovision with the use of a blue long pass no filter (emission wavelength: 397 nm), green band pass

filter (emission wavelength: 515-565 nm) and two red filters (emission wavelength: 590 nm; band pass: 630/75 nm). All dyes used in experiments were purchased from Molecular Probes (Invitrogen).

5.1.4. Fusion Assays

Cells were grown in tissue culture dishes until 80% confluency, detached by trypsinization; then resuspended in appropriate growth media, and centrifuged for 10min at 1000rpm. The medium was then removed, and a portion of the resuspended cells were added to hemacytometer for cell counting. Negative control data were obtained by with the same assay protocol without added boronic acids. Polyethylene glycol (PEG) was used as a reference for interpretation of cell-cell fusion (Data not shown). Statistical analysis was performed by collecting 10 images randomly, in the magnification field using phase contrast, DIC, and fluorescent microscopy with cell compartmental staining. Cell-cell fusion index was calculated by the number of fused cells (F) divided by number of cells in magnification field (NF), [F/NF*100] for percentile. Syncytia index was determined by the number of nuclei per cell. Each experiment was done in triplicates. FACS was also used for validation of cytoplasm assay. In addition cell survival and cell cycle assays were determined using this method. Preparation of a FACS sample is as follows: to a 5 ml tube a suspension of ca. 1×10^6 cells in 500 µl FACS buffer was added to FACS tubes and analyzed with FACScan. Each boronic acid derivative was dissolved in 1 ml of DMSO to obtain concentrations between 5-11 mg/ml to be used as stock solutions.

5.1.5. Nuclear staining.

Method 1. 10 µl of boronic acid was added in 500 µl of appropriate medium. The homogeneous mixture was added to a suspension of 2M/ml of cells in centrifuge tube. This mixture was stirred for 2 min at 37 °C. Afterwards the volume was raised with medium to 5 ml and allowed to stir two additional min at 37 °C. Next, the tube was incubated for 5 min at 37°C and lastly centrifuged for 10 min at 1000 rpm. The supernatant was then removed and cells were seeded in 6 well plates 1M/well. The cells were viewed between 18-72 h. Revised Method 1. Five hundred µl of boronic acid in suitable growth medium (according to cell type) was added to a cell suspension of 0.5-1.0 $\times 10^6$ in 2 ml medium. The centrifuge tubes were then placed on a shaker at 37 °C for 15 min and then centrifuged for 10 min at 1000 rpm. The supernatant was then removed and cells were seeded in 6 well plates or Petri dishes. Cells were allowed to fuse up to 3 days. After cell-cell fusion process, cells were fixed with 3.7% formaldehyde for 30 min. After washings with PBS cells were stained with DAPI [4',6-diamidino-2-phenylindole] (Molecular Probes). Nucleus was viewed by fluorescence (blue pass filter) and DIC microscopy. To determine the amount of nuclei present per cell the fluorescent images were analyzed by Zeiss fluorescent particle counter software.

5.1.6. Cytoplasmic staining.

Prior to fusion, adherent cells were stained at concentration of 0.5-10 µM for 45minutes in medium containing FBS for 45 minutes at 37°C, using either 5-chloromethylfluorescein diacetate (CMFDA) or (5-(and-6)-(((4-chloromethyl) benzoyl)amino) tetramethylrhodamine (CMTMR) (Molecular Probes). After washing cells were further incubated at least 30 minutes at 37°C. Medium was removed and cells

were allowed to adjust overnight. A density of 0.5-2.0 × 10^6 M/ml 1:1 mixture (homo- or heterogeneous) cell types were suspended in 2 ml of suitable growth media in a centrifuge tube. A solution (500 µl) containing boronic acid was added to the suspension over a period of one minute with constant stirring with the tip of a pipet. Afterwards, the centrifuge tube was placed on a controlled temperature shaker for 15 min at 37 °C. The tube was then removed and centrifuged for 10 min at 1000 rpm (room temperature). The supernatant was removed and the pellet was then resuspended in 5-10% FBS and proper medium was added. After fusion process, a density of 1-5 × 10^5 M/ml of cells were seeded in duplicates in 6-well plates or 0.5-1 × 10^6 M/ml in petri dishes and then incubated for 1-3 days. Dual–labeled cytoplasm (color ranging from yellow to orange upon overlay of filters) was imaged by phase contrast and fluorescent (red and green pass filters) microscopy and/or analyzed by flow cytometry.

5.1.7. Plasma membrane staining (artificial lectin).

After fusion assay described above (with the exception of cytoplasmic dye), the cells were fixed with 1-4% formalin for 15 minutes at 37°C, followed by addition of alexafluoro-WGA (0.5-1µM) and Hoescht for nuclear staining (1-2µM) in PBS or HBSS for 10minutes at room temperature. The cells were washed with PBS twice and viewed with phase contrast and fluorescent (red and blue filters) microscopy.

5.1.8. DNA ploidy or cell cycle assay.

After cell fusion process described in section 5.1.6, cells were detached with 0.25% trypsin, then centrifuged. The supernatant was removed and then washed with PBS. After aspiration of PBS, 500 µl of 70% ethanol added dropwise. The cells were allowed

to incubate for 15 min on ice or at -20 °C overnight. The centrifuge tubes were then centrifuged and ethanol was removed. Then 1 ml of PI staining solution (10 ml of 0.1 Triton X-100/PBS, 0.40 ml of 500 µg/ml of PI (Propidium Iodide), and 2mg/ml of DNase-free RNase) were added to 1×10^6 cells, placed on ice for 30 min and then analyzed by FACS with a red filter.

5.1.9. Cell survival assay.

After cell fusion process, cells were trypsinized and then washed with cold PBS. The supernatant was then discarded. To a suspension of 1×10^6 cells in 1X annexin-binding buffer, 5 µl of alexa fluor 488 Annexin V and 1 µg/ml of 100 µg/ml of PI solution was added. The cells were incubated at room temperature for 15 min. After incubation period, 400 µl of additional 1X annexin-binding buffer was added. Cells were analyzed using a red and green filter with FACScan.

5.2. Chemistry

5.2.1. General

All ^1H and ^{13}C MHz were recorded at 400 MHz and 100 MHz, respectively, with tetramethylsilane as the internal reference. Elemental and mass spectral analyses were performed at Georgia State University Analytical Facilities. All commercial reagents were used without further purification unless otherwise noted. Acetonitrile (CH_3CN) and dichloromethane (CH_2Cl_2) were distilled from CaH_2. Tetrahyrofuran (THF) was distilled from Na and benzophenone.

5.2.2 Synthesis and Structural Analysis

Trans-Dispiro[oxirane-2,9'(10'H)-anthracene-10',2''-oxirane] (30).[76]

Compound **(29)** (1.0 g, 4.8 mmol) and sodium hydride (60% oil dispersion) (0.43g, 17.9 mmol) was added to a round bottom flask in 30 ml of anhydrous DMSO, followed by dropwised addition of trimethylsulfonyl iodide (2.2g, 10.8 mmol) in 30 ml of anhydrous DMSO. The reaction was allowed to stir at room temperature for two h under nitrogen. After completion the reaction was vacuum filtrated and then poured into 600 ml of ice water and allowed to stand for 20 min. The crystals were collected and then washed with water to obtain an isolated (0.97 g, 86% yield).

^{1}H NMR($CDCl_3$, 400 MHz) δ: 7.38-7.37 (m, 8H), 3.24 (s, 4H).

10-(Hydroxylmethyl)-9-anthraldehyde (31).[76]

Compound **30** (2.88 g, 12.2 mmo1) and lithium bromide (4.87 g, 56.0 mmol) was refluxed in 182 ml of dry acetonitrile in the dark at 70 °C for 16h. The reaction was then cooled and placed in a -40 °C dry ice-acetone bath. The resulting yellow crystals were collected by filtration and washed with water to give a (2.45 g, 85% yield).

^{1}H NMR($CDCl_3$, 400 MHz) δ: 11.54 (s, 1H), 8.93-8.91 (d, J = 8.4 Hz, 2H), 8.55-8.53 (d, J = 8 Hz, 2H), 7.71-7.64 (m, 4H), 5.75 (s, 2H).

(10-Methylaminomethyl-anthracen-9-yl)-methanol (32).

To a solution of compound **31** (1.57 g, 6.6 mmol) in MeOH (47 ml) and THF (74 ml) was added an aqueous solution of methylamine (40% wt, 34 ml). The mixture was then allowed to stir for 16 h and then sodium borohydride (1.27 g, 33.4 mmol) was added and allowed to stir an additional 2 h. The resulting mixture was evaporated. The residue was

then dissolved in (25 ml) of ethyl acetate and washed with 10% HCl (3 × 50 ml). The aqueous layer was cooled to 0 °C and was made basic with ammonium hydroxide. This was followed by washing (3 × 100ml) with ethyl acetate. The combined organic layers was washed with brine; then dried over magnesium sulfate, suction filtrated, and evaporated under vacuo to give a yellow solid in (1.17g, 71% yield).

^{1}H NMR($CDCl_3$, 400 MHz) δ: 8.39-8.36 (m, 2H), 8.27-8.26 (m, 2H), 7.51-7.46 (m, 4H), 5.56 (s, 2H), 4.57 (s, 2H), 2.58 (s, 3H).

(10-Methylaminomethyl-anthracen-9-ylmethyl)-methyl-carbamic acid *tert*-butyl ester (33).

Compound **32** (1.22g, 4.86 mmol) was dissolved in MeOH (55 ml), then di-*tert*-butyldicarbonate and triethylamine (11 ml) was added. The solution was allowed to stir for 12 h. The solution was then evaporated, after which 50 ml of dichloromethane (DCM) was added. The organic layer was separated and washed (3 × 20ml) with water, then 20 ml of brine. The resulting organic layer was then dried over magnesium sulfate, filtered and solvent was removed under reduced pressure. The residue was then purified by silica gel flash chromatography eluting with DCM/MeOH (95:5) to yield 1.21 g of a yellow solid (71% yield).

^{1}H NMR($CDCl_3$, 400 MHz) δ: 8.50-8.40 (m, 4H), 7.58-7.54 (m, 4H), 5.69 (s, 2H), 5.45 (s, 2H), 2.45 (s, 3H), 1.54 (s, 9H).

(10-Azidomethyl-anthracen-9-ylmethyl)-methyl-carbamic acid *tert*-butyl ester (34).

Triphenylphosphine (717 mg, 2.74 mmol), carbon tetrachloride (1 ml), and 2 ml of dry DMF was added to a round bottom flask followed by alcohol derivative **33** (300 mg, 0.856 mmol, in 3 ml of dry DMF). After disappearance of **33** as monitored by TLC,

sodium azide (208 mg, 3.16 mmol) was added. The reaction was allowed to stir at room temperature until completion as inidicated by TLC and GC-MS analysis. Ice water (10 ml) was added to reaction and the reaction mixture was stirred for 5 min. Then the reaction solution was diluted with ether (50 ml). The organic layer was washed (2 × 10ml) with water and brine, dried over anhydrous magnesium sulfate, and concentrated. The residue was purified by flash chromatography with ethyl acetate/hexanes (15:85) to produce a yellow oil, (277mg, 90% yield).

^{1}H NMR($CDCl_3$, 400 MHz) δ: 8.52-8.36 (m, 4H), 7.64-7.59 (m, 4H), 5.57 (s, 2H), 5.37 (s, 2H), 2.51 (s, 3H), 1.59 (s, 9H); ^{13}C-NMR ($CDCl_3$, 100 MHz): 155.8, 131.0, 130.4, 127.1, 126.5, 126.1, 126.0, 125.1, 124.3, 79.9, 46.5, 42.7, 31.8, 28.5; ESI MS: [M+(Na)] calculated 400.2, found 400.1.

(10-Aminomethyl-anthracen-9-ylmethyl)-methyl-carbamic acid *tert*-butyl ester (35).

Compound **34** (154 mg, 0.410 mmol) and triphenylphosphine (268 mg, 1.02 mmol) in aqueous THF (1:100) was stirred at rt for 16 h. The solution was then concentrated and purified by means of flash chromatography with CH_2Cl_2/MeOH (90:10) to give 122 mg of a yellow solid, 85% yield.

^{1}H NMR($CDCl_3$, 400MHz) δ: 8.45-8.38 (m, 4H), 7.57-7.52 (m, 4H), 5.50 (s, 2H), 4.83 (s, 2H), 2.47 (s, 3H), 1.55 (s, 9H); ^{13}C-NMR ($CDCl_3$): 155.8, 135.8, 131.2, 129.0, 128.5,125.8, 125.7, 125.1, 124.5, 79.7, 42.5, 38.4, 31.7, 28.5; MS(EI) calculated 350, found 350.

General procedure for preparation of Boc-protected diamides (36).

The di-acid (0.543 mmol, 1 equivalent), *N*-hydroxybenzotriazole (HOBt, 1.9 mmol, 1.47 mg), 1-(2-dimethylaminopropyl)-3-ethylcarbodiimide (EDCI, 1.07 mmol, 213 mg), and then compound **35** (1.14 mmol, 400 mg) was added to round bottom flask, followed by the addition of 30 ml of dry CH_2Cl_2. The solution was allowed to mix for 30 min at 0° C,

then triethylamine (TEA) was added to obtain a slight basic solution. Then the reaction temperature was slowly raised to room temperature and allowed to stir for 18 hr. The the reaction mixture was washed with 5% sodium bicarbonate (10 ml), 5% citric acid (10 ml), and brine (10 ml). The organic layer was dried over anhydrous magnesium sulfate, gravity filtered, and concentrated. The crude product was purified by flash chromatography with CH_2Cl_2/MeOH or precipitation from CH_2Cl_2/Hexanes.

[10-({[4-({10-[(*tert*-Butoxycarbonyl-methyl-amino)-methyl]-anthracen-9-ylmethyl}-methyl-carbamoyl)-benzoyl]-aminomethyl)-anthracen-9-ylmethyl]-methyl-carbamic acid *tert*-butyl ester (36a). 80% yield. ^{1}H NMR($CDCl_3$, 400 MHz) δ: 8.49-8.39 (m, 8H), 7.70-7.59 (m, 8H), 6.27 (s, 2H), 5.64 (s, 4H), 5.54 (s, 4H), 2.49 (s, 6H), 1.57 (s, 18H). MS data for di-amides were not useful for spectral analysis. The molecular ion was not present; MS (ESI+) [$-C_2H_4$] calculated 803.4, found 803.3.

[10-({[4-({10-[(*tert*-Butoxycarbonyl-methyl-amino)-methyl]-anthracen-9-ylmethyl}-methyl-carbamoyl)-pyridine-2-carbonyl]-aminomethyl)-anthracen-9-ylmethyl]-methyl-carbamic acid *tert*-butyl ester (36b). 60% yield. ^{1}H NMR($CDCl_3$, 400 MHz) δ: 8.68 (s, 1H), 8.42-8.40 (m, 2H), 8.35-8.31 (m,6H), 8.12 (s, 1H), 8.05 (s, 1H), 7.53-7.44 (m, 8H), 5.58 (d, J = 4.4 Hz, 2H), 5.45 (s, 4H), 5.31 (s, 2H), 2.42 (s, 3H), 2.36 (s, 6H), 1.51 (s, 18H). MS data for di-amides were not useful for spectral analysis. The molecular ion was not present; MS (ESI+) [$-C_2H_5$] calculated 803.3, found 803.1.

[10-({[4-({10-[(*tert*-Butoxycarbonyl-methyl-amino)-methyl]-anthracen-9-ylmethyl}-methyl-carbamoyl)-imidazole-4-carbonyl]-aminomethyl)-anthracen-9-ylmethyl]-methyl-carbamic acid *tert*-butyl ester (36c). 43% yield ^{1}H NMR($CDCl_3$, 300 MHz) δ: 8.37-8.31 (m, 8H), 7.59 (s, 1H), 7.57-7.55 (m, 8H), 5.96 (s, 2H), 5.38 (s, 2H), 2.43 (s, 6H), 1.52 (s, 18H). MS data for di-amides were not useful for spectral analysis. The molecular ion was not present.

[10-({[4-({10-[(*tert*-Butoxycarbonyl-methyl-amino)-methyl]-anthracen-9-ylmethyl}-methyl-carbamoyl)-pyrazine-2-carbonyl]-aminomethyl)-anthracen-9-ylmethyl]-methyl-carbamic acid *tert*-butyl ester (36d). 50% yield ^{1}H NMR($CDCl_3$, 400 MHz) δ: 9.22-9.20 (m, 1H), 8.51-8.40 (m, 8H), 8.05-8.04 (m, 1H), 7.2-7.56 (m, 8H), 5.67 (s, 4H), 5.54 (s, 4H), 2.52 (s, 6H), 1.66 (s, 18H). MS data for di-amides were not useful for spectral analysis. The molecular ion was not present; MS (ESI+) [$-C_2H_6$] calculated 803.4, found 803.4.

General procedure for preparation of the symmetrical diboronic acids (37).

Deprotection of the amine moiety of diamide **35** was accomplished by dissolving it in dry CH_2Cl_2 (15 ml) followed by trifluoroacetic acid addition and stirring at room temperature 15 min. After removal of Boc-protected group, the residue was concentrated and dried in vacuo for 3 hr. The reaction mixture was then subsequently placed in a round bottom flask. Then dry acetonitrile (35 ml), potassium carbonate (2.2 mmol, 305 mg), catalytic amount of potassium iodide, and compound **38** (0.88 mmol, 251 mg) were added to the same flask. The reaction mixture was allowed to stir for 18h. The insoluble materials were filtered, and the filtrate was evaporated under vacuo. The resulting residue was dissolved in CH_2Cl_2, 20 ml of 10% sodium bicarbonate, and 8 ml of water for the removal of protecting group of the boronate motif. The mixture was stirred for 4h. The organic phase was washed with brine and dried over anhydrous magnesium sulfate. The solvent was removed under reduced pressure. The crude material was precipitated from THF/Hexanes.

Diboronic acid (37a). 28% yield. ^{1}H NMR(CD_3OD, 400MHz) δ: 8.43-8.41 (m, 4H), 8.23-8.21 (m, 4H), 7.72-7.71 (m, 4H), 7.62-7.56 (m, 8H), 7.38-7.31 (m, 8H), 5.38 (s, 4H), 5.03 (s, 4H), 4.37 (s, 4H), 2.42 (s, 6H); HRMS(+H/D)[$-H_2O$] calculated 882.4124, found 882.4105.

Diboronic acid (37b). 25% yield. ^{1}H NMR(CD_3OD, 400 MHz) δ: 8.71-8.70 (m, 1H), 8.52-8.44 (m, 4H), 8.24-8.19 (m, 4H), (m, 1H), 7.69-7.66 (m, 2H), 7.57-7.51 (m, 9H), 7.37-7.32 (m, 4H), 7.29-7.26 (m, 2H), 5.59 (s, 1H), 5.54 (s, 1H), 5.49 (s, 2H), 5.00 (s, 4H), 4.31 (s, 4H), 2.38 (s, 6H); HRMS(+H)[$-H_2O$] calculated 882.3997, found 882.4001.

Diboronic acid (37c). 15% yield. ^{1}H NMR(CD_3OD, 400MHz) δ: 8.42-8.41 (m, 4H), 8.23-8.21 (m, 4H), 7.72-7.56 (m, 11H), 7.38-7.31 (m, 6H), 5.35 (s, 4H), 5.04 (s, 4H), 4.37 (s, 4H), 2.40 (s, 6H); MS ES(+) [$-3H_2O$] : 835.4

Diboronic acid (37d). 20% yield. ^{1}H NMR(CD_3OD, 400MHz) δ: 9.09 (s, 2H), 8.53-8.51 (m, 4H), 7.71-7.69 (m, 2H), 7.60-7.52 (m, 8H), 7.37-7.33 (m, 4H), 7.30-7.28 (m, 2H), 5.60 (s, 4H), 5.49 (s, 4H), 4.29 (s, 4H), 4.29 (s, 4H), 2.37 (s, 6H), HRMS(+H)[$-H_2O$] calculated 883.3951, found 883.3978.

General Procedures for synthesis of the boronic acid derivatives (42).

[4-Carboxy,2-nitro(phenyl boronic acid)] (40). Twelve ml of fuming nitric acid was added to a flask along with 13 ml of sulfuric acid. The solution was chilled to 0 °C, then **39** (2.01 g, 0.012 mol) was added in portions over 15 min. Then the mixture became yellow. After determining completion by thin layer chromatography, the solution was then poured over crushed ice. A white precipitate formed and was collected through vacuum filtration and dried under vacuum. The resulting crude solid was purified with flash chromatography eluting with CH_2Cl_2/MeOH (95:5) to give a (1.65 g, 65% yield).

[4-Acyl chloride,2-nitro(phenyl boronic acid)] (41). To a flask was added compound **40** (300 mg, 1.42 mmol), thionyl chloride in 6 ml, with and a drop of DMF. The reaction was refluxed for 48hr. Solvent was removed and the reaction mixture dried overnight to

remove remaining thionyl chloride. No isolation was performed; the crude product was used directly for the next step.

[4–Caboxyamide,2-nitro(phenyl boronic acid)] (42). To compound **41** (1 eq.), 7ml of dry tetrahydrofuran (THF) was added. The mixture was allowed to chill to 0 °C, then appropriate alkylamine was added dropwise (1.1eq.). Then the reaction was allowed to warm up to room temperature. The completion of reaction was monitored by thin layer chromatography. The solution was concentrated and the residue was purified by column chromatography with a dichloromethane/methanol (95:5) mixture. Each compound was oxidized with hydrogen peroxide in the presence of sodium hydroxide (pH ca. 9) for further verification of characterization and spectral analysis.

[4-(*N*-octyl)carboxamido,2-nitro(phenyl boronic acid)] (42a). 39% yield.

^{1}H NMR($CDCl_3$ with a drop of CD_3OD, 400 MHz) δ: 8.62 (s, 1H), 8.16-8.14 (dd, *J* = 7.6, 1.6 Hz, 1H), 7.57-7.55 (d, *J* = 7.6 Hz, 1H), 3.47-3.40 (m, 2H), 1.68-1.60 (m, 2H), 1.39-129(m, 10H), 0.90-0.86 (t, *J* = 6.8 Hz, 3H); ^{13}C NMR($CDCl_3$ with a drop of CD_3OD, 100 MHz) δ: 165.7, 150.5, 136.6, 132.8, 132.0, 121.4, 40.5, 31.7, 29.4, 29.2, 27.0, 22.5, 13.8; MS (ESI-) calculated 321.16, found 321.53.

[4-(*N*-octyl)carboxamido,2-nitrophenol] (42aa). ^{1}H NMR ($CDCl_3$, 400 MHz) δ: 8.51-8.50 (d, *J* = 2.0 Hz, 1H), 8.08-8.05 (dd, *J* = 8.8, 2.4 Hz, 1H), 7.24-7.22 (d, *J* = 8.8 Hz, 1H), 3.49-3.43 (m, 2H), 1.66-1.59 (m, 2H), 1.38-1.25 (m,10H), 0.90-0.86 (t, *J* = 6.8 Hz, 3H); MS (ESI-) calculated 293.15, found 293.17; Elemental analysis: calculated % C: 61.21, %H: 7.53, %N: 9.52, found %C: 61.50, %H: 7.92, %N: 9.06.

[4-(*N*-dodecyl)carboxamido,2-nitro(phenyl boronic acid)] (42b). 33% yield. ^{1}H NMR ($CDCl_3$ with a drop of CD_3OD, 400MHz) δ: 8.62 (s, 1H), 8.16-8.14 (dd, *J* = 7.6, 1.6 Hz, 1H), 7.57-7.55 (d, *J* = 7.6 Hz, 1H), 3.47-3.40 (m, 2H), 1.68-1.60 (m, 2H), 1.39-1.29 (m, 18H), 0.90-0.86 (t, *J* = 6.8 Hz, 3H); ^{13}C NMR ($CDCl_3$ with a drop of CD_3OD, 100 MHz) δ: 165.4, 150.4, 136.5, 132.7, 132.0, 121.2, 40.3, 31.8, 29.5, 29.2, 26.9, 22.5, 13.8; MS (ESI-) calculated 377.22, found 377.04.

[4-(*N*-dodecyl)carboxamido,2-nitrophenol] (42bb). ^{1}H NMR ($CDCl_3$, 400MHz) δ: 8.59-8.58(d, *J* = 2.0 Hz, 1H), 8.10-8.07 (dd, *J* = 8.8, 2.0 Hz, 1H), 7.23-7.21 (d, *J* = 8.8 Hz, 1H), 3.44-3.39 (m, 2H), 1.64-1.58 (m, 2H), 1.34-1.26 (m, 18H), 0.90-0.86 (t, *J* = 6.8 Hz, 3H); No of protons does not match the structure!!(28 protons correct) MS (ESI-) calculated 349.21, found 349.23; Elemental analysis: calculated %C: 65.12, %H: 8.63, %N: 7.99, found %C: 65.14, %H: 9.04, %N: 7.33.

[4-(*N*-hexadecyl)carboxamido,2-nitro(phenyl boronic acid)] (42c). 28% yield. ^{1}H NMR($CDCl_3$,dropCD_3OD, 400 MHz) δ: 8.50 (s, 1H), 8.08-8.06 (dd, *J* = 7.6, 1.6 Hz, 1H), 7.57-7.55 (d, *J* = 7.6 Hz 1H), 3.47-3.40 (m, 2H), 1.68-1.60 (m, 2H), 1.39-129 (m, 26H), 0.90-0.86 (t, *J* = 6.8 Hz, 3H); ^{13}C NMR ($CDCl_3$ with a drop of CD_3OD, 100 MHz) δ: 165.4, 150.3, 136.5, 132.7, 132.0, 121.2, 40.3, 31.8, 29.4, 29.2, 27.0, 22.5, 13.8; HRMS (-H) calculated 433.2874, found 433.2889.

[4-(*N*-hexadecyl)carboxamido,2-nitrophenol] (42cc). ^{1}H NMR ($CDCl_3$, 400 MHz) δ: 8.60-8.59 (d, *J* = 2.0 Hz, 1H), 8.10-8.07 (dd, *J* = 8.8, 2.0 Hz, 1H), 7.23-7.21 (d, *J* = 8.8 Hz, 1H), 3.43-3.38 (m, 2H), 1.64-1.60 (m, 2H), 1.34-1.26 (m, 26H), 0.90-0.86 (t, *J* = 6.8 Hz, 3H); MS (ESI-) calculated 405.27, found 405.29; Elemental analysis: calculated %C: 67.95, %H: 9.42, %N: 6.89, found %C: 66.92, %H: 9.67, %N: 5.94.

[4-(*N*-octadecyl)carboxamido,2-nitro(phenyl boronic acid)] (42d). 29% yield. ^{1}H NMR (DMSO, 400 MHz) δ: 8.78 (s, 1H), 8.58 (s, 1H), 8.30 (s, 2H), 8.20-8.18 (d, *J* = 7.6 Hz, 1H) 7.66-7.64 (d, *J* = 7.6 Hz, 1H), 3.18-3.17 (m, 2H), 1.54 (m, 2H), 1.24 (m, 30H), 0.86-0.84 (m, 3H); ^{13}C NMR (DMSO, 100 MHz) δ: 164.00, 150.11, 138.19, 135.72, 132.54, 121.22, 39.10, 31.29, 29.03, 28.92, 26.49, 22.09, 13.93; MS (ESI-) calculated 461.32, found 461.85.

[4-(*N*-octadecyl)carboxamido,2-nitrophenol] (42dd). ^{1}H NMR (DMSO, 400 MHz) δ: 8.29-8.28 (d, *J* = 2.8 Hz, 1H), 7.47-7.44 (dd, *J* = 9.2, 2.4 Hz, 1H), 6.30-6.28 (d, *J* = 9.2 Hz, 1H), 3.17-3.13 (m, 2H), 1.47-1.45 (m, 2H), 1.23 (m, 30H), 0.87-0.83 (t, *J* = 6.8 Hz, 3H); MSI (ES-) calculated 433.30, found 433.10.

6. Closing Remarks and Future Directions

6.1. Fluorescent Probes for Cell Surface Carbohydrates

Carbohydrates serve as a source of energy and provide structural framework for RNA and DNA, among others. A particular property of carbohydrates is its involvement in cell-cell adhesion interactions, as it has been correlated with metastatic behavior of various cancer types.[3, 5, 6] Several oligosaccharides such as sLea, sLex, Lex, and Ley have been identified as cell identification biomarkers in the development and progression of such cancers, thus making these carbohydrates an attractive target for sensor design.

The essential components of a sensor are: 1) molecular recognition; 2) functional group interactions; 3) selectivity toward target molecule, and 4) signal output. Boronic acids have been employed as drug transporters,[110] intermediates in Suzuki cross-coupling reaction,[111] enzyme inhibitors,[112] and many others. One of the most interesting properties of boronic acid is its ability to covalently react with 1,2 or 1,3 cis diols to form five or six membered cyclic esters in aqueous media.[14] This unique attribute makes boronic acid ideal receptor for the molecular recognition of biological carbohydrates.

Sialyl Lewis X has been chosen as the initial target due to implications in the development of liver and colon cancer.[5, 6] Secondly, fluorescence has been chosen as the signal output, as it provides high sensitivity, and requires very little sample. The approach in designing a fluorescent probe for sLex is to develop a system in which there is an off and on state of detection (Figure 6.1).

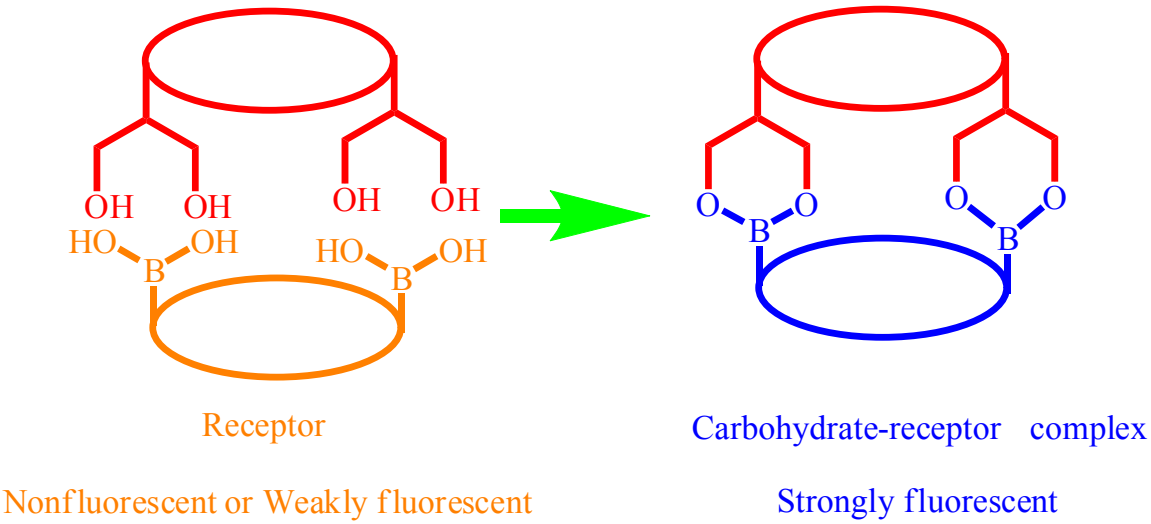

Figure 6.1 The approach of the design of a fluorescent receptor for sLex**.**

The fluorescent anthracene-boronic acid system was chosen as the initial design. This system was first introduced in 1992 by the Czarnik group, [35] and was later used by Shinkai to incorporate a 1,5 relationship between an amine and boron to create more electron density around the boron center. In doing so, they developed monoboronic acid **16**, which is intrinsically selective for fructose, and a diboronic derivative also selective for glucose.[22] In this system the amine regulates the fluorescence intensity. The anthracene moiety is quenched by an excited state photoinduced electron transfer, whish is considered to be the 'off' state of the sensor. Upon addition of a diol, the fluorescence intensity increases, which represent the 'on' state of the sensor. There are two proposed mechanism in literature that have been introduced as the mechanism which stops the queching process of the anthracene motif.[22, 36] Shinkai and co-workers proposed that there is a B-N bond formation which stops the quenching process. Upon addition of a diol, leading to the formation of a boronic ester; the pK_a of the boron species decrease. This causes the amine to

react with the boron, forming a B-N bond, stopping the quenching process. Later, the Wang group published a paper with detailed experimentations providing

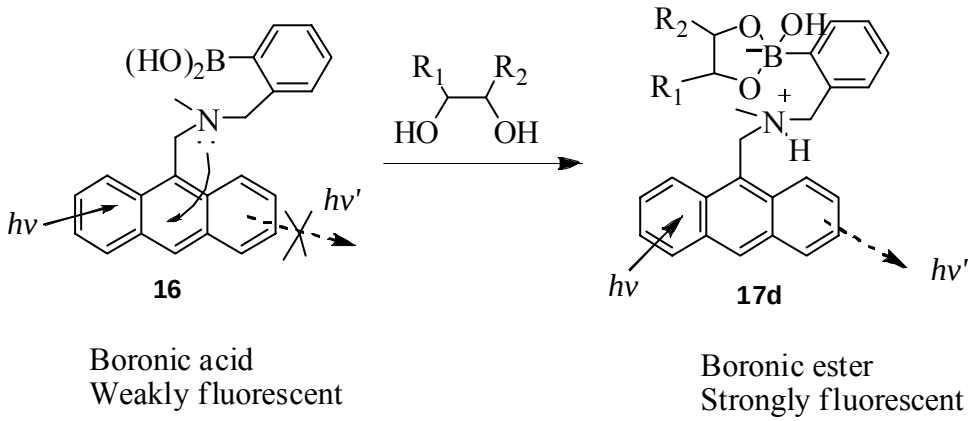

Figure 6.2 Signaling unit for anthracene based photoinduced electron transfer (PET) system.

additional insight as to the mechanism in which the quenching process is eliminated in aqueous medium. They proposed the mechanism is stopped through a hydrolysis mechanism. The B-N bond is labile, as a result it is hydrolyzed. The amine is then protonated, stopping the quenching process. There has been much success with this system, and the Wang group has used this system to develop the first fluorescent probe for sLex in hepatocellular carcinoma cell line.[104] This bis-anthracene-boronic acid compound has begun the quest of the future design for fluorescent probes for cell surface carbohydrates, and was used as the lead compound for the initial design of this project. The di-carboxylic acid motif of this system, **28** was slightly changed to increase hydrophilicity, as this is the major intermolecular interaction with the natural ligand.[78] Three ring substitutions with heteroatom(s) were introduced within the di-carboxylic acid unit; an imidazole, pyridine, and a pyrazine ring. The imidazole added a ring contraction

effect. The tertiary amine attached to the di-carboxylic acid unit was changed to a secondary amine. These changes were made in hopes to increase selectivity toward sLex. Compound **28** labeled HEPG2 cell line at a concentration of 1 μM. The protocols were mimicked. The HEPG2 cell line expressing sLex and COS7 non-expressing cell line were adapted. The cell lines were stained with the different di-anthraceneboronic acid **(28)** analogs between concentrations of 0.5-10 μM. The results were analyzed using fluorescent microscopy with the use of a blue filter.

Compound **37c** labeled the HEPG2 cell line selectively at a concentration as low as 0.5 μM. It is possible that the observed effect with **37c** was due to the ring contraction and additional hydrogen bonding capability. This type of intermolecular interaction is associated with the natural lectin ligand for sLex.[78]

In conclusion, there is an obvious need for a recognition moiety as a diagnostic tool to monitor the presence of sialyl Lewis X as it is associated with the progression and the metastatic behavior of certain cancer and tumor cell types. With the appropriate boronic acid scaffold to detect this oligosaccharide one could begin to design selectin inhibitors to block the abnormalities that occur in this particular pathway, possibly aiding in the therapeutic realm of autoimmune diseases and cancer. In addition, it could be used as a diagnostic tool to pursue the effector mechanisms that govern this pathogenesis of cancer and autoinflammatory diseases. With that said, additional exploratory computational and/or molecular modeling design could aid in the discovery of a boronic acid with the appropriate scaffold to serve as lectin mimics or a diagnostic tool to monitor the progression of various cancers, among other possibilities.

6.2. Phenylboronic Acid as Fusogens

Cell-cell fusion is a process in which two or more different types of cells are fused to produce one cell with a common cytoplasm and a single continuous plasma membrane (Figure 6.3). Cell-cell fusion has been employed as a technique used in traditional

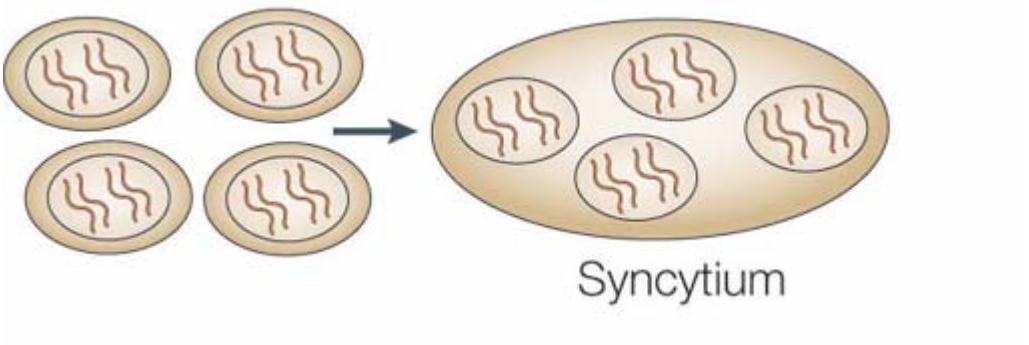

Figure 6.3 Cell-cell fusion process.[113]

hybridoma technology to obtain specific monoclonal antibodies to be used as therapeutic agents for cancer, autoimmune diseases and infections, among others.[82] In addition, the new "wave" vaccine therapy has shown promising results with minor side effects.[98] As of now, cell-cell fusion is accomplished by 'nature' spontaneously and by, viruses, PEG, or electrofusion. Due to boronic acid ability to recognize and covalently react with 1,2 and 1,3 cis diols, makes it ideal for tethering two cells together to induce the cascade of events required for cell-cell fusion. With that in mind, four [4–caboxyamide,2-nitro(phenyl boronic acid)] derivatives were synthesized to test the fusogenicity with the use of human cancer cells. The hypothesis is that the boronic acid will serve as a receptor for a carbohydrate substituent on one cell and the fatty aliphatic side chain will migrate in the bilayer of the adjacent cell merging the cells together. Cancer cells

spontaneously fuse together, and to validate the hypothesis, boronic acid derivatives were added as fusogens to induce cell-cell fusion above basal activity in human cancer cell lines.

Several cell lines were tested as possible cell based assays. The final selection chosen were, Hela (cervical cancer), Messa (uterine sarcoma), and CHO (Chinese hamster ovarian cell line). The approach began with fusing cells of the same type together. Immuno-fluorescence microscopy was used to give indication of cell-cell fusion. The first assay began with, dyeing the nuclei directly after the cell-cell fusion process with DAPI. This procedure was viewed with a blue filter, followed by analysis using a cell counting software. It was hard to establish cell-cell fusion events from cell-cell adhesion using this protocol alone. Next, an artificial lectin tagged with a red dye was used for plasma membrane labeling, along with a dye to stain the nucleus, Hoescht. This dye combination system helped to eliminate confusion between cell-cell fusion and cell-cell adhesion. The boronic acid derivatives, using this protocol in Hela and CHO cell lines did not increase fusion beyond basal activity. However, in the Messa cell line, **37d** increased over 2-folds above basal activity. This was further validated using a dual cytoplasmic dye staining protocol. One half of the cells were stained with a red dye and the other half with a green dye. If cell-cell fusion occurred, a yellow to orange color would appear; which could be viewed by fluorescence microscopy or FACS analysis. Results from FACS analysis contradicted with the results obtained through plasma membrane staining. A further experiment was conducted to determine the DNA content using PI. This experiment did not display any tetraploid peaks, meaning double the amount of chromosomal content in normal somatic cells. With the analysis combined,

the fusion of the same cell type was abandoned. The project was geared toward fusion between two cells from different species.

Hela (cervical cancer) and CHO (Chinese hamster ovarian) cell lines were chosen as the cell based assay. Each line was subjected to the fusion process, and cell survival assays were conducted to gain a reference point of the toxicity concentration limit of each phenylboronic acid derivative. The concentrations were reduced if cell death occurred above 5%. Next, Hela and CHO cell lines were labeled with red or green dye and fused together for 3 days; then analyzed by FACS analysis. The results show compounds **37b**, **37c**, and **37d** increased up to 10-folds above basal activity, with compound **37c** showing the greatest potential of fusogenic properties.

Next endeavors in this project will be geared toward actually implementing boronic acid derivatives in immunotherapeutic applications. In addition, to increase our knowledge in the mechanism at which the PBA derivatives induces cell fusion; the design of fluorescent boronic acid dyes are in route, which will be monitored by Time Lapse Video Microscopy.

7. References

1. Fukuda, M., Cell surface carbohydrates and cell development. *Ed.; CRC: Boca Raton* **1992**, pp.127-161.

2. Fukuda, M.; Hindsgaul, O., *Molecular Glycobiology; Oxford University Press: New York* **1994**.

3. Idikio, H. A., Sialyl-lewis-X, Gleason grade and stage in non-metastatic human prostate cancer. *Glycoconjugate J.* **1997,** 14, 875-877.

4. Jørgensen, T.; Berner, A.; Kaalhus, O.; Tveter, K. J.; Danielsen, H. E.; Bryne, M., Up-regulation of the oligosaccharide sialyl lewis^X: a new prognostic parameter in metastatic prostate cancer. *Cancer Res.* **1995,** 55, 1817-1819.

5. Fujiwara, Y.; Shimada, M.; Takenaka, K.; Kajiyama, K.; Shirabi, K.; Sugimachi, K., The sialyl Lewis X expression in potential predictor for the emergence of hepatocarcinogenesis: hepatocellular carcinoma. *Heoatogastroenterology* **2002,** 49, 213-217.

6. Weston, B. W.; Hiller, K. M.; Mayben, J. P.; Manousos, G. A.; Bendt, K. M.; Liu, R.; Cusack, J. C., Jr., Expression of human α(1,3) fucosyltransferase antisense sequences inhibits selectin-mediated adhesion and liver metastasis of colon carcinoma cells. *Cancer Res.* **1999,** 59, 2127-2135.

7. Eggert, H.; Frederiksen, J.; Morin, C.; Norrild, J. C., A new glucose-selective fluorescent bisboronic Acid. first report of strong α-furanose complexation in aqueous solution at physiological pH. *J. Org. Chem.* **1999,** 64, 3846-3852.

8. Gao, X.; Zhang, Y.; Wang, B., Naphthalene-based water-soluble fluorescent boronic acid isomers suitable for ratiometric and off-on sensing of saccharides at physiological pH. *New J. Chem.* **2005,** 29, 579-586.

9. James, T. D.; Shinmori, H.; Shinkai, S., Novel fluorescence sensor for 'small' saccharides. *Chem. Commun.* **1997**, 71-72.

10. Yang, W.; Yan, J.; Springsteen, G.; Deeter, S.; Wang, B., A novel type of fluorescent boronic acid that shows large fluorescence intenisty changes upon binding with a carbohydrate in aqueous solution at physiological pH. *Bioorg. Med. Chem. Lett.* **2003,** 13, 1019-1022.

11. Zhao, J.; Davidson, M. G.; Mahon, M. F.; Kociok-Köhn, G.; James, T. D., An enantioselective fluorescent sensor for sugar acids. *J. Am. Chem. Soc.* **2004,** 126, 16179-16186.

12. Pizer, R.; Tihal, C., Equilibria and reaction mechanism of the complexion of methylboronic acid with polyols. *Inorg. Chem.* **1992,** 31, 3243-3247.

13. Pizer, R.; Babcock, L., Mechanism of complexion of boronic acids with catechol and substituted catechols. *Inorg. Chem.* **1977,** 16, 1677-1681.

14. Lorand, J. P.; Edwards, J. O., Polyol complexes and structure of the benzeneboronate ion. *J. Org. Chem.* **1959,** 24, 769-774.

15. Vandenberg, R.; Peters, J. A.; Vanbekkum, H., The structure and (local) stability-constants of borate esters of monosaccharides and disasaccharides as studied by B-11 and C-13 NMR spectroscopy. *Carbohydr. Res.* **1994,** 253, 1-12.

16. Vanduin, M.; Peters, J. A.; Kieboom, A. P. G.; Vanbekkum, H., The pH-dependence of the stability of esters of boric acid and borate in aqueous-medium as studied by B-11 NMR. *Tetrahedron* **1984,** 40, 2901-2911.

17. Zhu, L.; Shagufta, S.; Gray, M.; Lynch, V.; Sorey, S.; Anslyn, E. V., A structural investigation of the B-N interaction in an o-(*N*,*N*-diakylaminomethyl)arylboronate system. *J. Am. Chem. Soc.* **2006,** 128, 1222-1232.

18. James, T. D.; Shinkai, S., Artificial receptors as chemosensors for carbohydrates. *Topics Curr. Chem.* **2002,** 218, 160-197.

19. Fang, H.; Kaur, G.; Wang, B., Progress in boronic acid-based fluorescent glucose sensors. *J. Fluorescence* **2004,** 14, (5), 481-489.

20. Springsteen, G.; Wang, B., A detailed examination of boronic acid-diol complexation. *Tetrahedron* **2002,** 58, (26), 5291-5300.

21. Yan, J.; Springsteen, G.; Deeter, S.; Wang, B., The relationship among pKa, pH, and binding constants in the interactions between boronic acids and diols-it is not as simple as it appears. *Tetrahedron* **2004,** 60, 11205-11209.

22. Ni, W.; Kaur, G.; Springsteen, G.; Wang, B.; Franzen, S., Regulating the fluorescence intensity of an anthracene boronic acid system: B-N bond or a hydrolysis mechanism? *Bioorg. Med. Chem. Lett.* **2004,** 32, 571-581.

23. Franzen, S.; Ni, W.; Wang, B., Study of the mechanism of electron-transfer quenching by boron-nitrogen adducts in fluorescent sensors. *J. Phys. Chem. B* **2003,** 107, 12942-12948.

24. Singhal, R. P.; Ramamurthy, B.; Govindraj, N., New ligand for boronate affinity-chromatography-synthesis and properties. *J. Chromatogr.,A* **1991,** 687, 61-69.

25. Van Diun, M.; Peters, J. A.; Kieboom, A. P. G.; Van Bekkum, H., Studies on borate esters 1: The pH dependence of the stability of esters of boric acid and borate in aqueous medium as studied by ^{11}B NMR. *Tetrahedron* **1984,** 40, 2901-2911.

26. Biot, M., *Compt. rend.* **1841,** 14.

27. Szebelladj, L.; Tomay, S. Z., Beitrage Zum Nachweis der Borsaure Mit Alizarin. *Z Anal. Chem.* **1936,** 107, 26-30.

28. Rama, M. J. R.; Medina, A. R.; Diaz, A. M., A flow injection renewable surface sensor for the fluorimetric determination of vanadium(V) with Alizarin Red S. *Talanta* **2005,** 66, 1333-1339.

29. Jansen, J. H.; Jahr, H.; Verhaar, J. A. N.; Pols, H. A. P.; Chiba, H.; Weinans, H.; Leeuwen, J. P. T. M. v., Stretch-induced modulation of matrix metalloproteinases in mineralizing osteoblasts via extracellular signal-regulated kinase-1/2. *J. Orthopaedic Res.* **2006,** 24, 1480-1488.

30. Palit, D.; Pal, H.; Mukherjee, T.; Mittal, J., Photodynamics of the S, state of some hydoxy- and amino-substituted naphthoquinones and anthraquinones. *J. Chem. Soc., Faraday Trans.* **1990,** 86, 3861-3869.

31. Springsteen, G.; Wang, B., Alizarin Red S. as a general optical reporter for studying the binding of boronic acids with carbohydrates. *Chem. Commun.* **2001**, 1608-1609.

32. Yan, J.; Fang, H.; Wang, B., Boronolectins and fluorescent boronolectins: an examination of the detailed chemistry issues important for the design. *Med. Res. Rev.* **2005,** 25, 490-520.

33. Pickup, J. C.; Hussain, F.; Evans, N. D.; Rolinski, O. J.; Birch, D. J. S., Fluorescence-based glucose sensors. *Biosen. and Bioelectron.* **2005,** 20, 2555-2565.

34. Cao, H.; Heagy, M., Fluorescent chemosensors for carbohydrates: a decade's worth of bright spies for saccharides in review. *J. Fluorescence.* **2004,** 14, (5), 569-584

35. Yoon, J.; Czarnik, A. W., Fluorescent chemosensors of carbohydrates. a means of chemically communicating the binding of polyols in water based on chelation-enhanced quenching. *J. Am. Chem. Soc.* **1992,** 114, 5874-575.

36. James, T. D.; Sandanayake, K. R. A. S.; Iguchi, R.; Shinkai, S., Novel saccharide-photoinduced electron transfer sensors based on the interaction of boronic acid amine. *J. Am. Chem. Soc.* **1995,** 117, 8982-8987.

37. Wulff, G.; Heide, B.; Helfmeier, G., Molecular recognition through the exact placement of functional groups on rigid matrices via a template approach. *J. Am. Chem. Soc.* **1986,** 108, 1089-1091.

38. Wang, Z.; Zhang, D.; Zhu, D., A new saccharide sensor based on a tetrathiafulvalene-anthracene dyad with a boronic acid. *J. Org. Chem.* **2005,** 70, 5729-5732.

39. Yang, W.; Fan, H.; Gao, X.; Gao, S.; Karnati, V. V. R.; Ni, W.; Hooks, B.; Carson, J.; Weston, B.; Wang, B., The first fluorescent diboronic acid sensor specific for hepatocellular carcinoma cells expressing sialyl lewis X. *Chem. & Bio.* **2004,** 11, 439-448.

40. Karnati, V. V.; Gao, X.; Gao, S.; Yang, W.; Ni, W.; Sankar, S.; Wang, B., A glucose-selective fluorescence sensor based on boronic acid-diol recognition. *Bioorg. & Med. Chem. Lett.* **2002,** 12, 3373-3377.

41. Wiskur, S. L.; Lavigne, J. J.; Ait-Haddou, H.; Lynch, V.; Chiu, Y. H.; Canary, J. W.; Anslyn, E. V., pKa Values and Geometries of Secondary and Tertiary Amines Complexed to Boronic Acids-Implications for Sensor Design. *Org. Lett.* **2001,** 3, 1311-1314.

42. Norrild, J. C., An illusive chiral aminoalkylferroceneboronic acid. Structural assignment of a 1:1 sorbitol and new insight into boronate-polyol interactions. *J. Chem. Soc. Perkin Trans 2* **2001,** 2, 719-726.

43. Wang, J.; Jin, S.; Lin, N.; Wang, B., Fluorescent indolylboronic acids that are useful reporters for the synthesis of boronolectins. *Chem. Biol. Drug Des.* **2006,** 67, (2), 137-44.

44. Sun, X. Y.; Liu, B., The fluorescence sensor for saccharide based on internal conversion. *Luminescence* **2005,** 20, (4-5), 331-3.

45. Yang, W.; Yan, J.; Springsteen, G.; Deeter, S.; Wang, B., A novel type of fluorescent boronic acid that shows large fluorescence intensity changes upon binding with a carbohydrate in aqueous solution at physiological pH. *Bioorg Med Chem Lett* **2003,** 13, (6), 1019-22.

46. DiCesare, N.; Lakowicz, J. R., Charge transfer fluorescent probes using boronic acids for monosaccharide signaling. *J. Biomed. Opt.* **2002,** 7, (4), 538-45.

47. Arimori, S.; Bell, M. L.; Oh, C. S.; James, T. D., A modular fluorescence intramolecular energy transfer saccharide sensor. *Org. Lett.* **2002,** 4, 4249-4251.

48. Cao, H.; McGill, T.; Heagy, M. D., Substituents effect on monoboronic acid sensors for saccaharides based on *N*-phenyl-1,8-naphthalenecarboximide. *J. Org. Chem.* **2004,** 69, 2959-2966.

49. Brownlee, M.; Cerami, A., Glycosated insulin complexed to concanavalin A. Biochemical basis for a closed loop insulin delivery system. *Diabetes* **1983,** 32, 499-504.

50. Badugu, R.; Lakowicz, J. R.; Geddes, C. D., Boronic acid fluorescent sensors for monosaccharide signaling based on the 6-methoxyquinolinium heterocyclic nucleus: progress toward noninvasive and continuous glucose monitoring. *Bioorg. Med. Chem. Lett.* **2005,** 13, 113-119.

51. Shinmori, H.; Takeuchi, M.; Shinkai, S., Spectrscopic sugar sensing by a stilbene derivative with push (Me_2N-)- pull ((OH_2B-)-type substituents. *Tetrahedron* **1995,** 51, 1893-1902.

52. DiCesare, N.; Lakowicz, J. R., Spectral properties of fluorophores combining the boronic acid group with electron donor or withdrawing groups. implication in the development of fluorescence probes for saccharides. *J. Phys. Chem. A* **2001,** 105, 6834-6840.

53. Gao, X.; Zhang, Y.; Wang, B., New boronic acid fluorescent reporter compounds. 2. a naphthalene-based on-off sensor functional at physiological pH *Org. Lett.* **2003,** 5, 4615-4618.

54. Seppo, A.; Turunen, J. P.; Penttila, L.; Keane, A.; Renkonen, O.; Renkonen, R., Synthesis of a tetravalent sialyl Lewis x glycan, a high-affinity inhibitor of L-selectin-mediated lymphocyte binding to endothelium. *Glycobiology* **1996,** 6, (1), 65-71.

55. Kaji, M.; Ishikura, H.; Kishimoto, T.; Omi, M.; Ishizu, A.; Kimura, C.; Takahashi, T.; Kato, H.; Yoshiki, T., E-selectin expression induced by pancreas-

carcinoma-derived interleukin-1 alpha results in enhanced adhesion of pancreas-carcinoma cells to endothelial cells. *Int J Cancer* **1995,** 60, (5), 712-7.

56. Matsushita, Y.; Kitajima, S.-i.; Goto, M.; Tezuka, Y.; Sagara, M.; Imamura, H.; Tanabe, G.; Tanaka, S.; Aikou, T.; Sato, E., *Cancer Lett* **1998,** 133, 151-160.

57. Ley, K., The role of selectins in inflammation and disease. *Trends Mol Med* **2003,** 9, (6), 263-8.

58. Steinhauer, D. A.; Wharton, S. A.; Skehel, J. J.; Wiley, D. C., Studies of the Membrane Fusion Activities of Fusion Peptide Mutants of Influenza Virus Hemagglutinin. *Journal of Virology* **1995,** 69, 6643-6651.

59. Springer, T. A., Traffic signals for lymphocyte recirculation and leukocyte emigration: the multistep paradigm. *Cell* **1994,** 76, 301-314.

60. Vestweber, D.; Blanks, J. E., Mechanisms that regulate the function of the selectins and their ligands. *Physiol. Rev.* **2001,** 79, 181-213.

61. Alberts, B.; Johnson, A.; Lewis, J.; Raff, M.; Roberts, K.; Walter, P., *Molecular Biology of the Cell; Garland Science: New York* **2002**.

62. Dey, M. P.; Witczak, Z. J., Functionalized S-thio-di and S-oligosaccharide precursors as templates for novel $sle^{x/a}$ mimetic antimetastatic agents. *Mini Rev. Med. Chem.* **2003,** 3, 271-280.

63. Varki, A.; Varki, N. M., P-selectin, carcinoma metastasis and heparin: novel mechanistic connections with therapeutic implications. *Braz. J. Med. Biol. Res.* **2001,** 34, 711-717.

64. Kneuer, C.; Ehrhardt, C.; Radomski, M.; Bakowsky, U., Selectin - potential pharmacological targets? *Drug Discovery Today* **2006,** 11, 1034-1040.

65. Marshall, D.; Haskard, D. O., Clinical overview of leukocyte adhesion and migration: where are we now? *Semin. Immunol.* **2002,** 14, 133-140.

66. Weiser, M. R.; Gibbs, S. A.; Valeri, C. R.; Shepro, D.; Hechtman, H. B., Anti-selectin therapy modifies skeletal muscle ischemia and reperfusion injury. *Shock* **1996,** 5, (6), 402-7.

67. Whitcup, S. M.; Kozhich, A. T.; Lobanoff, M.; Wolitzky, B. A.; Chan, C. C., Blocking both E-selectin and P-selectin inhibits endotoxin-induced leukocyte infiltration into the eye. *Clin Immunol Immunopathol* **1997,** 83, (1), 45-52.

68. Theoret, J. F.; Chahrour, W.; Yacoub, D.; Merhi, Y., Recombinant P-selectin glycoprotein-ligand-1 delays thrombin-induced platelet aggregation: a new role for P-selectin in early aggregation. *Br J Pharmacol* **2006,** 148, (3), 299-305.

69. Wienrich, B. G.; Krahn, T.; Schon, M.; Rodriguez, M. L.; Kramer, B.; Busemann, M.; Boehncke, W. H.; Schon, M. P., Structure-function relation of efomycines, a family of small-molecule inhibitors of selectin functions. *J Invest Dermatol* **2006,** 126, (4), 882-9.

70. Proudfoot, A., Chemokine Receptors: Multifacted Therapeutic Targets. *Nat. Rev.* **2002,** 2, 106-115.

71. Ribeiro, S.; Horuk, R., The clinical potential of chemokine receptor antagonists. *Pharm. & Therap.* **2005,** 107, 44-58.

72. Mulder, W. J. M.; Strijkers, J. G.; Griffioen, A. W.; Bloois, L. v.; Storm, G.; Koning, G. A.; Nicolay, K., A liposomal system for contrast-enhanced magnetic resonance imaging of molecular targets. *Bioconjugate Chem.* **2004,** 15, 799-806.

73. Azarmi, S.; Huang, Y.; Chen, H.; McQuarne, S.; Abrams, D.; Roa, W.; Finlay, H.; Miller, G.; Löbenberg, R., Optimization of a two-step desolvation method for preparing gelation nanoparticles and cell uptake cancer cells. *J. Pharm. Pharmaceut. Sci.* **2006,** 9, 124-132.

74. Matsushita, Y.; Kitajima, S.-i.; Goto, M.; Tezuka, Y.; Sagara, M.; Imamura, H.; Tanabe, G.; Tanaka, S.; Aikou, T.; Sato, E., Selectins induced by interleukin-1ß on the human liver endothelial cells act as a ligands for sialyl Lewis X-expressing human colon cancer cell metastasis. *Cancer Lett* **1998,** 133, 151-160.

75. Wright, L. M.; Kreikemeier, J. T.; Fimmel, C. J., A concise review of serum markers for hepatocellular cancer. *Cancer Detect. Prev.* **2007,** 31, (1), 35-44.

76. Lin, Y.; Lang, S. A.; Seifert, C. M.; Child, R. G.; Morton, G. O.; Fabio, P. F., Aldehyde syntheses. Study of the preparation of 9,10-anthracenedicarboxaldehyde. *J. Org. Chem.* **1979,** 25, 4701-4705.

77. Kaur, G.; Fang, H.; Gao, X.; Li, H.; Wang, B., Substituent effect on anthracene-based bisboronic acid glucose sensors. *Tetrahedron* **2006,** 62, 2583-2589.

78. Chhabra, S. R.; Rahim, A. S. A.; Kellam, B., Recent progress in the design of selectin inhibitors. *Mini Rev. Med. Chem.* **2003,** 3, 679-687.

79. Horsley, V.; Pavlath, G., Forming a multinucleated cell: molecules that regulate myoblast fusion. *Cells Tissue Organs* **2004,** 176, 67-78.

80. Frank, H.-G.; Bose, P.; Albieri-Borges, A.; Borges, M.; Greindl, A.; Neulen, J.; Pötgens, A. J. G.; Kaufmann, P., Evaluation of fusogenic trophoblast surface epitopes as targets for immune contraception. *Contraception* **2005,** 71, 282-293.

81. Black, S.; Kadyrov, M.; Kaufmann, P.; Ugele, B.; Emans, N.; Huppertz, B., Syncytial fusion of human trophoblast depends on caspase 8. *Cell Death Differ.* **2004** 11, 90-98.

82. Brekke, O. H.; Sandlie, I., Therapeutic antibodies for human diseases at the dawn of the twenty-first century. *Nature Rev.* **2003,** 2, 52-61.

83. Davis, T.; Grillo-López, J.; White, C.; McLaughlin, P.; Czuczman, M.; Link, B.; Maloney, D.; Weaver, R.; Rosenberg, J.; Levy, R., Rituximab anti-CD20 monoclonal antibody therapy in non-Hodgkin's lymphoma: safety and efficacy of re-treatment. *J. Clin. Oncol.* **2000,** 18, 3135-3143.

84. Goldenberg, M., Trastuzumab, a recombinant DNA-derived humanized monoclonal antibody, a novel agent for the treatment of metastatic breast cancer *Clin. Therapeu.* **1999,** 21, 309-318.

85. Lindner, M.; Schirrmacher, V., Tumour cell-dendritic cell fusions for cancer immunotherapy: comparison of therapeutic efficiency polyethylen-glycol versus electro-fusion protocols. *Eur. J. Clin. Invest.* **2002,** 32, 207-217.

86. Kugler, A.; Walden, G. S.; Zoller, G.; Zobwalski, A.; Brossart, P.; Trefzer, U.; Ullrich, S.; Müller, C. A.; Becker, V.; Gross, A. J.; Hemmerlein, B.; Kanz, L.; Ringert, G. A. M. R.-H., Regression of human metastatic renal cell carcinoma after vaccination with tumor cell-dendritic cell hybrids. *Nature Med.* **2000,** 6, (3), 332-336.

87. Gong, J.; Koido, S.; Chen, D.; Kashiwaba, M.; Kufe, D., Induction of antitumor activity by immunization with fusions of dendritic and carcinoma cells. *Nature Med.* **1997,** 3, (5), 558-561.

88. Chen, E. H.; Olson, E. N., Unveiling the mechanisms of cell-cell fusion. *Science* **2005,** 308, 369-373.

89. Duelli, D.; Lazebnik, Y., Cell fusion: a hidden enemy? *Cancer Cell* **2003,** 3, 445-448.

90. Armstrong, D. G.; Newfield, J. T.; Gillespie, R., Orthopedic management of osteopetrosis: results of a survey and review of the literature. *J. Pediatr. Orthop.* **1999,** 19, 122-132.

91. Miller, F. R.; McInerney, D.; Rogers, C.; Miller, B. E., Spontaneous fusion between metastatic mammary tumor subpopulations. *J. Cellular Biochem.* **2004,** 36, 129-136.

92. Sakamoto, T.; Ushijima, H.; Okitsu, S.; Susuki, E.; Sakai, K.; Morikawa, S.; Müller, W., Establishment of an HIV cell-cell fusion assay by using two genetically modified HeLa cell lines and reporter gene. *J. Virol. Methods* **2003,** 114, 159-166.

93. Steinhauer, D.; Wharton, S.; Skehel, J.; Wiley, D., Studies of the membrane fusion activities of fusion peptide mutants of influenza virus hemaggutinin. *J. Virol.* **1995,** 1995, 6643-6651.

94. Mastrobattista, E.; Koning, G. A.; Storm, G., Immunoliposomes for the targeted delivery of antitumor drugs. *Adv. Drug Deliv. Rev.* **1999,** 40, 103-127.

95. Gao, X.; Zhang, Y.; Wang, B., A highly fluorescent water-soluble boronic acid reporter for saccharide sensing that shows ratiometric UV changes and significant fluorscence changes. *Tetrahedron* **2005,** 61, 9111-9117.

96. Davis, C.; Gallo, M.; Corvalan, J., Transgenic mice as a source of fully human antibodies for the treatment of cancer. *Cancer and Metastasis Rev.* **1999,** 18, 421-425.

97. Alberts, B.; Johnson, A.; Lewis, J.; Raff, M.; Roberts, K.; Walter, P., Molecular biology of the cell. *Garland Science: New York* **2002**.

98. Gong, J.; Koido, S.; Chen, D.; Tanaka, Y.; Huang, L.; Avigan, D.; Anderson, K.; Ohnio, T.; Kufe, D., Immunization against murine multiple with myeloma with fusions of dendritic and plasmacytoma cells is potentiated by interleukin 12. *Blood* **2002,** 99, (7), 2512-2517.

99. Terada, N.; Hamazaki, T.; Oka, M.; Hoki, M.; Mastalerz, D.; Nakano, Y.; Meyer, E.; Morel, L.; Petersen, B.; Scott, E., Bone marrow cells adopt the phenotype of other cells by spontaneous fusion. *Nature* **2002,** 416, 542-545.

100. Ying, Q.; Nichols, J.; Evans, E.; Smith, A., Changing potency by spontaneous fusion. *Nature* **2002,** 416, 545.

101. Keryer, G.; Alsat, E.; Taskén, K.; Evian-Brion, D., Cyclic AMP-dependent protein kinases and human trophoblast cell differentiation in vitro. *J. Cell Sci.* **1998,** 111, 995-1004.

102. Hui, S. W.; Kuhl, T. L.; Guo, Y. Q.; Israelachvili, J., Use of poly(ethylene glycol) to control cell aggregation and fusion. *Colloids and Surfaces B: Biointerfaces* **1999,** 14, 213-222.

103. Zheng, S.-L.; Reid, S.; Lin, N.; Wang, B., Microwave-assisted synthesis of ethynylarylboronates or the construction of boronic acid-based fluorescent sensors for carbohydates. *Tetrahedron Letters* **2006,** 47, 2331-2335.

104. Yang, W.; Gao, S.; Gao, X.; Karnati, V. V. R.; Ni, W.; Wang, B.; Hooks, W. B.; Carson, J.; Weston, B., Diboronic acids as fluorescent probes for cells expressing sialyl lewis X. *Bioorganic & Medicinal Chemistry Letters* **2002,** 12, 2175-2177.

105. Wang, W.; Gao, S.; Wang, B., Building fluorescent sensors by template polymerization: The preparation of a fluorescent sensor for D-fructose. *Org. Lett.* **1999,** 1, (8), 1209-1212.

106. Sugasaki, A.; Sugiyasu, K.; Ikeda, M.; Takeuchi, M.; Shinkai, S., First successful molecular design of an artificial lewis Ooigosaccharide binding System utilizing positive homotropic allosterism. *J. Am. Chem. Soc.* **2001,** 123, 10239-10244.

107. Borges, M.; Frank, H.; Kaufmann, P.; Pötgens, J., A two-colour fluorescence assay for the measurement of syncytial fusion between trophoblast-derived cell lines. *Placenta* **2003,** 24, 959-964.

108. Foster, T.; Alvarez, X.; Kousoulas, K., Plasma membrane topology of syncytial domains of Herpes Simplex Virus type 1 glycoprotein K (gK): the UL20 protein enables cell surface localization of gK but not gK-mediated cell-cell fusion. *J. Virol.* **2003,** 77, 499.

109. Hiddemann, W.; Schumann, J.; Andreeff, M.; Barlogie, B.; Herman, C.; Leif, C.; Mayall, H.; Murphy, F.; Sanberg, A., Convention on nomemclature for DNA cytometry. *Cytometry* **1984,** 5, 445-446.

110. Draffin, S. P.; Duggan, P. J.; Duggan, S. A. M., Highly fructose selective transport promoted by boronic acids based on a pentaerythritol. *Org. Lett.* **2001,** 3, 917-920.

111. Ahmed, Z.; Langer, P., Suzuki cross-coupling reactions of gamma-alkylidenebutenolides: application to the synthesis of vulpinic acid. *J Org Chem* **2004,** 69, (11), 3753-7.

112. Adams, J., Proteasome inhibition in cancer: development of PS-341. *Semin Oncol* **2001,** 28, (6), 613-9.

113. Bjerkvig, R.; Tysnes, B.; Aboody, K.; Najbauer, J.; Terzis, A. J., The origin of the cancer stem cells; current controversies and new insight. *Nature Rev.* **2005,** 5, 899-904.

8. Appendix

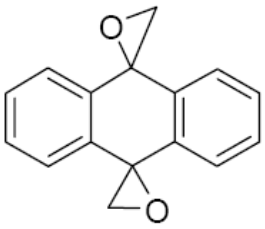

Trans-Dispiro[oxirane-2,9'(10'H)-anthracene-10',2''-oxirane] **(30).**

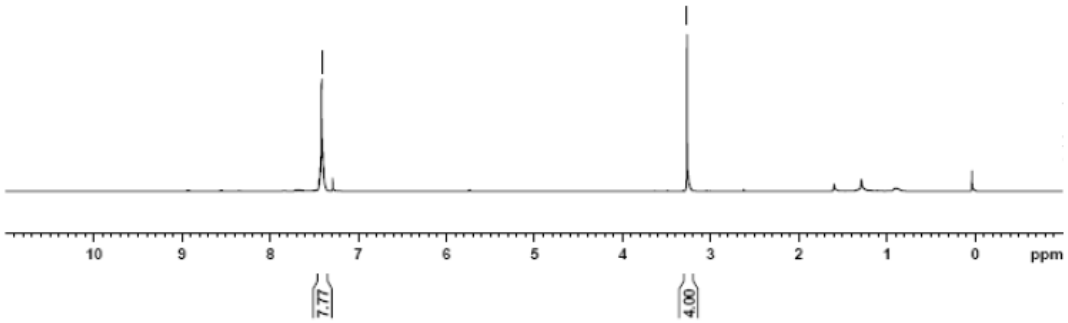

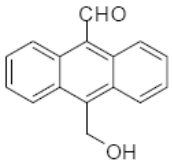

10-(Hydroxylmethyl)-9-anthraldehyde **(31)**

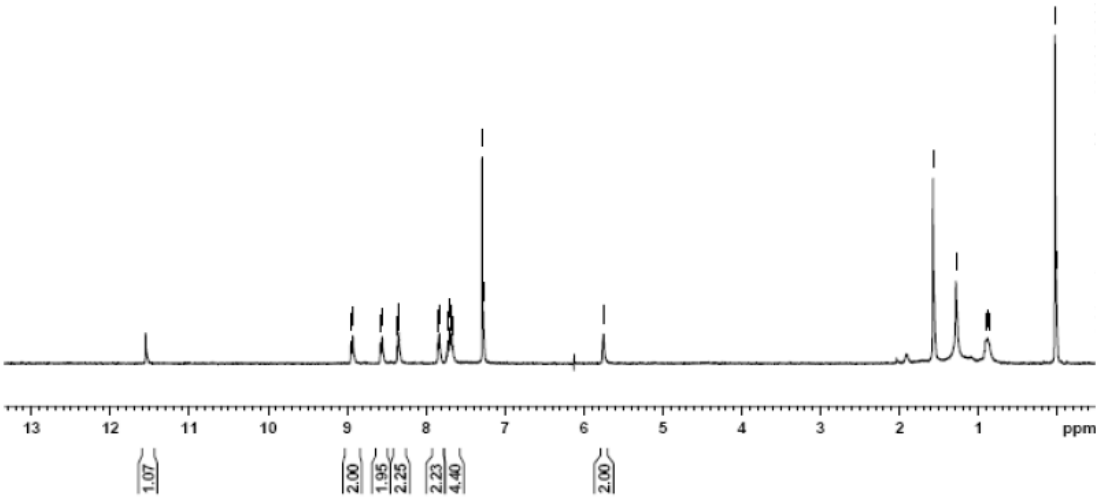

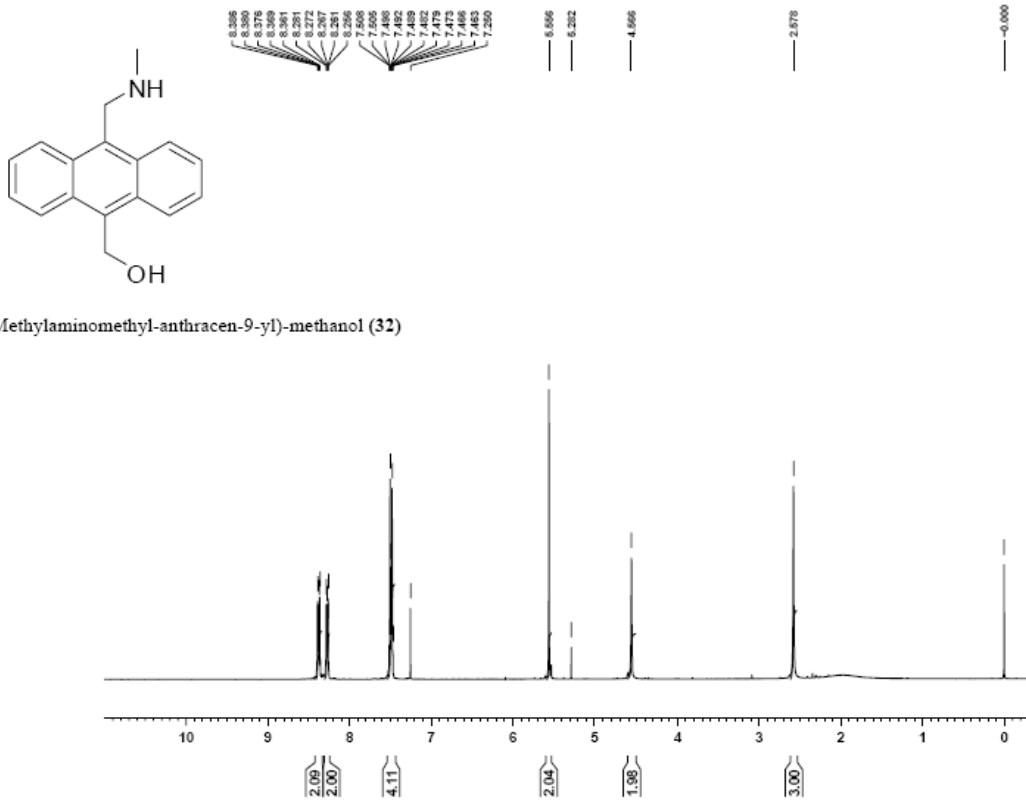

(10-Methylaminomethyl-anthracen-9-yl)-methanol (**32**)

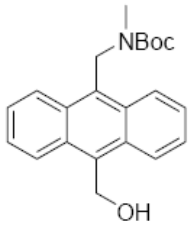

10-Methylaminomethyl-anthracen-9-ylmethyl)-methyl-carbamic acid *tert*-butyl ester (**33**)

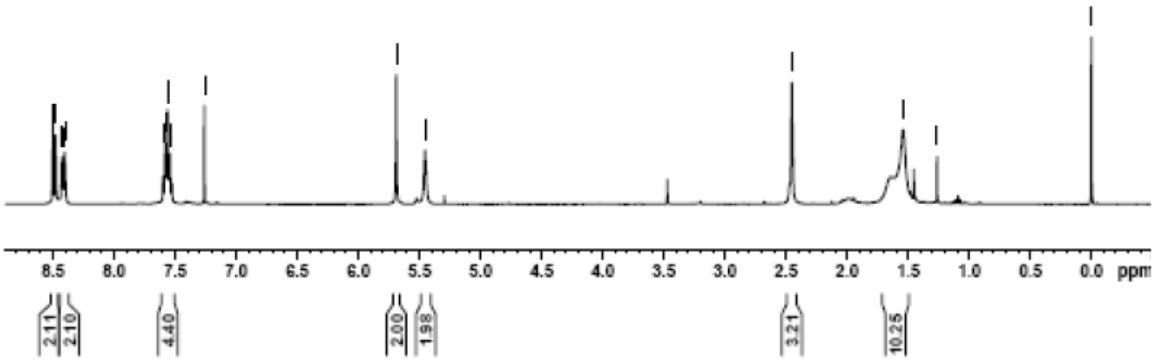

(10-Azidomethyl-anthracen-9-ylmethyl)-methyl-carbamic acid *tert*-butyl ester **(34)**

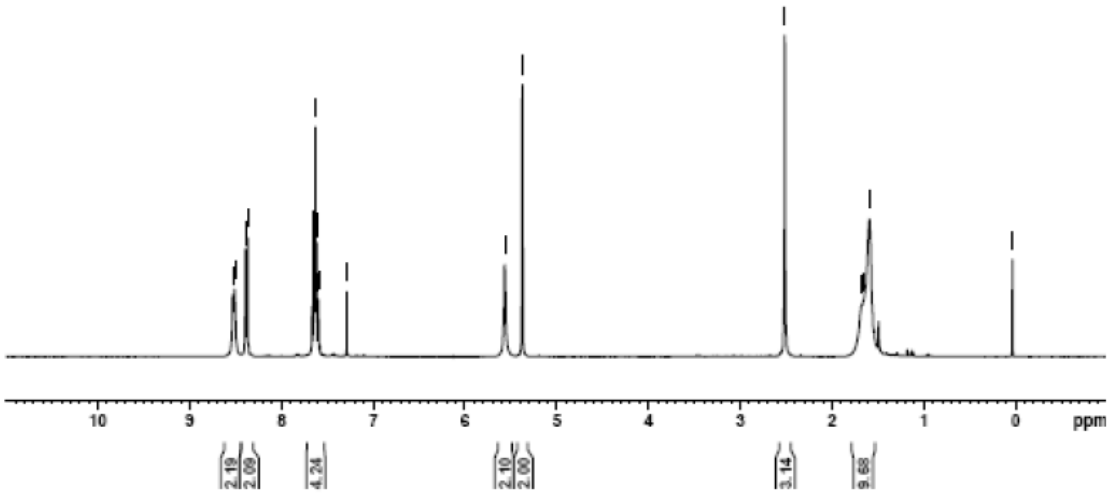

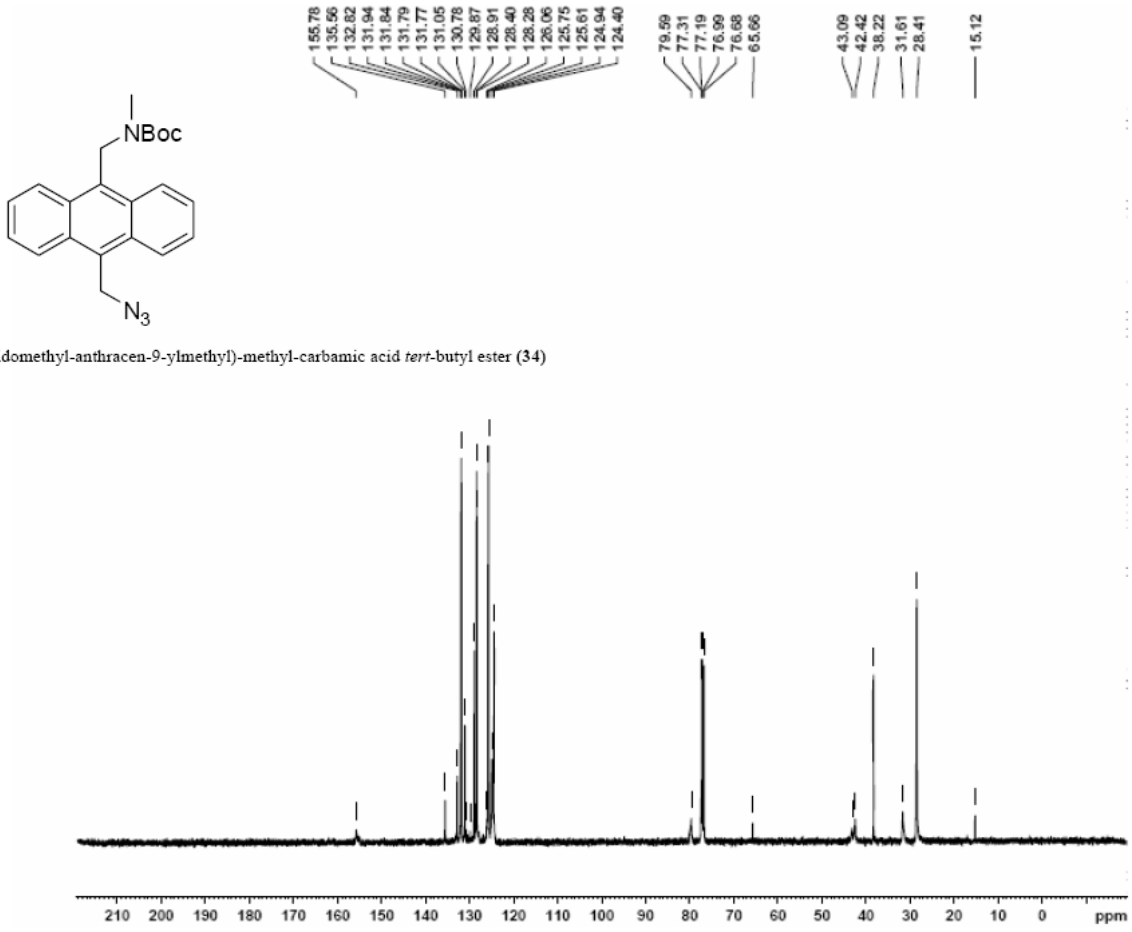

(10-Azidomethyl-anthracen-9-ylmethyl)-methyl-carbamic acid *tert*-butyl ester (**34**)

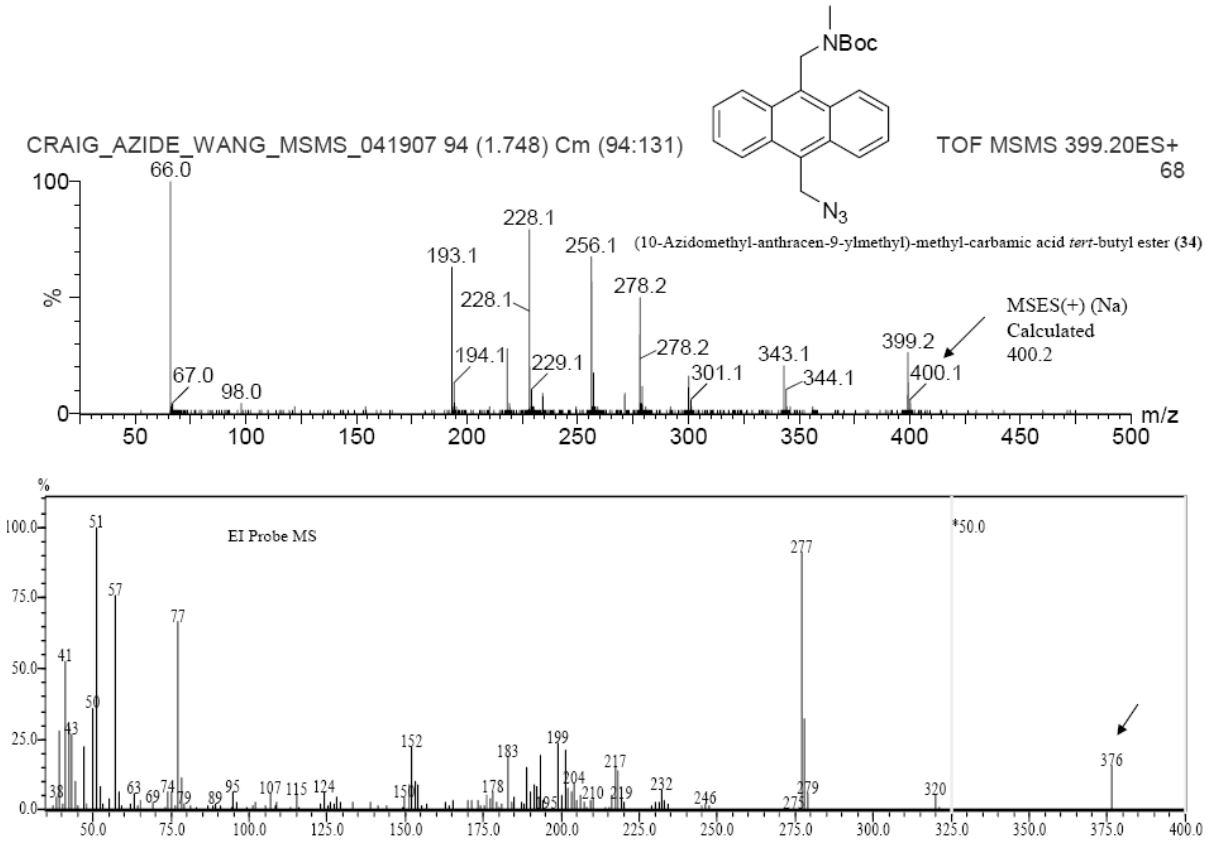
NBoc
N3
CRAIG_AZIDE_WANG_MSMS_041907 94 (1.748) Cm (94:131)
TOF MSMS 399.20ES+
68
(10-Azidomethyl-anthracen-9-ylmethyl)-methyl-carbamic acid tert-butyl ester (34)
MSES(+) (Na)
Calculated
400.2
m/z
EI Probe MS
*50.0

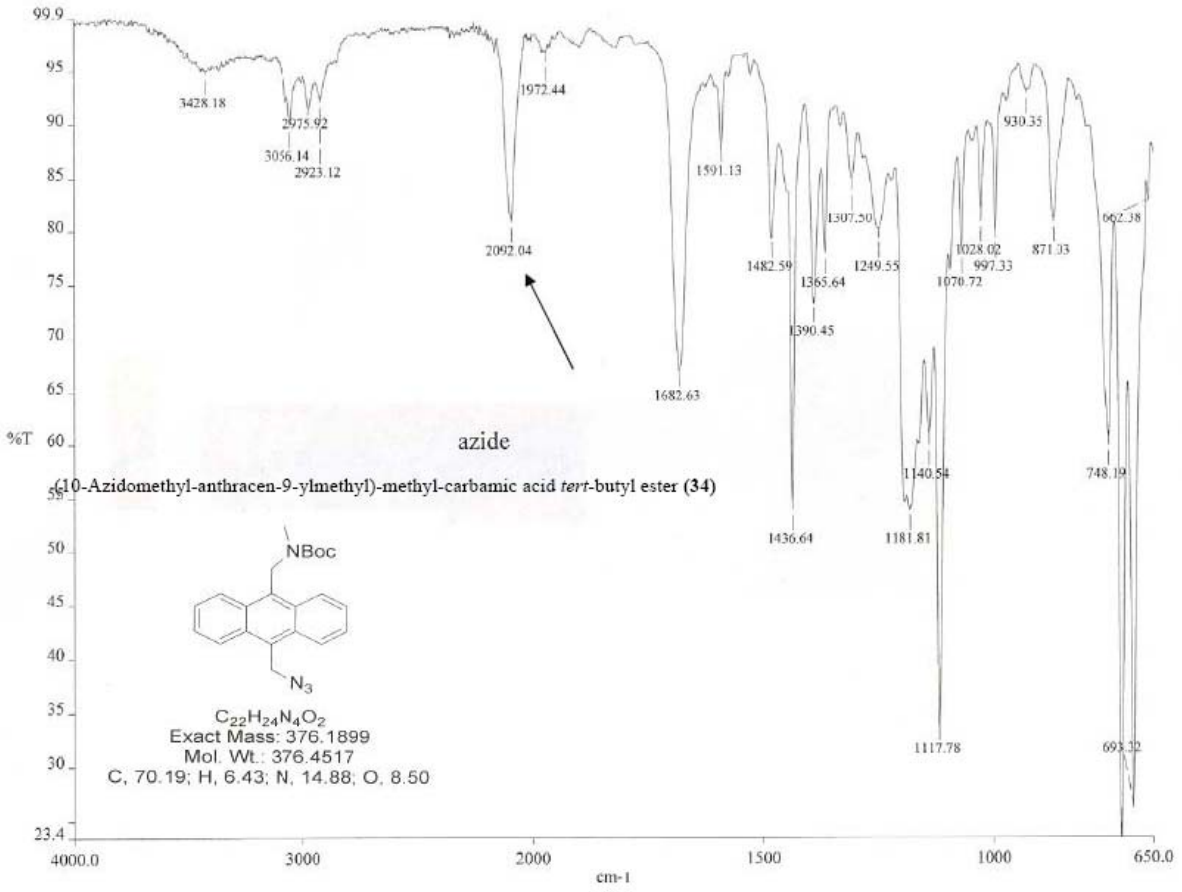
azide
(10-Azidomethyl-anthracen-9-ylmethyl)-methyl-carbamic acid tert-butyl ester (34)
NBoc
N3
C22H24N4O2
Exact Mass: 376.1899
Mol. Wt.: 376.4517
C, 70.19; H, 6.43; N, 14.88; O, 8.50
%T
cm-1
3428.18
3056.14
2975.92
2923.12
2092.04
1972.44
1682.63
1591.13
1482.59
1436.64
1390.45
1365.64
1307.50
1249.55
1181.81
1140.54
1117.78
1070.72
1028.02
997.33
930.35
871.33
748.19
693.32
662.38

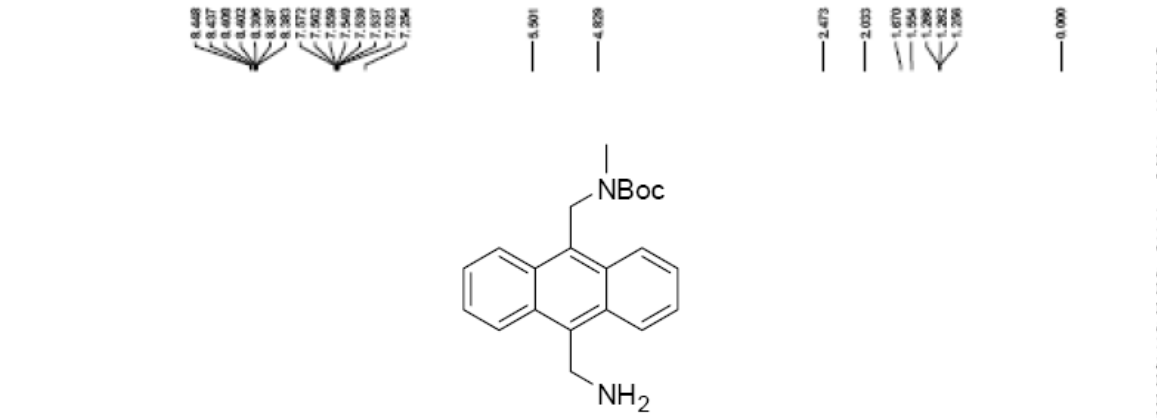

(10-Aminomethyl-anthracen-9-ylmethyl)-methyl-carbamic acid *tert*-butyl ester (**35**)

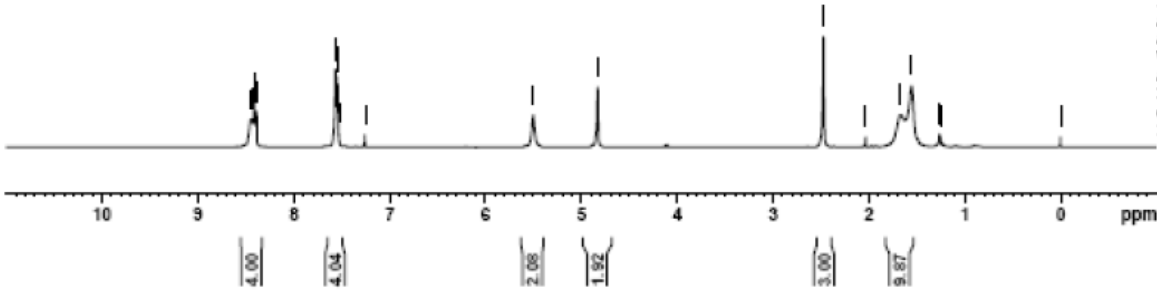

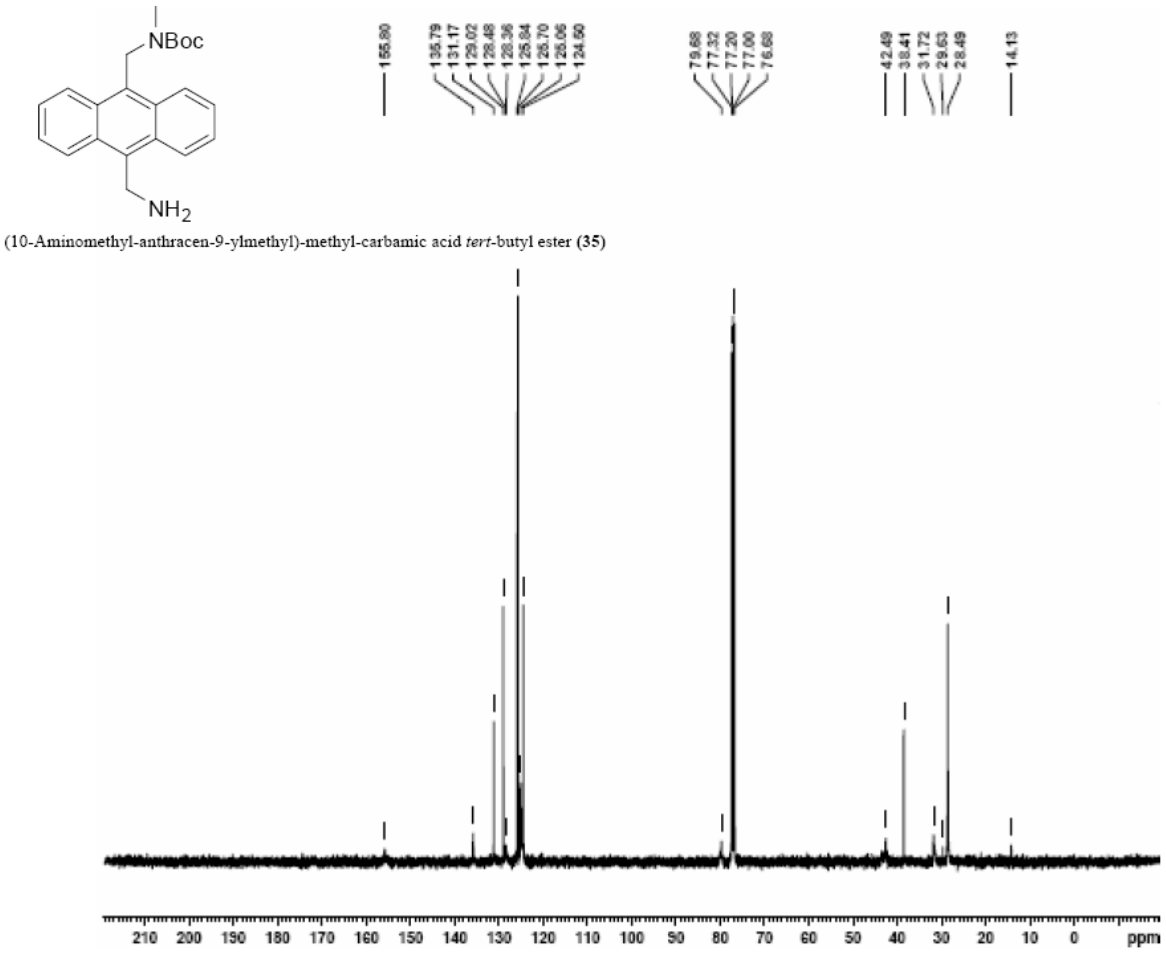

(10-Aminomethyl-anthracen-9-ylmethyl)-methyl-carbamic acid *tert*-butyl ester **(35)**

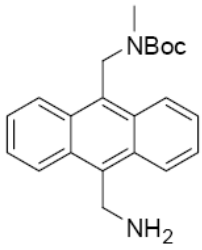

(10-Aminomethyl-anthracen-9-ylmethyl)-methyl-carbamic acid *tert*-butyl ester (**35**)

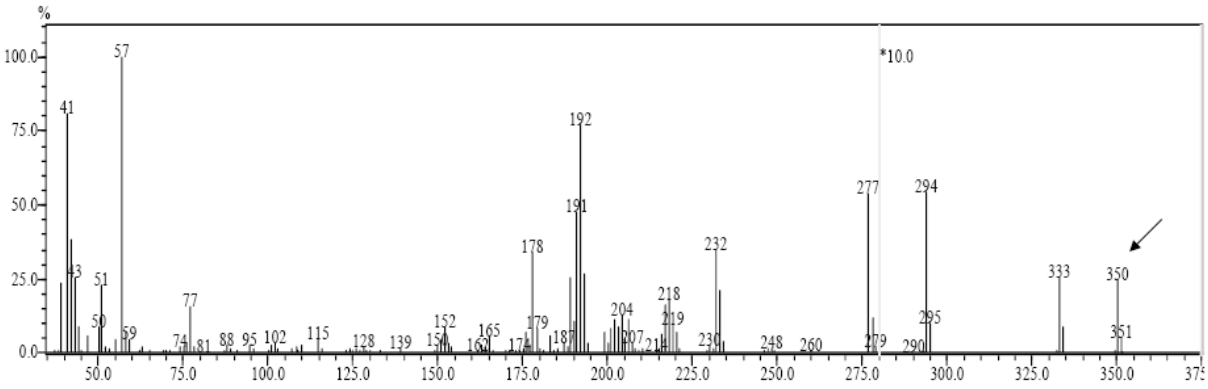

EI Probe MS

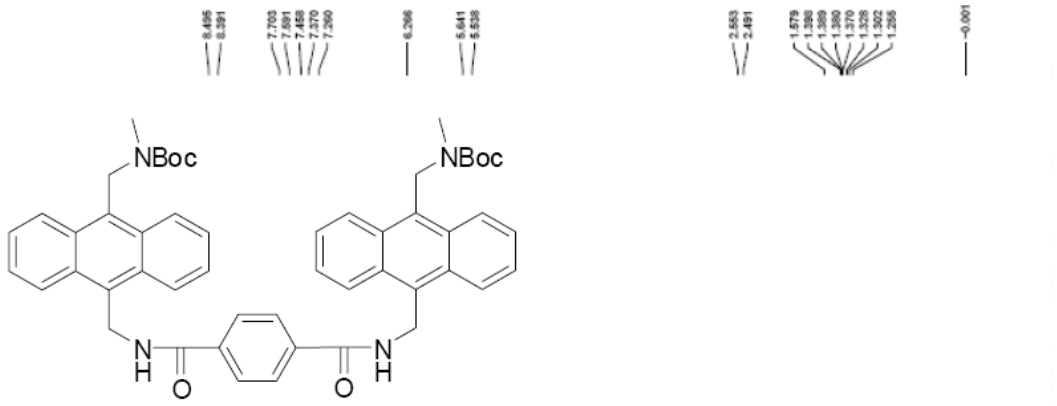

[10-({[4-({10-[(*tert*-Butoxycarbonyl-methyl-amino)-methyl]-anthracen-9-ylmethyl}-methyl-carbamoyl)-benzoyl]-aminomethyl)
-anthracen-9-ylmethyl]-methyl-carbamic acid *tert*-butyl ester **(36a)**

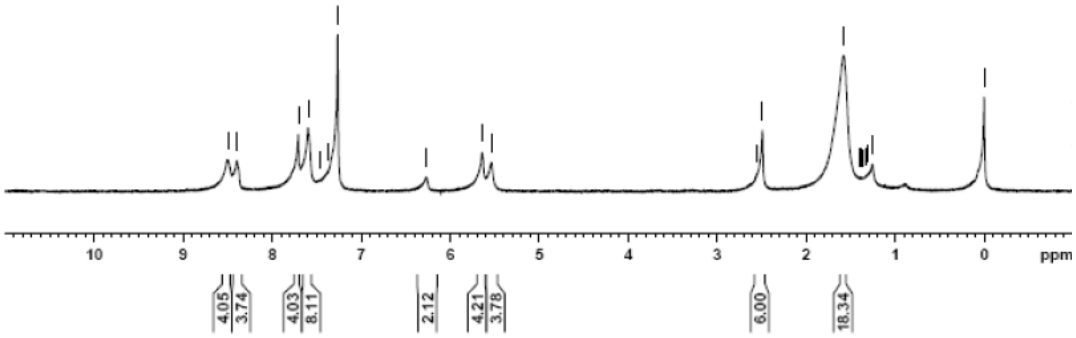

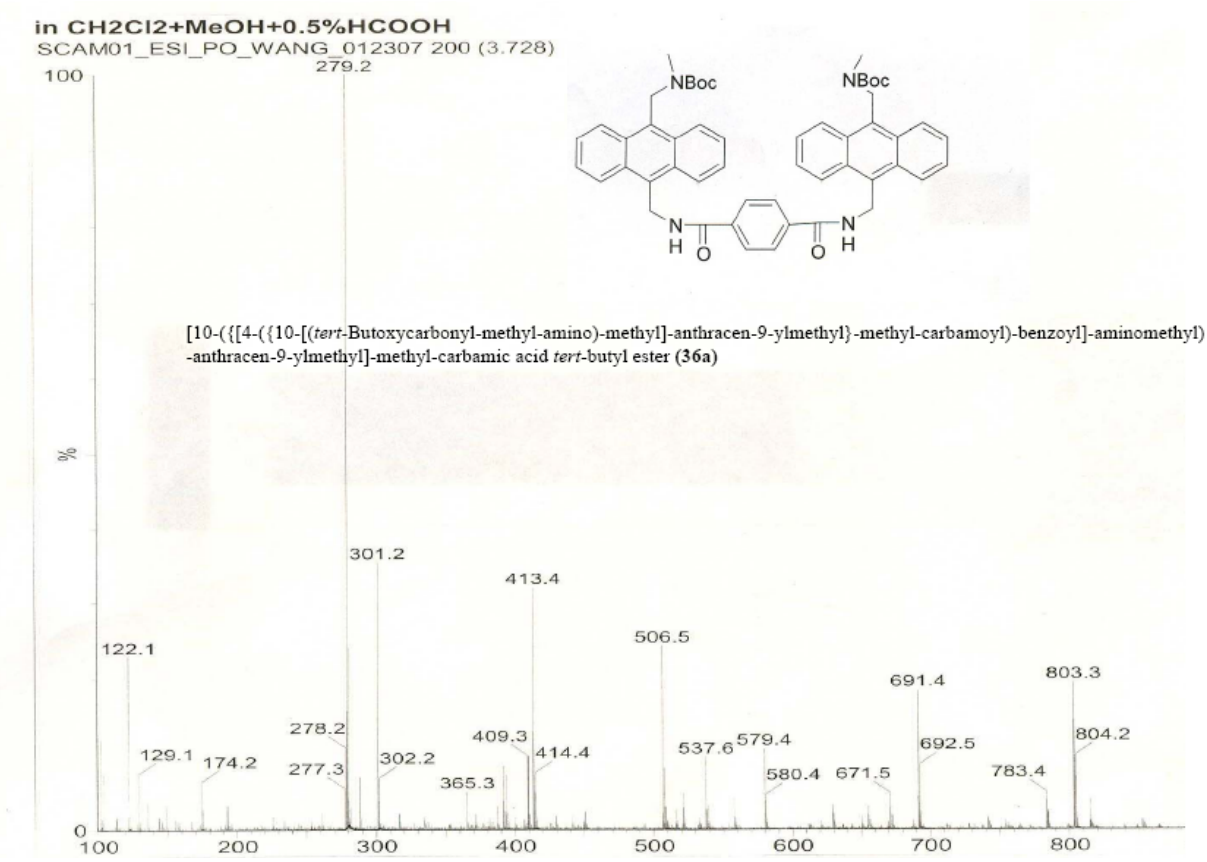

[10-({[4-({10-[(*tert*-Butoxycarbonyl-methyl-amino)-methyl]-anthracen-9-ylmethyl}-methyl-carbamoyl)-benzoyl]-aminomethyl)-anthracen-9-ylmethyl]-methyl-carbamic acid *tert*-butyl ester (**36a**)

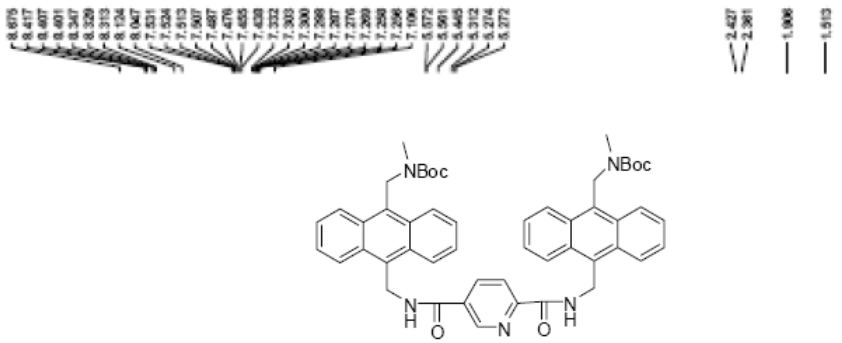

[10-({[4-({10-[(*tert*-Butoxycarbonyl-methyl-amino)-methyl]-anthracen-9-ylmethyl}-methyl-carbamoyl)-pyridine-2-carbonyl]-aminomethyl)-anthracen-9-ylmethyl]-methyl-carbamic acid *tert*-butyl ester (**36b**)

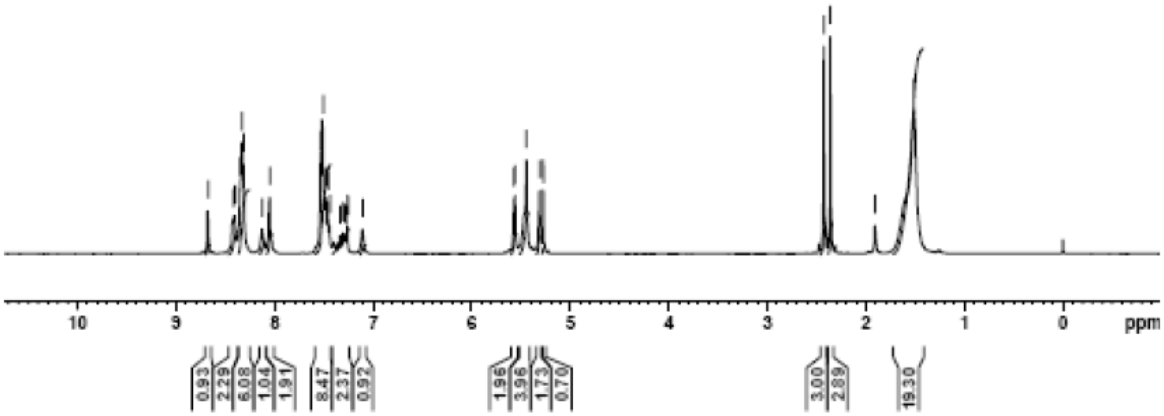

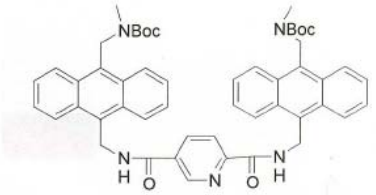

[10-({[4-({10-[(*tert*-Butoxycarbonyl-methyl-amino)-methyl]-anthracen-9-ylmethyl}-methyl-carbamoyl)-pyridine-2-carbonyl]-aminomethyl)-anthracen-9-ylmethyl]-methyl-carbamic acid *tert*-butyl ester **(36b)**

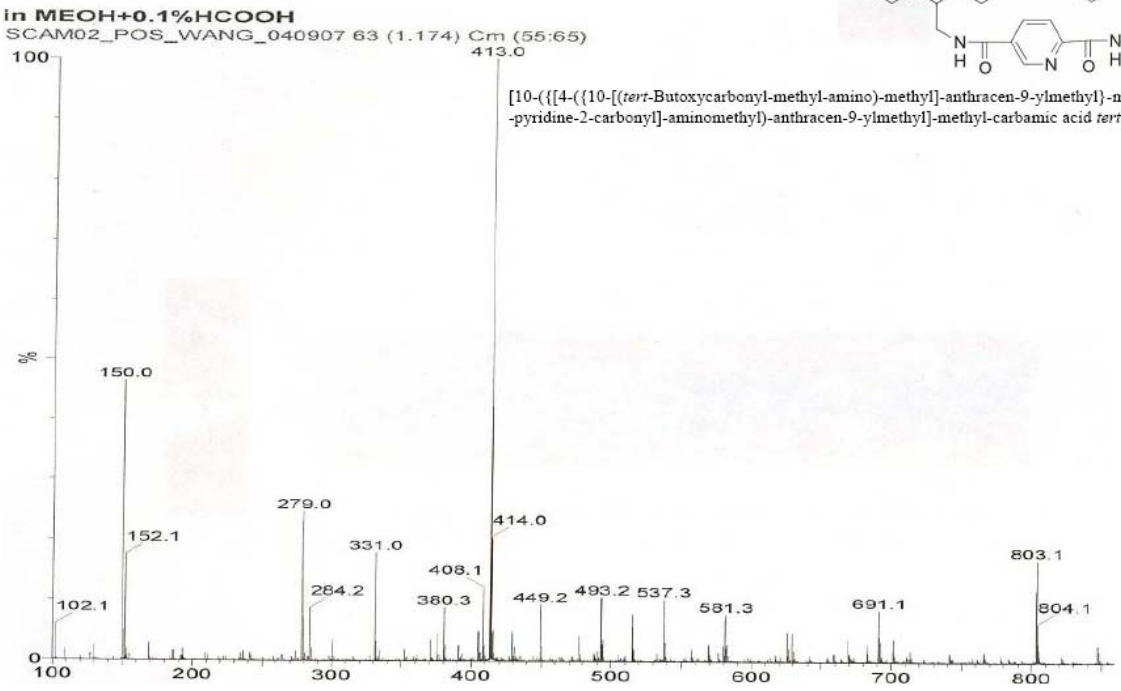

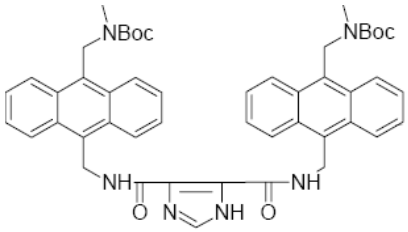

[10-({[4-({10-[(*tert*-Butoxycarbonyl-methyl-amino)-methyl]-anthracen-9-ylmethyl}-methyl-carbamoyl)-imidazole-4-carbonyl]-aminomethyl)-anthracen-9-ylmethyl]-methyl-carbamic acid *tert*-butyl ester **(36c)**

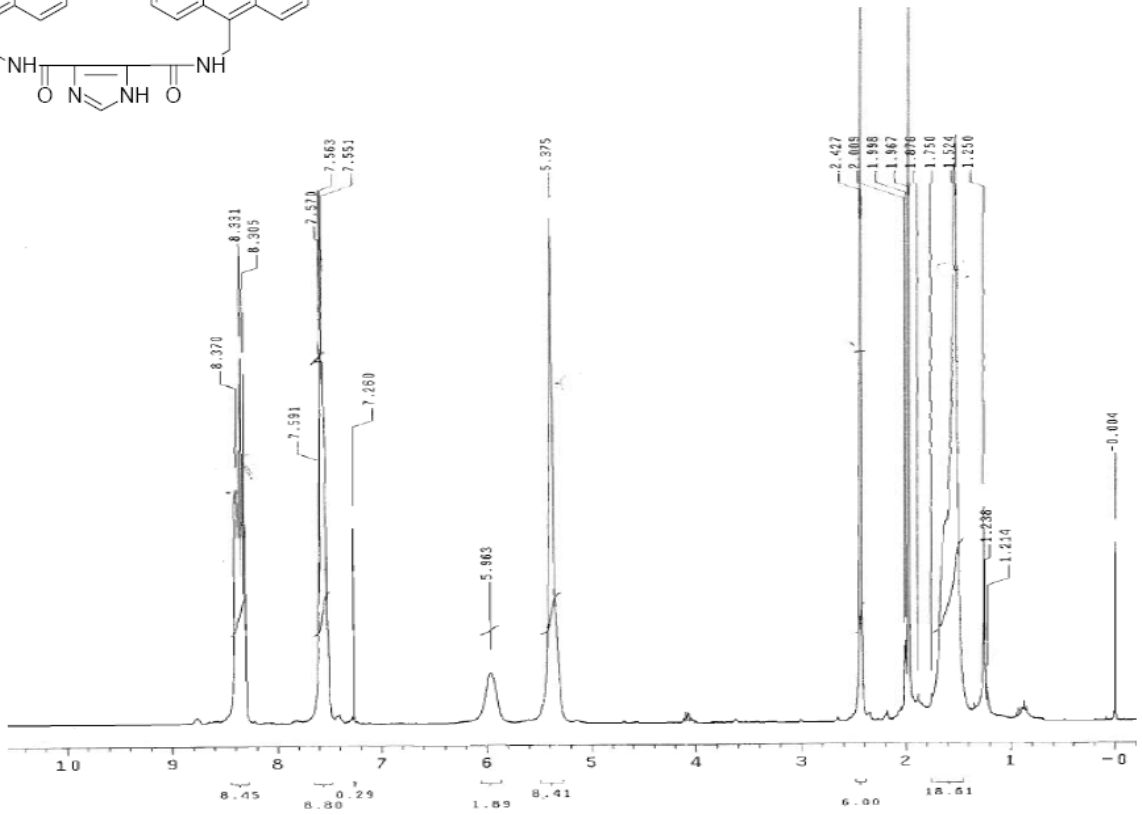

[10-({[4-({10-[(*tert*-Butoxycarbonyl-methyl-amino)-methyl]-anthracen-9-ylmethyl}-methyl-carbamoyl)-pyrazine-2-carbonyl]-aminomethyl)-anthracen-9-ylmethyl]-methyl-carbamic acid *tert*-butyl ester **(36d)**

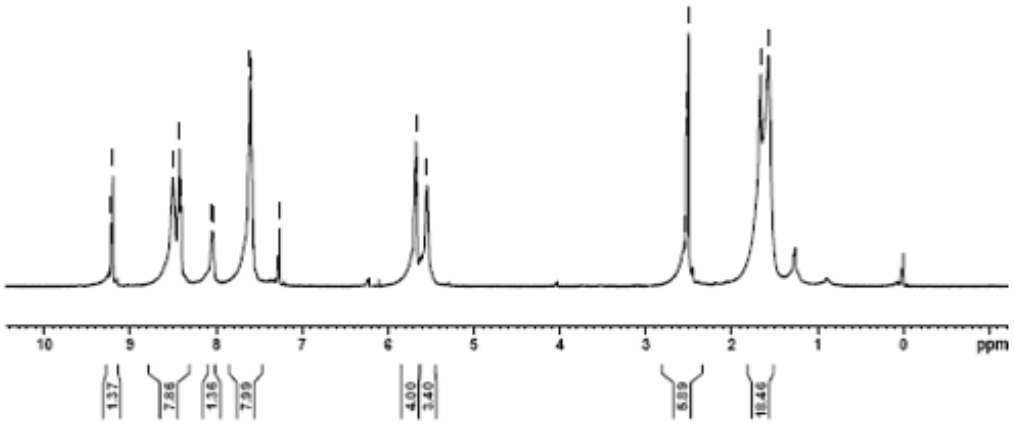

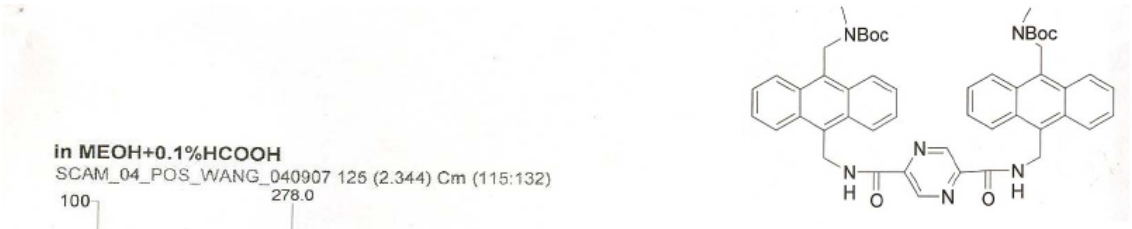

in MEOH+0.1%HCOOH

SCAM_04_POS_WANG_040907 125 (2.344) Cm (115:132)

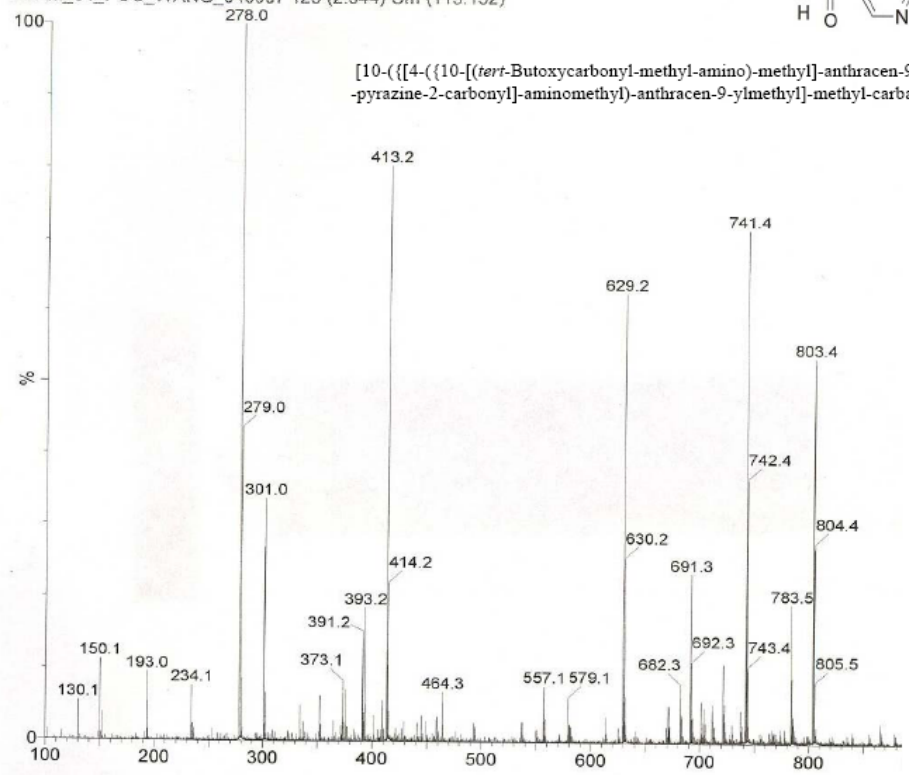

[10-({[4-({10-[(*tert*-Butoxycarbonyl-methyl-amino)-methyl]-anthracen-9-ylmethyl}-methyl-carbamoyl)-pyrazine-2-carbonyl]-aminomethyl)-anthracen-9-ylmethyl]-methyl-carbamic acid *tert*-butyl ester **(36d)**

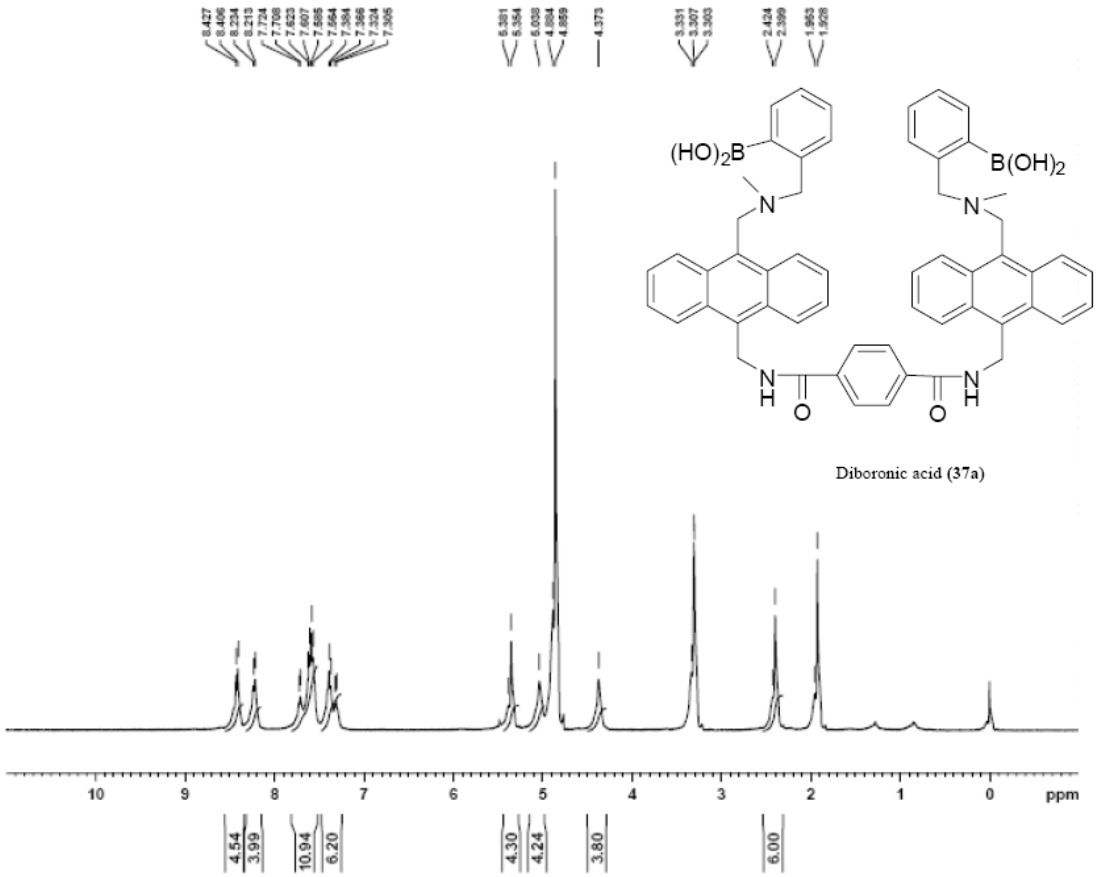
8.427
8.406
8.234
8.213
7.724
7.708
7.623
7.607
7.585
7.564
7.384
7.366
7.324
7.306
5.381
5.364
5.038
4.884
4.869
4.373
3.331
3.307
3.303
2.424
2.399
1.963
1.928
(HO)2B
B(OH)2
N
N
N
H
O
O
N
H
Diboronic acid (37a)
10
9
8
7
6
5
4
3
2
1
0
ppm
4.54
3.99
10.94
6.20
4.30
4.24
3.80
6.00

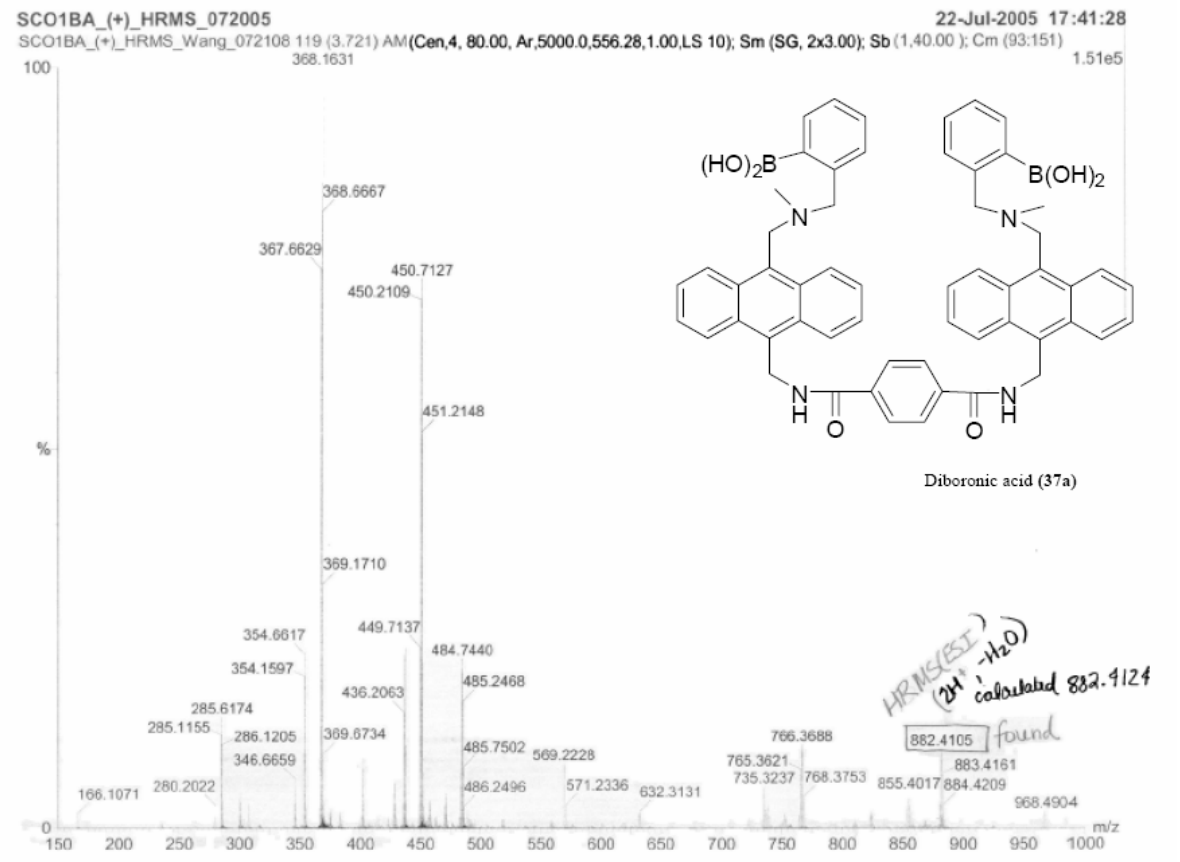
SCO1BA_(+)_HRMS_072005
22-Jul-2005 17:41:28
SCO1BA_(+)_HRMS_Wang_072108 119 (3.721) AM (Cen,4, 80.00, Ar,5000.0,556.28,1.00,LS 10); Sm (SG, 2x3.00); Sb (1,40.00); Cm (93:151)
1.51e5
100
%
0
m/z
150 200 250 300 350 400 450 500 550 600 650 700 750 800 850 900 950 1000
368.1631
368.6667
367.6629
450.7127
450.2109
451.2148
369.1710
449.7137
354.6617
484.7440
354.1597
485.2468
436.2063
285.6174
285.1155
286.1205
369.6734
346.6659
485.7502
569.2228
280.2022
166.1071
486.2496
571.2336
632.3131
766.3688
765.3621
735.3237
768.3753
855.4017
882.4105
883.4161
884.4209
968.4904
(HO)2B
B(OH)2
N
N
N
H
O
O
N
H
Diboronic acid (37a)
HRMS(ES+)
(2M+ -H2O)
calculated 882.4124
found

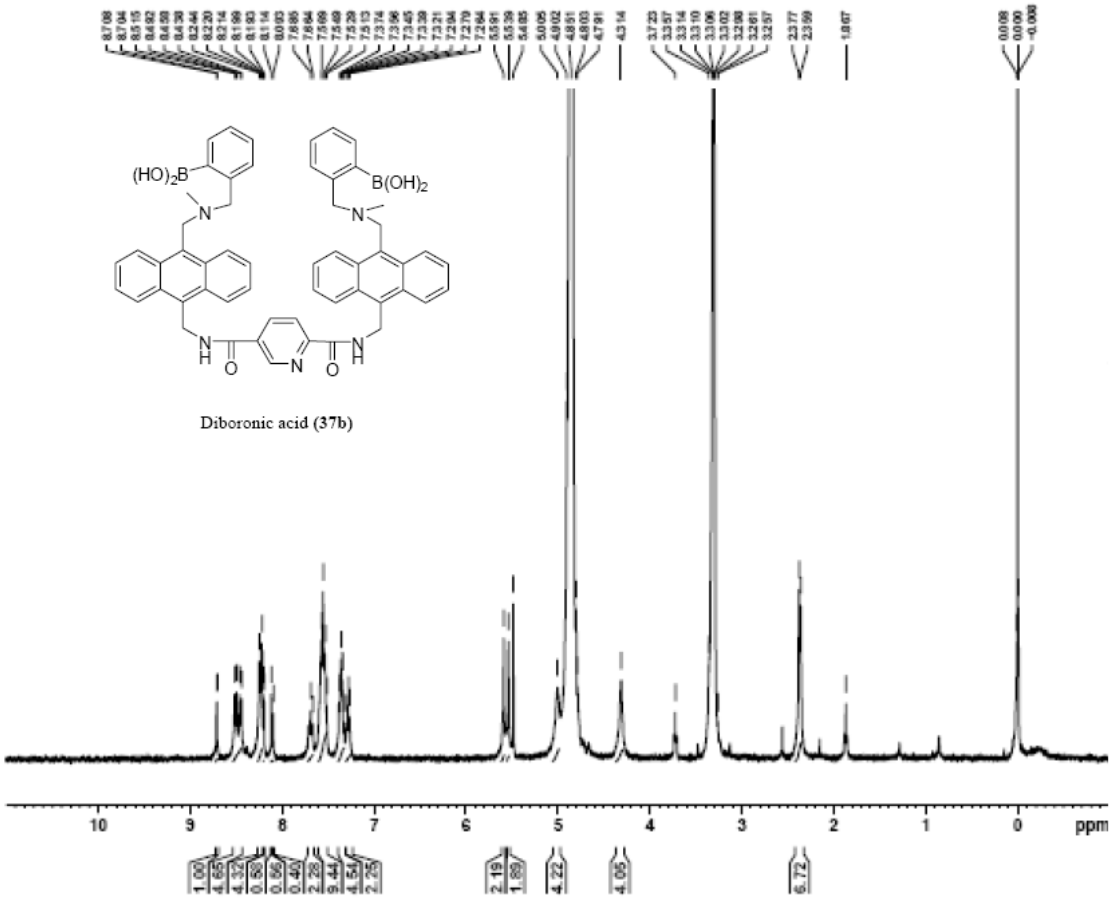

Diboronic acid (37b)

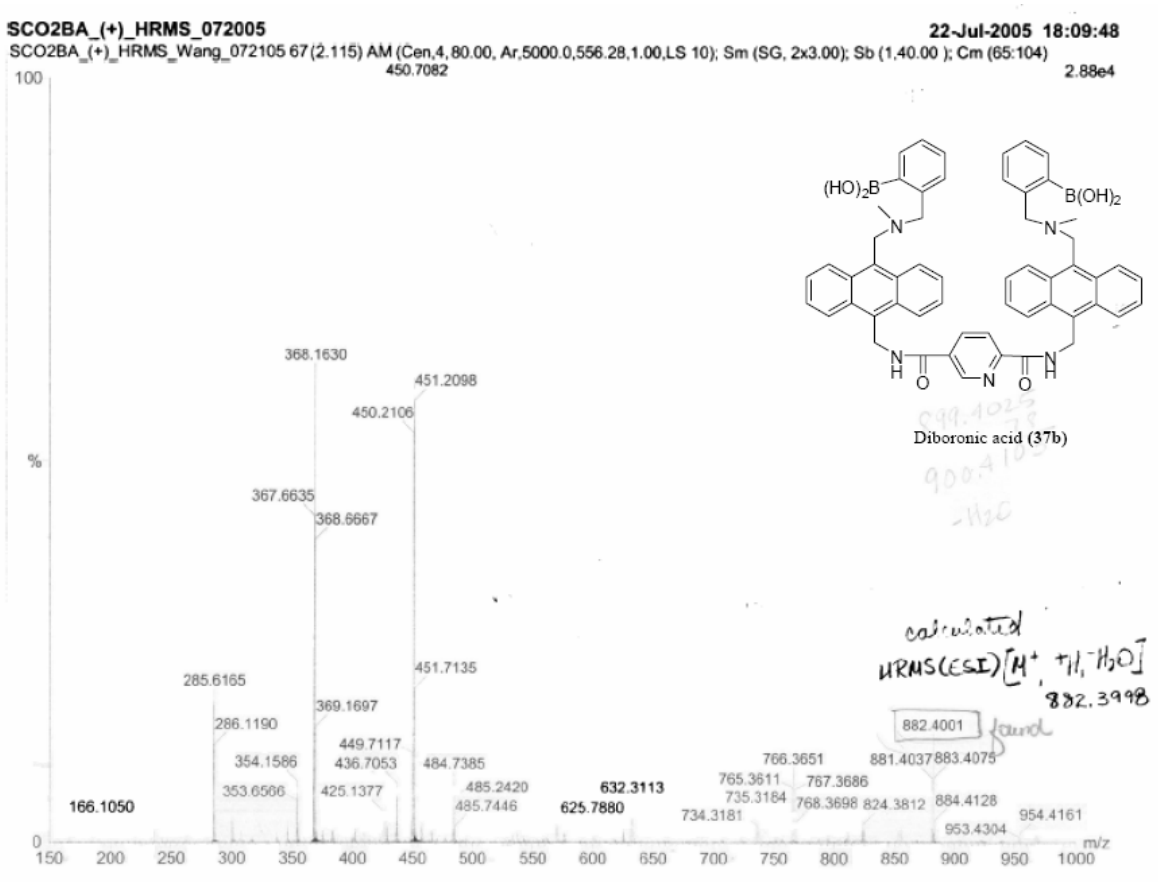
SCO2BA_(+)_HRMS_072005
22-Jul-2005 18:09:48
SCO2BA_(+)_HRMS_Wang_072105 67 (2.115) AM (Cen,4, 80.00, Ar,5000.0,556.28,1.00,LS 10); Sm (SG, 2x3.00); Sb (1,40.00); Cm (65:104)
450.7082
2.88e4
100
%
0
(HO)2B
B(OH)2
N
H
O
Diboronic acid (37b)
368.1630
451.2098
450.2106
367.6635
368.6667
451.7135
285.6165
369.1697
286.1190
449.7117
354.1586
436.7053
484.7385
353.6566
425.1377
485.2420
485.7446
632.3113
625.7880
166.1050
766.3651
881.4037
883.4075
765.3611
767.3686
735.3184
768.3698
824.3812
884.4128
734.3181
954.4161
953.4304
150
200
250
300
350
400
450
500
550
600
650
700
750
800
850
900
950
1000
m/z
calculated
HRMS(ESI)[M+H, -H2O]
882.3998
882.4001
found

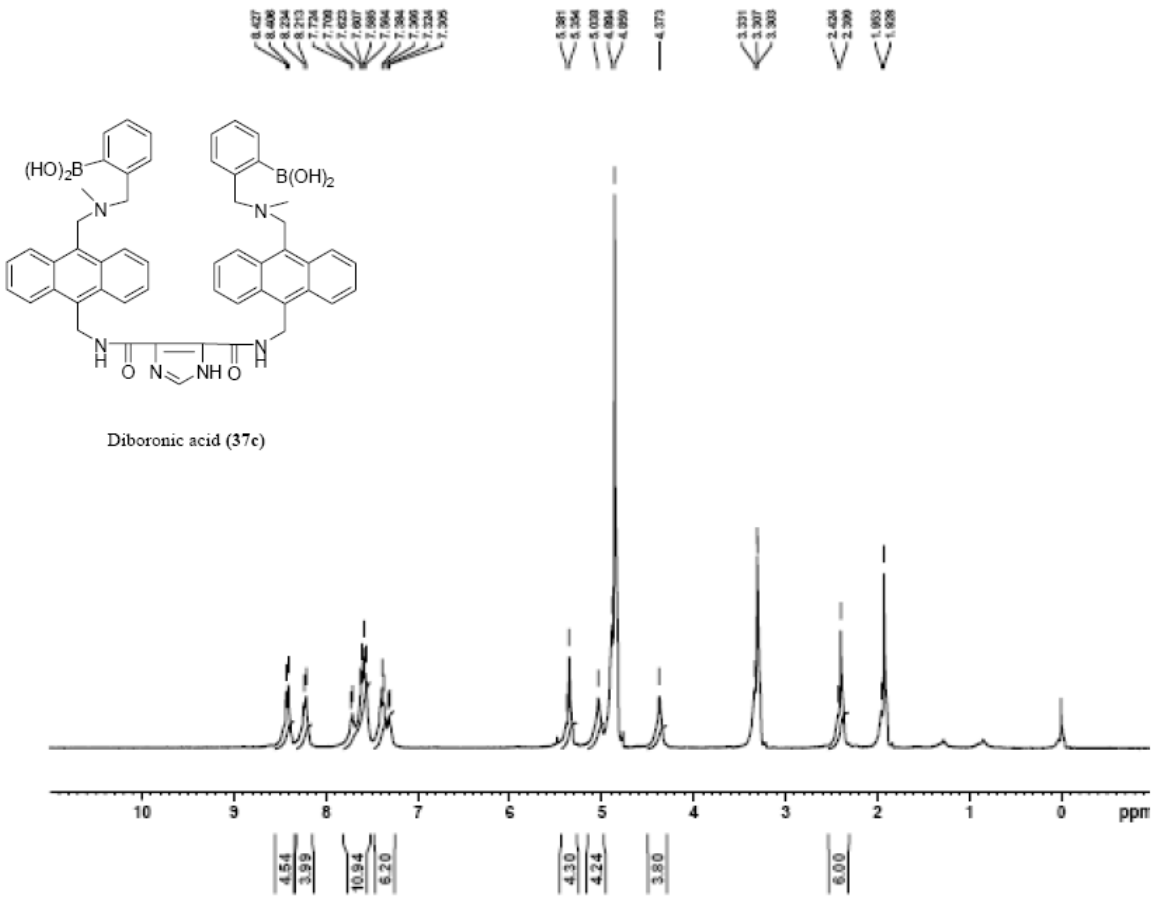

Diboronic acid (**37c**)

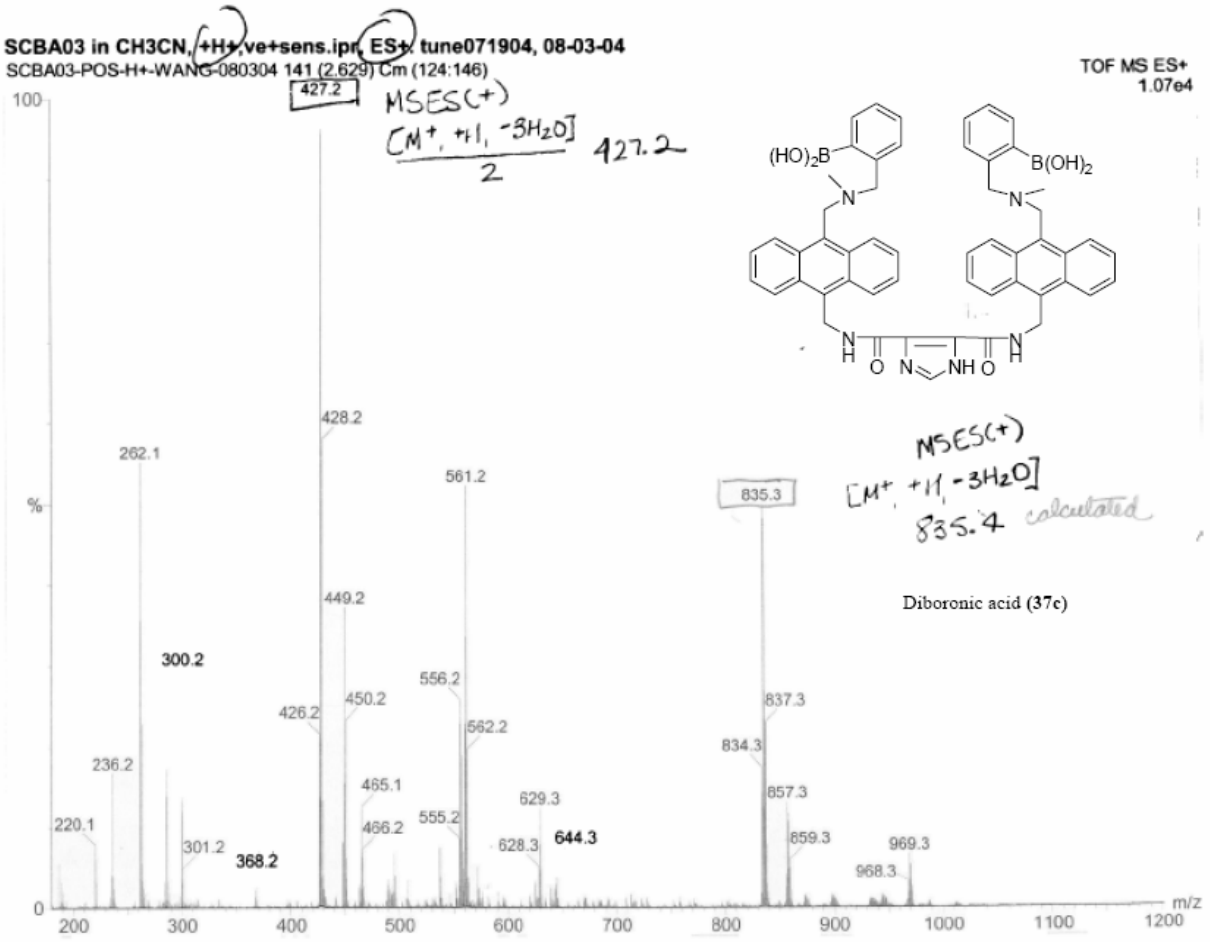
SCBA03 in CH3CN, (+H+,ve+sens.ipr, ES+ tune071904, 08-03-04
SCBA03-POS-H+-WANG-080304 141 (2.629) Cm (124:146)
TOF MS ES+
1.07e4
427.2
MSES(+)
[M+, +1, -3H2O]
2
427.2
(HO)2B
B(OH)2
N
N
N
H
O
N
NH
O
N
H
428.2
262.1
561.2
835.3
MSES(+)
[M+, +1, -3H2O]
835.4 calculated
%
449.2
Diboronic acid (37c)
300.2
556.2
450.2
837.3
426.2
562.2
834.3
236.2
465.1
629.3
857.3
220.1
555.2
466.2
644.3
659.3
969.3
301.2
628.3
368.2
968.3
0
m/z
200
300
400
500
600
700
800
900
1000
1100
1200

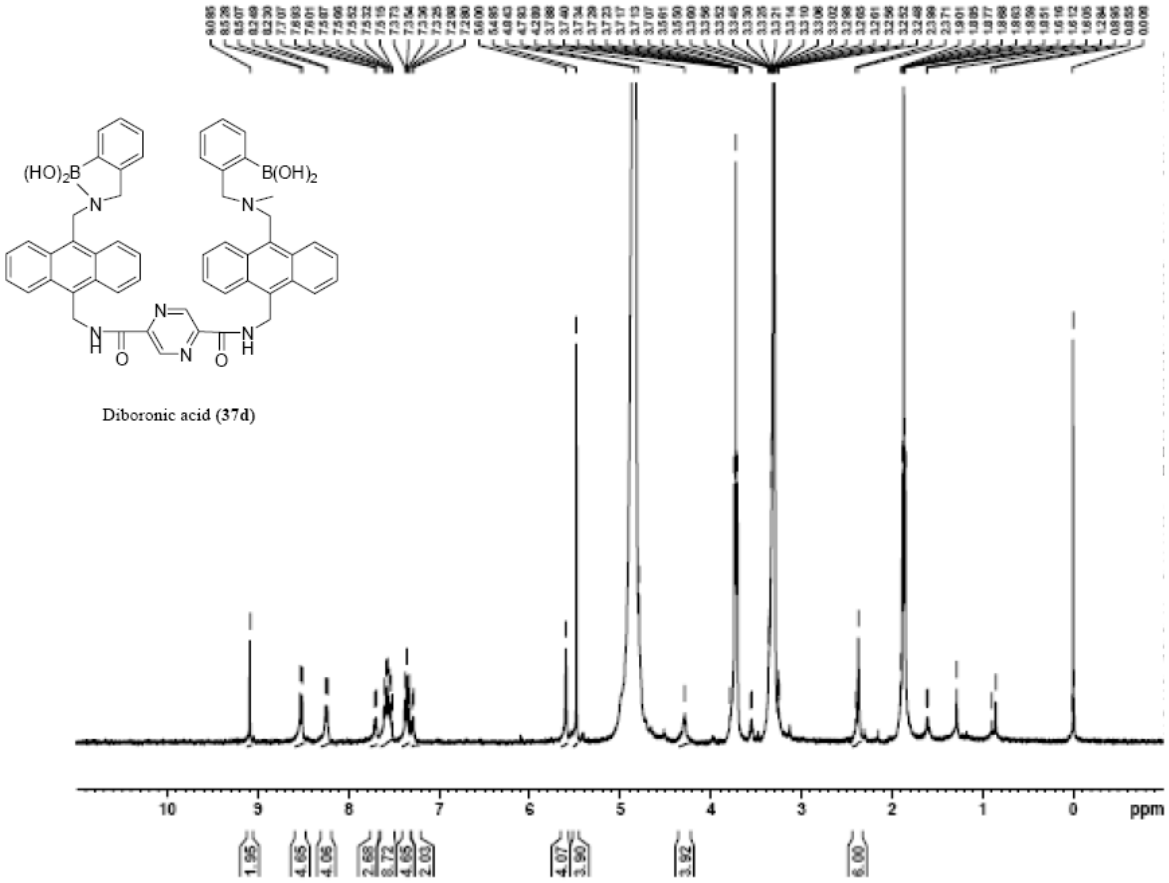

Diboronic acid (**37d**)

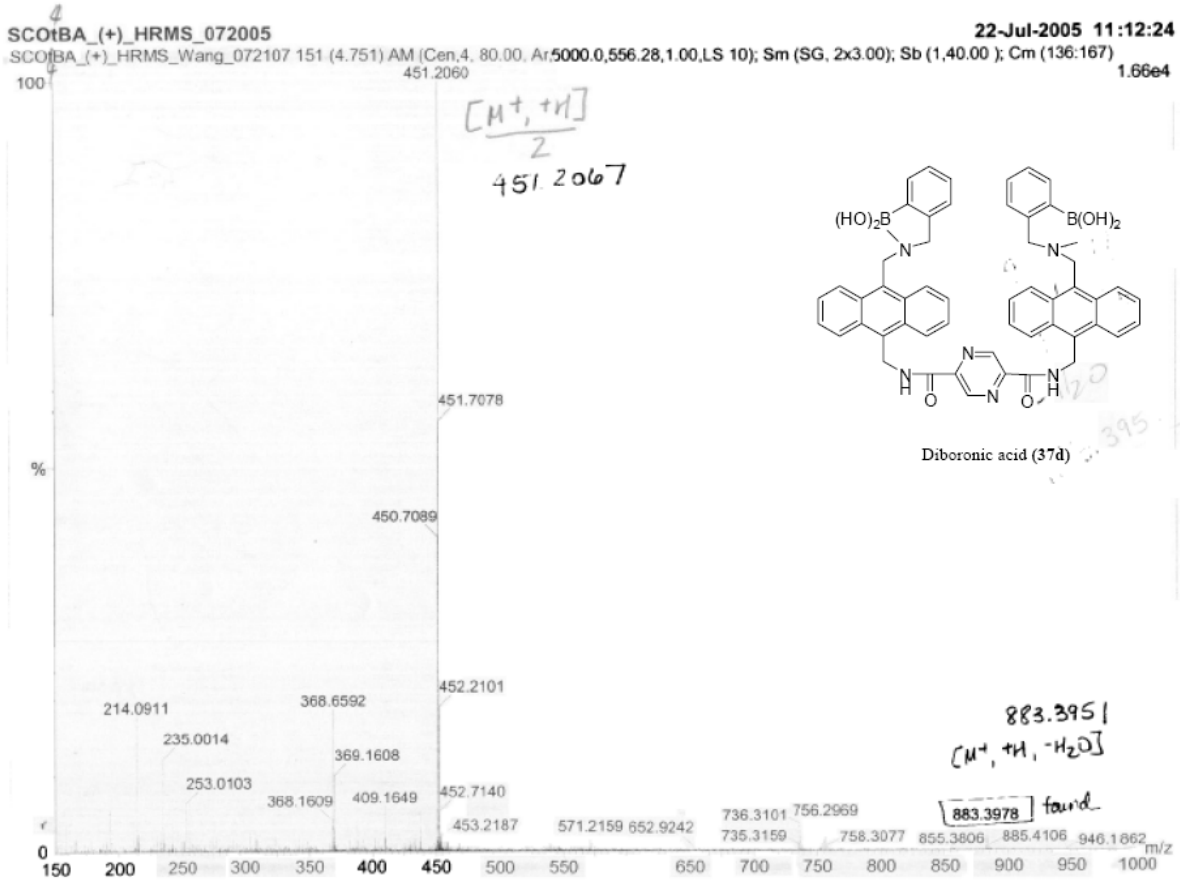
SCOtBA_(+)_HRMS_072005
22-Jul-2005 11:12:24
SCOtBA_(+)_HRMS_Wang_072107 151 (4.751) AM (Cen,4, 80.00, Ar,5000.0,556.28,1.00,LS 10); Sm (SG, 2x3.00); Sb (1,40.00); Cm (136:167)
1.66e4
451.2060
[M+, +H]
2
451.2067
(HO)2B
B(OH)2
Diboronic acid (37d)
451.7078
450.7089
452.2101
214.0911
368.6592
235.0014
369.1608
253.0103
368.1609
409.1649
452.7140
453.2187
571.2159
652.9242
736.3101
735.3159
756.2969
758.3077
883.3978
855.3806
885.4106
946.1862
883.3951
[M+, +H, -H2O]
found
%
m/z

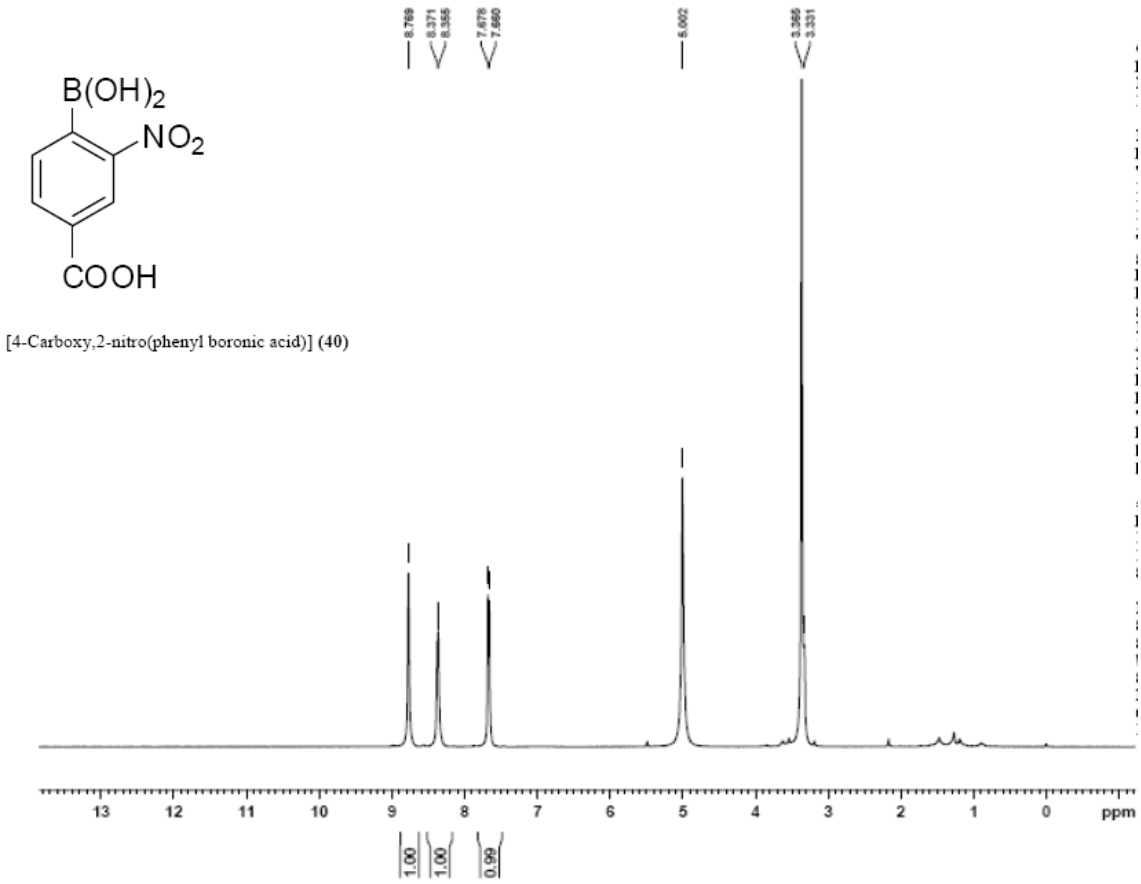

[4-Carboxy,2-nitro(phenyl boronic acid)] **(40)**

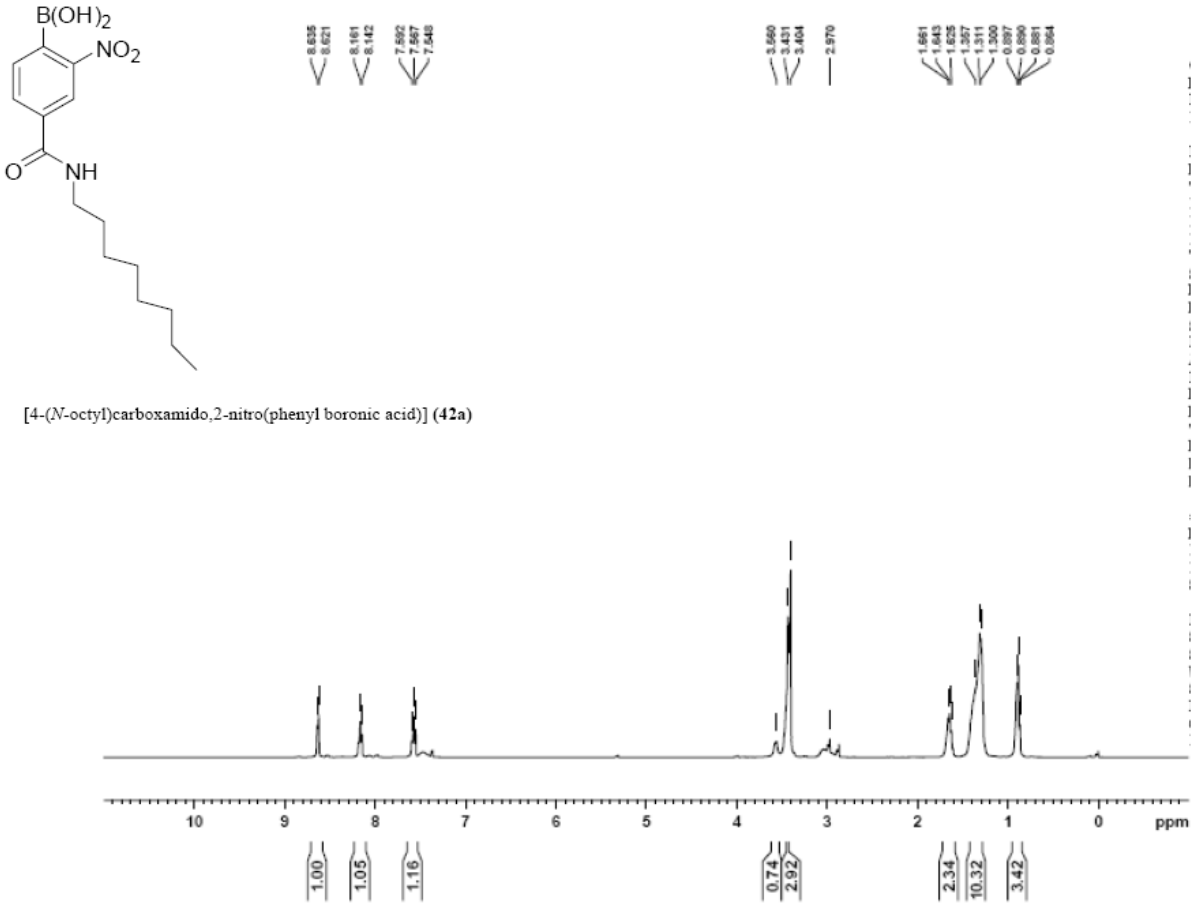

[4-(*N*-octyl)carboxamido,2-nitro(phenyl boronic acid)] (**42a**)

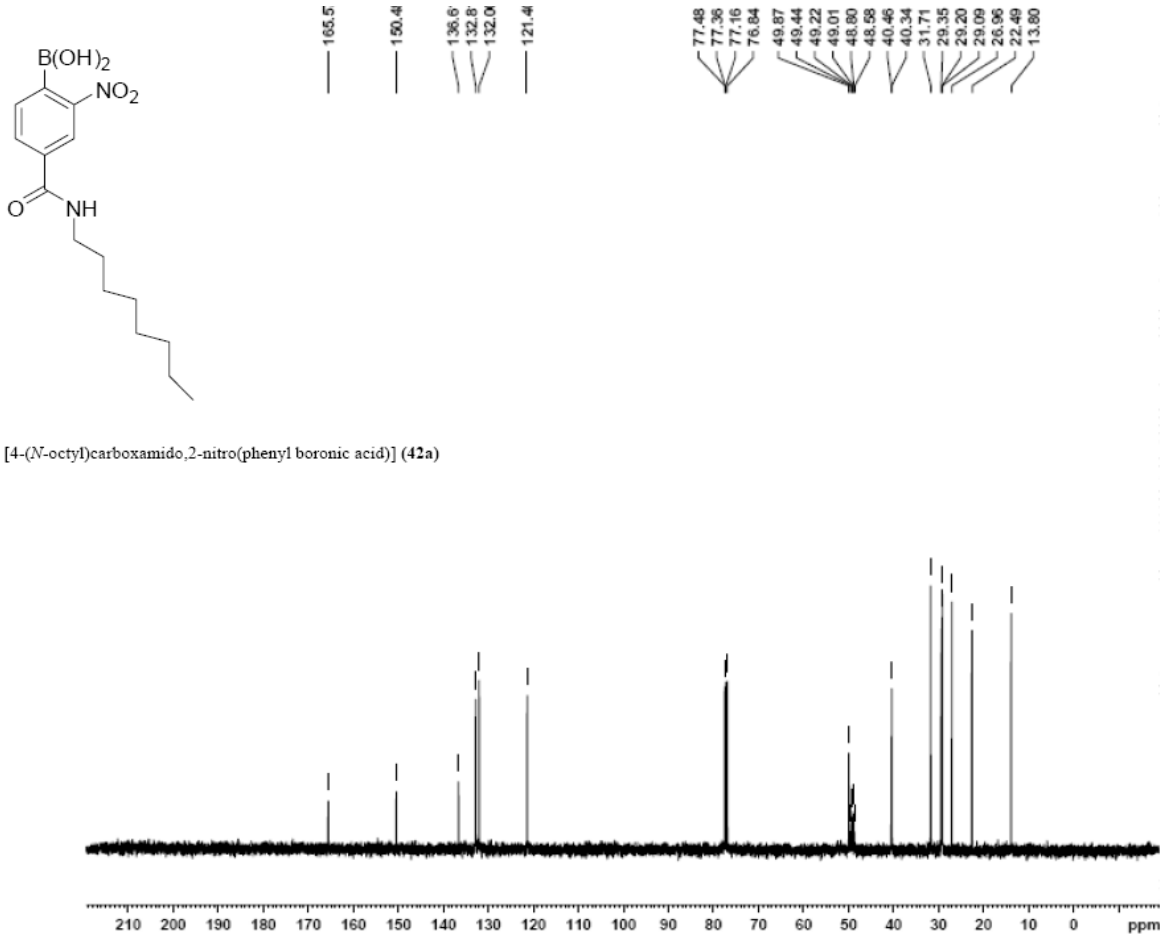

[4-(*N*-octyl)carboxamido,2-nitro(phenyl boronic acid)] (**42a**)

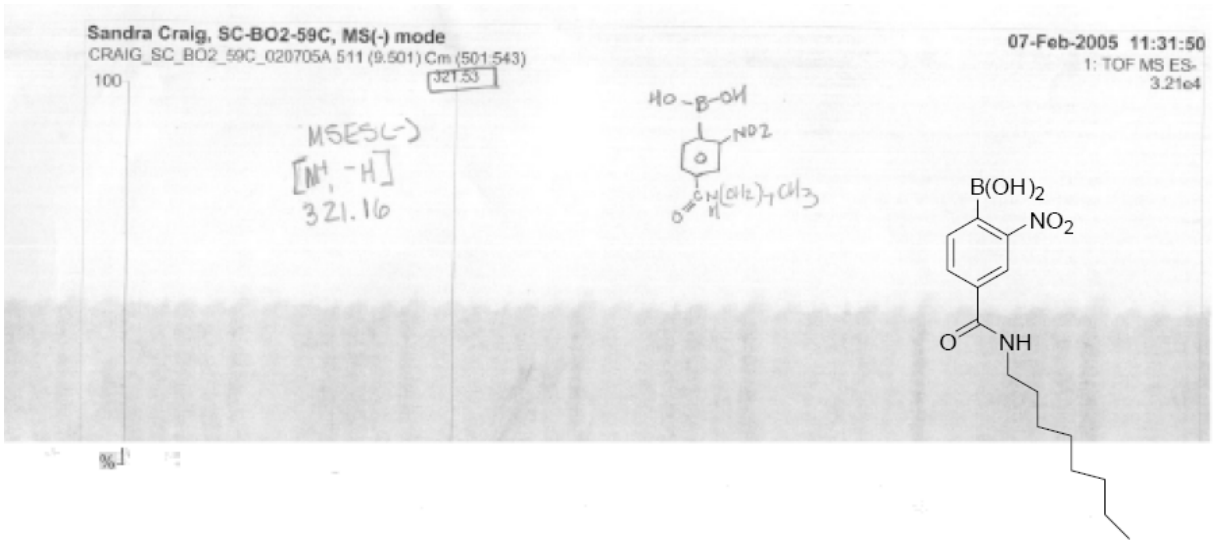

[4-(*N*-octyl)carboxamido,2-nitro(phenyl boronic acid)] (**42a**)

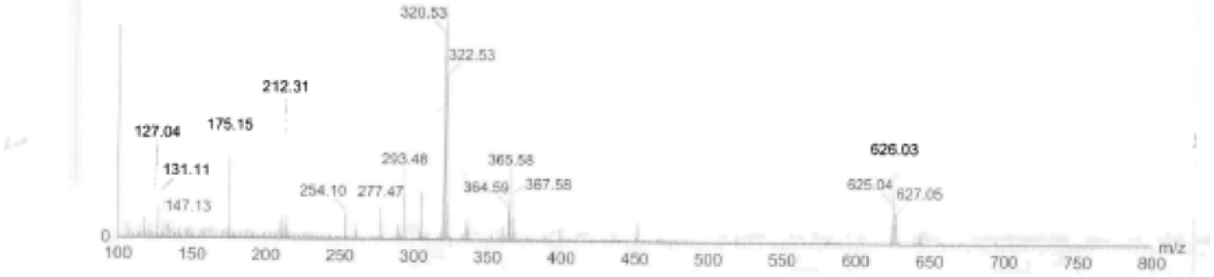

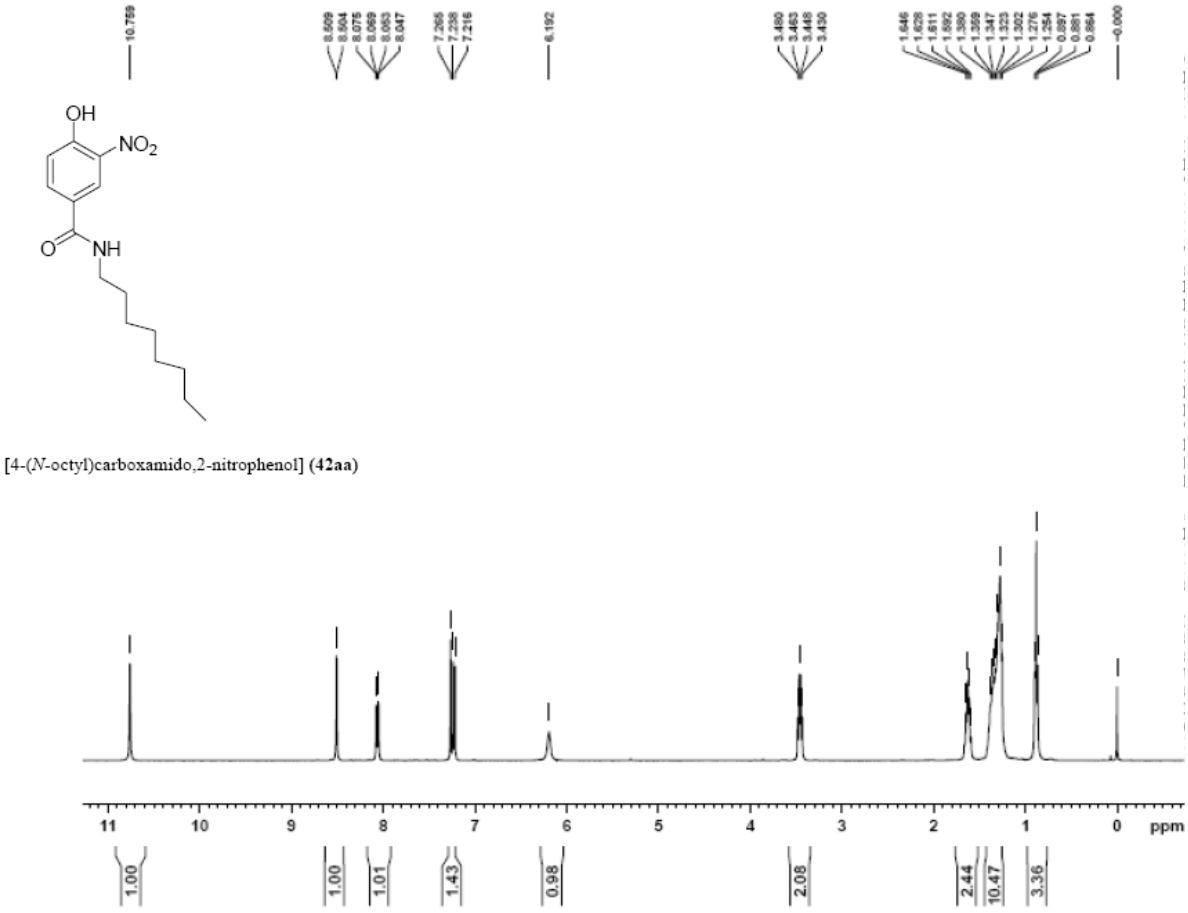

[4-(*N*-octyl)carboxamido,2-nitrophenol] (**42aa**)

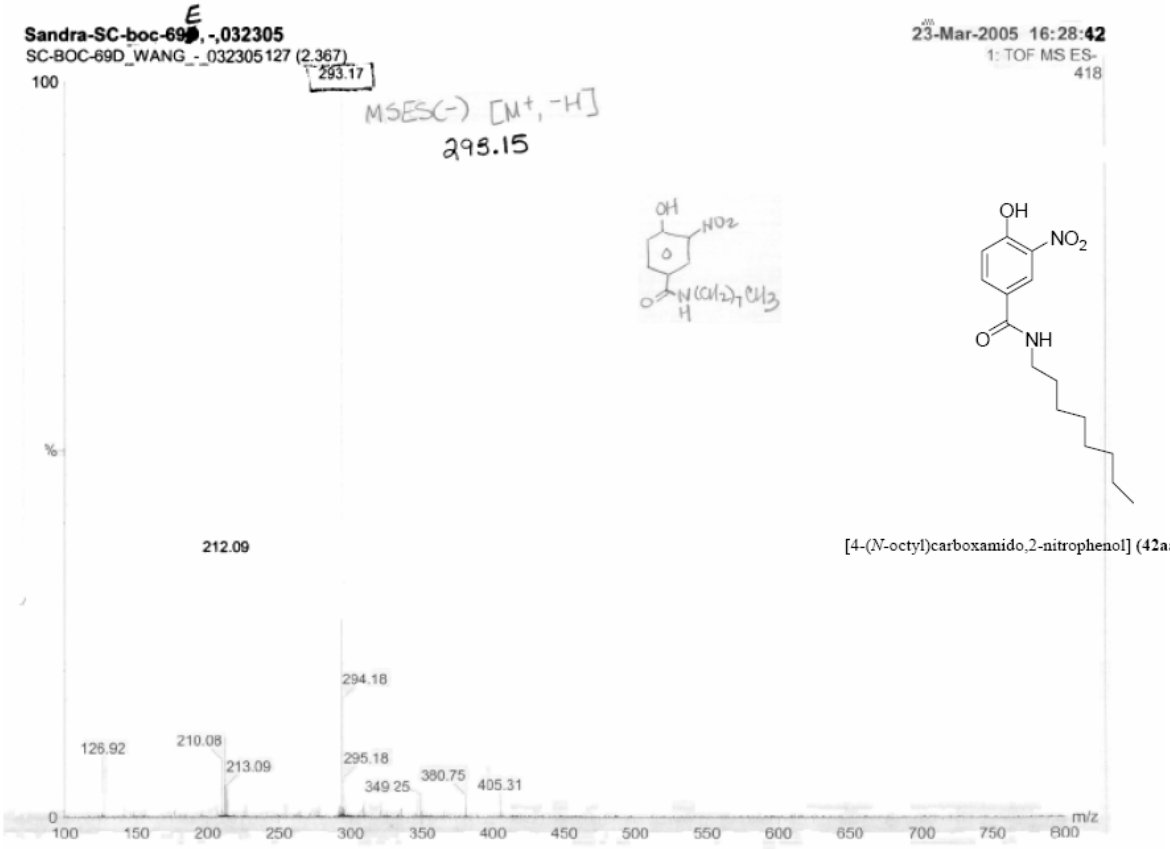

[4-(*N*-octyl)carboxamido,2-nitrophenol] (**42aa**)

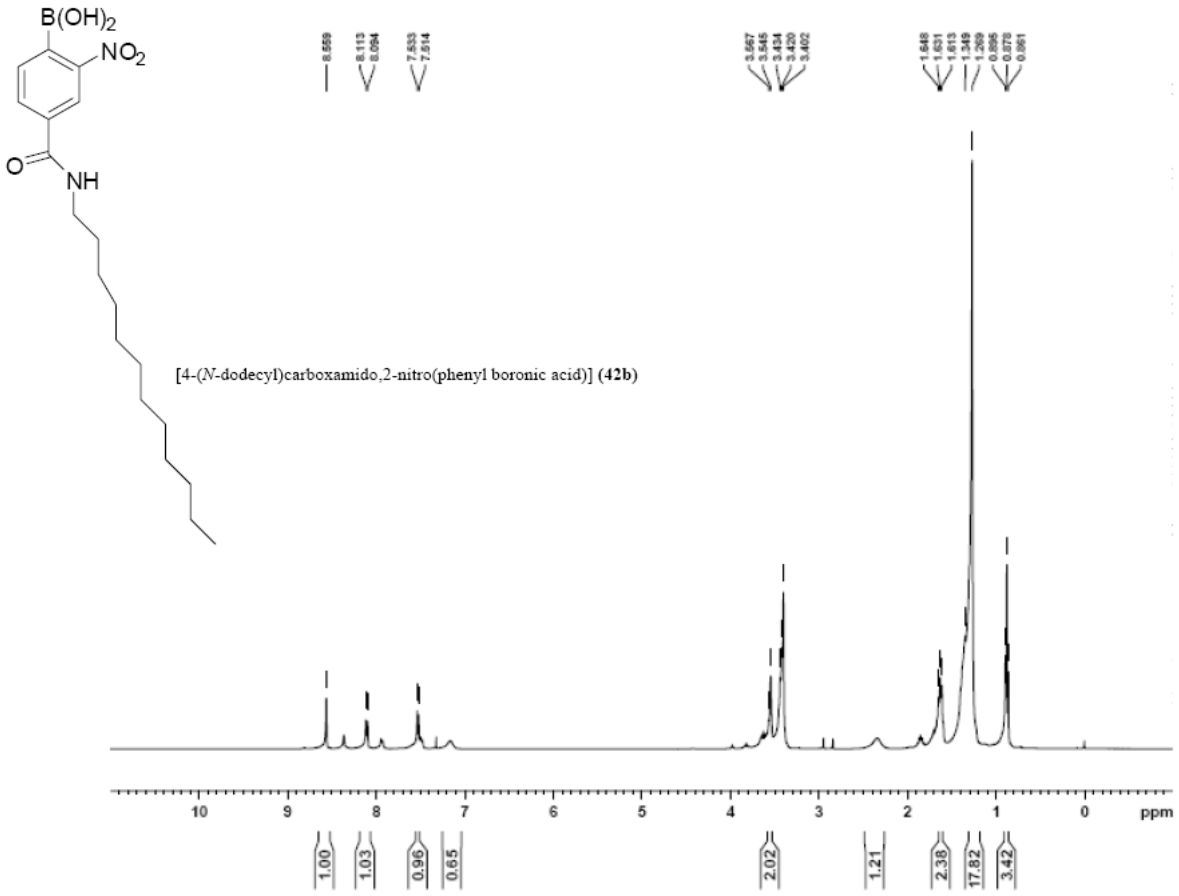

[4-(*N*-dodecyl)carboxamido,2-nitro(phenyl boronic acid)] **(42b)**

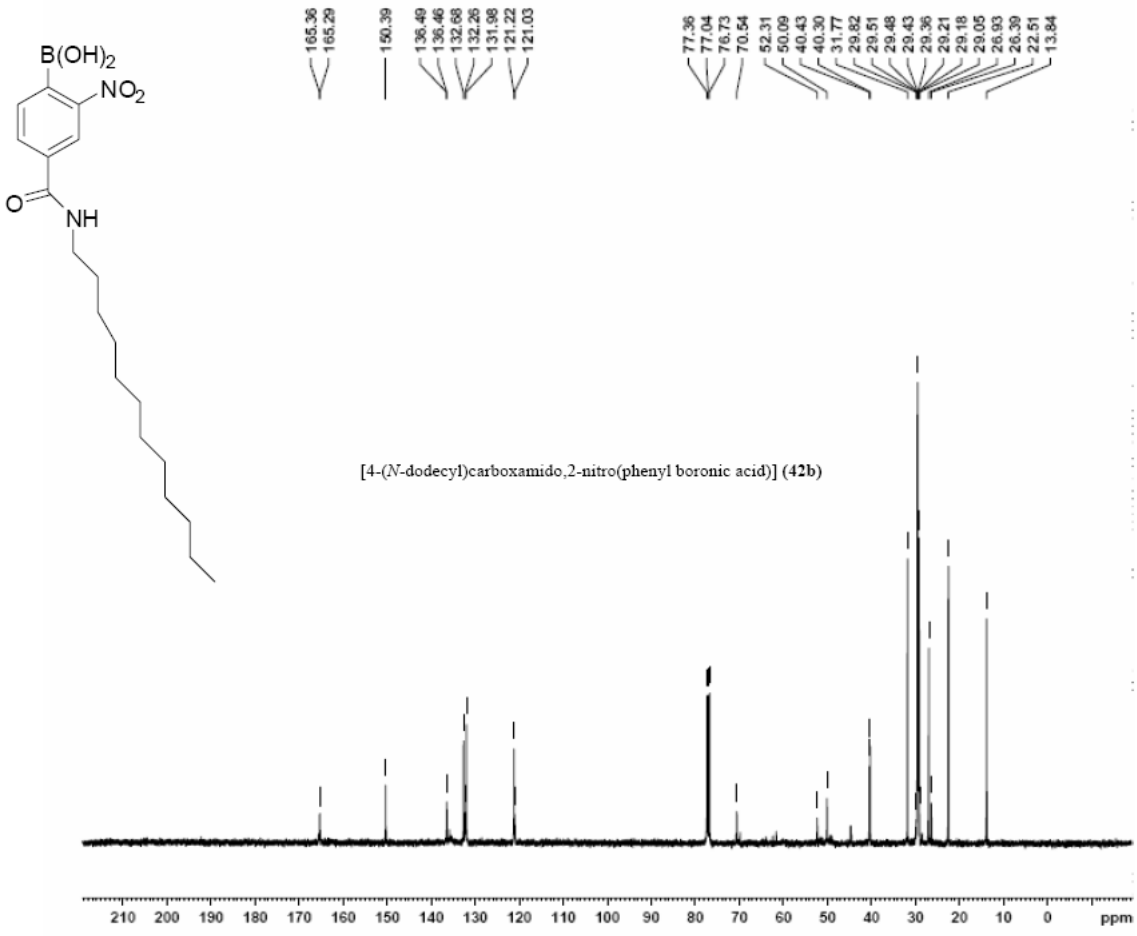
B(OH)2
NO2
O
NH
165.36
165.29
150.39
136.49
136.46
132.68
132.26
131.98
121.22
121.03
77.36
77.04
76.73
70.54
52.31
50.09
40.43
40.30
31.77
29.82
29.51
29.48
29.43
29.36
29.21
29.18
29.05
26.93
26.39
22.51
13.84
[4-(N-dodecyl)carboxamido,2-nitro(phenyl boronic acid)] (42b)
210 200 190 180 170 160 150 140 130 120 110 100 90 80 70 60 50 40 30 20 10 0 ppm

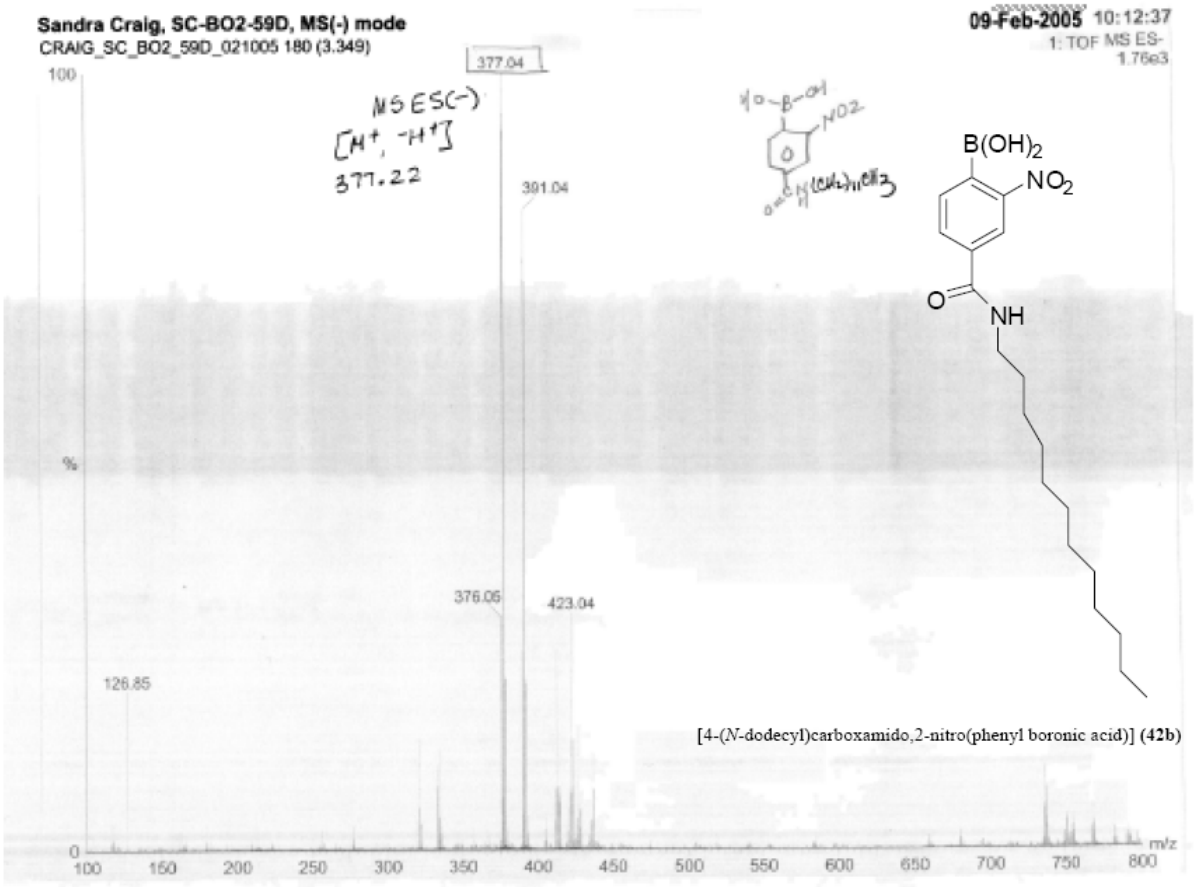
Sandra Craig, SC-BO2-59D, MS(-) mode
CRAIG_SC_BO2_59D_021005 180 (3.349)
09-Feb-2005 10:12:37
1: TOF MS ES-
1.76e3
377.04
391.04
376.06
423.04
126.85
NSESC-)
[M+, -H+]
377.22
B(OH)2
NO2
O
NH
%
m/z
100
150
200
250
300
350
400
450
500
550
600
650
700
750
800
[4-(N-dodecyl)carboxamido,2-nitro(phenyl boronic acid)] (42b)

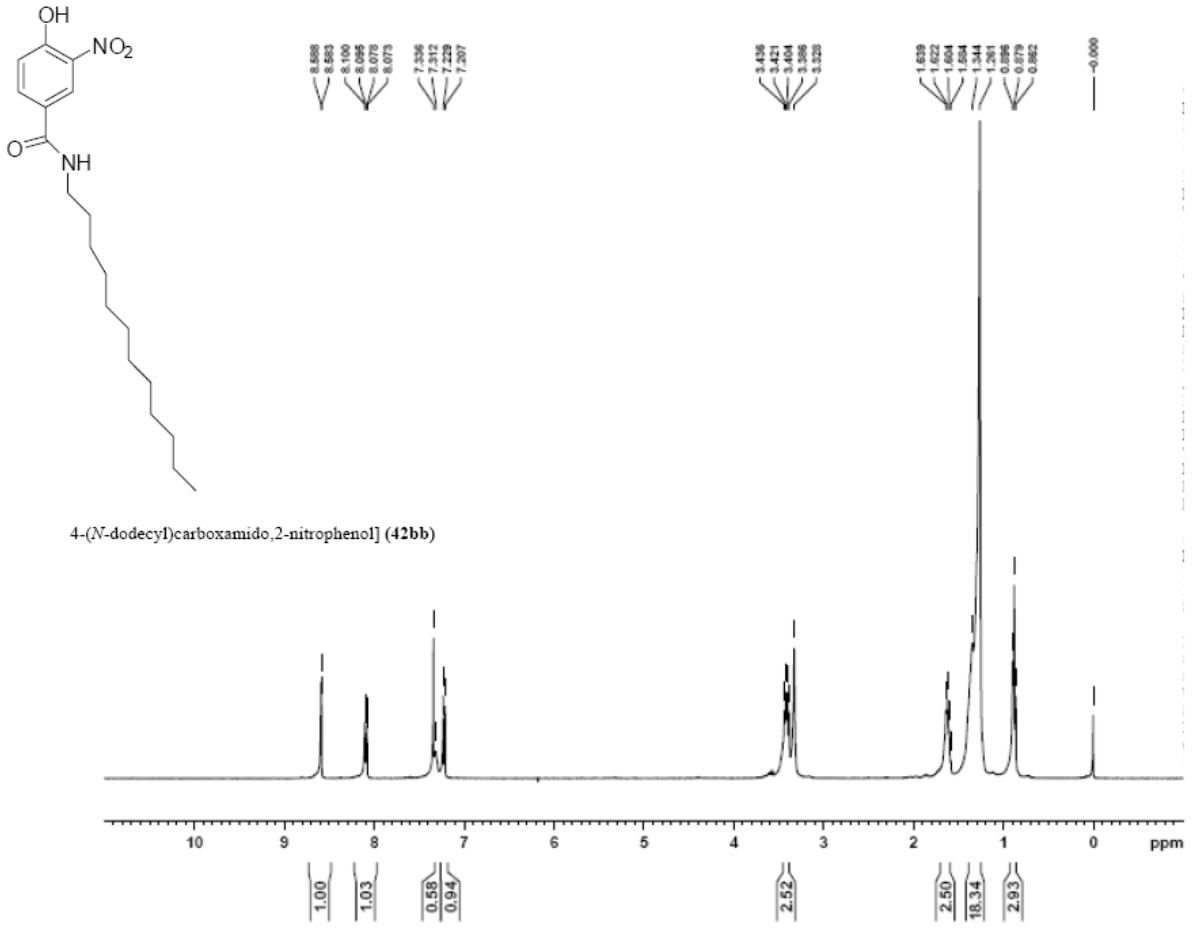

4-(*N*-dodecyl)carboxamido,2-nitrophenol] **(42bb)**

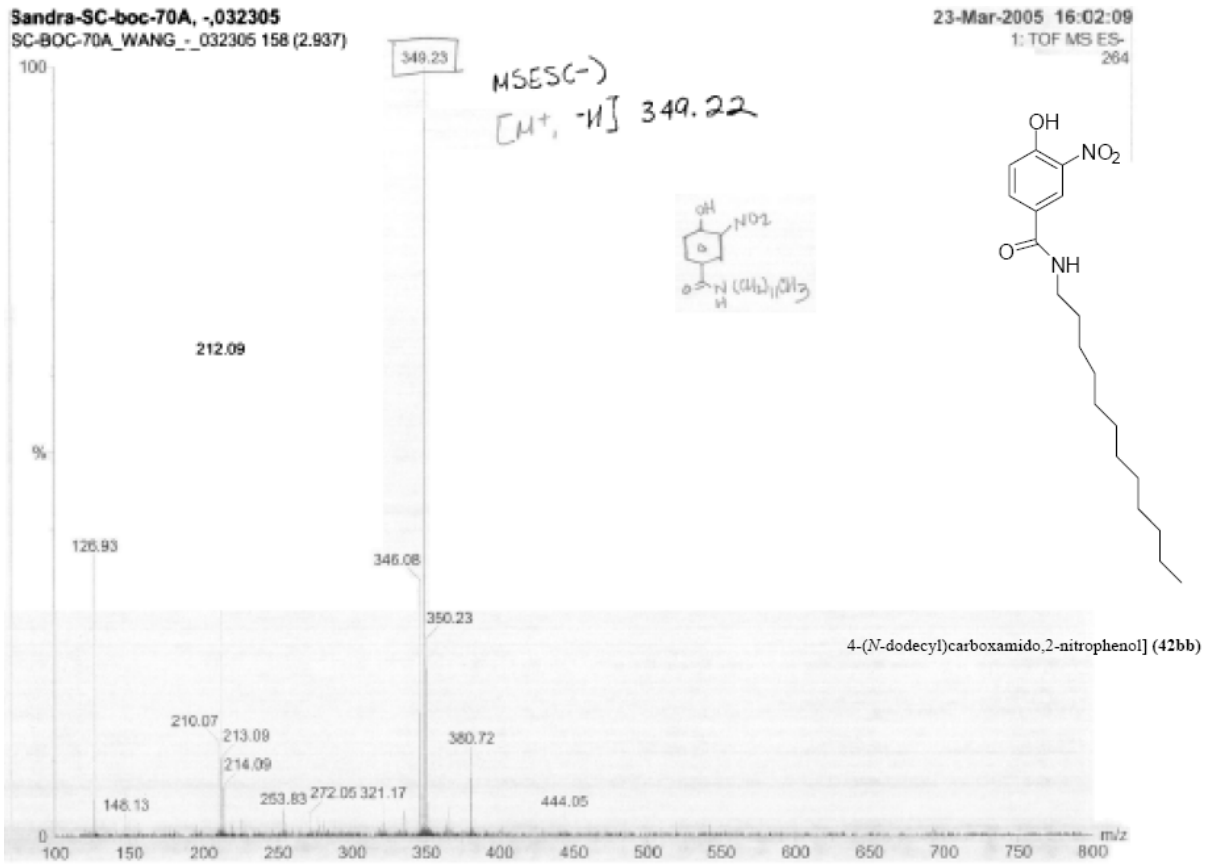

4-(*N*-dodecyl)carboxamido,2-nitrophenol] **(42bb)**

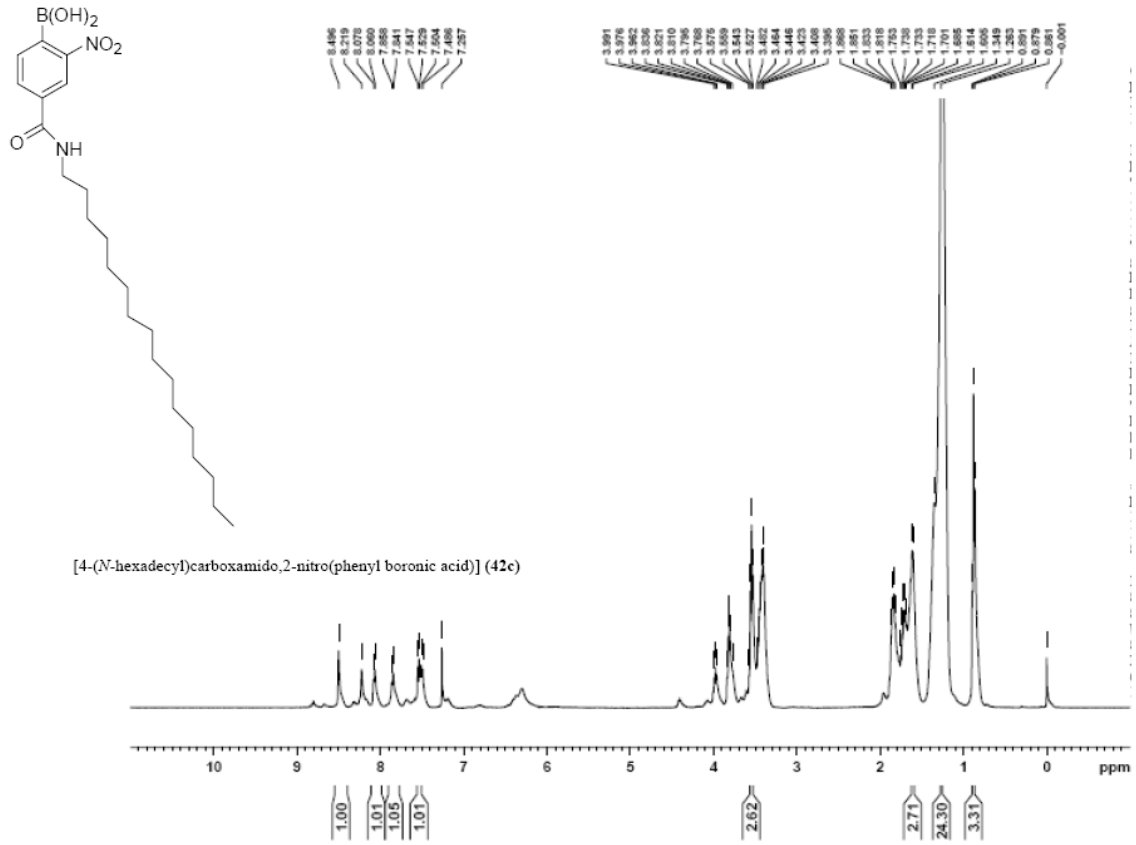

[4-(*N*-hexadecyl)carboxamido,2-nitro(phenyl boronic acid)] (**42c**)

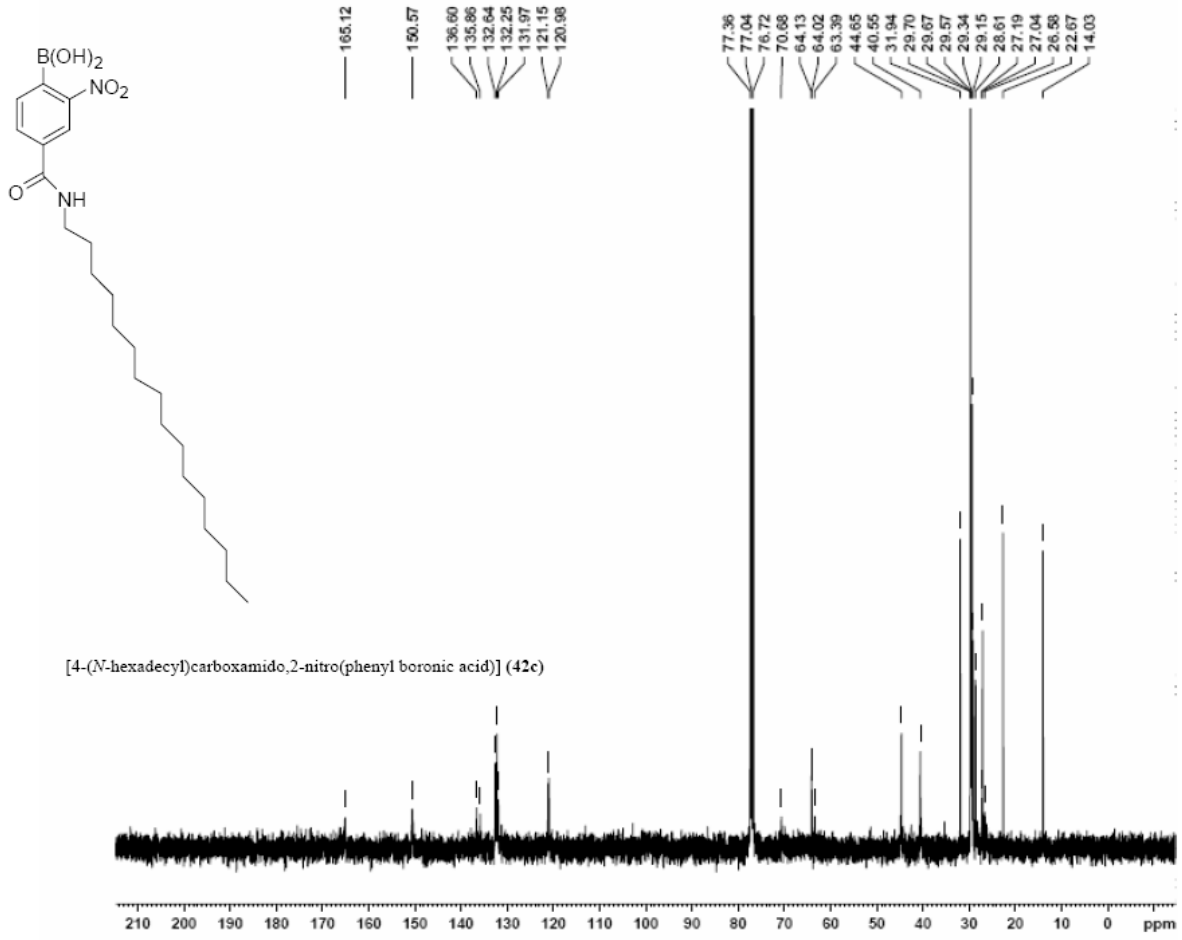

[4-(*N*-hexadecyl)carboxamido,2-nitro(phenyl boronic acid)] (**42c**)

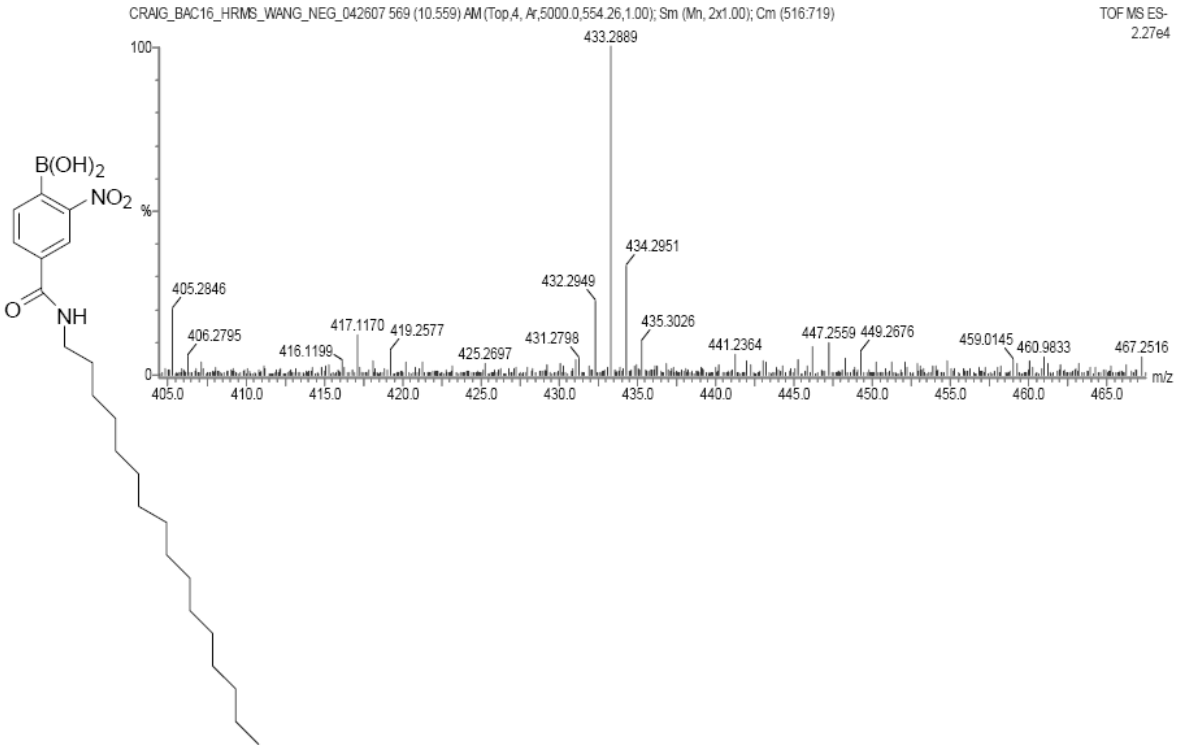

[4-(*N*-hexadecyl)carboxamido,2-nitro(phenyl boronic acid)] (**42c**)

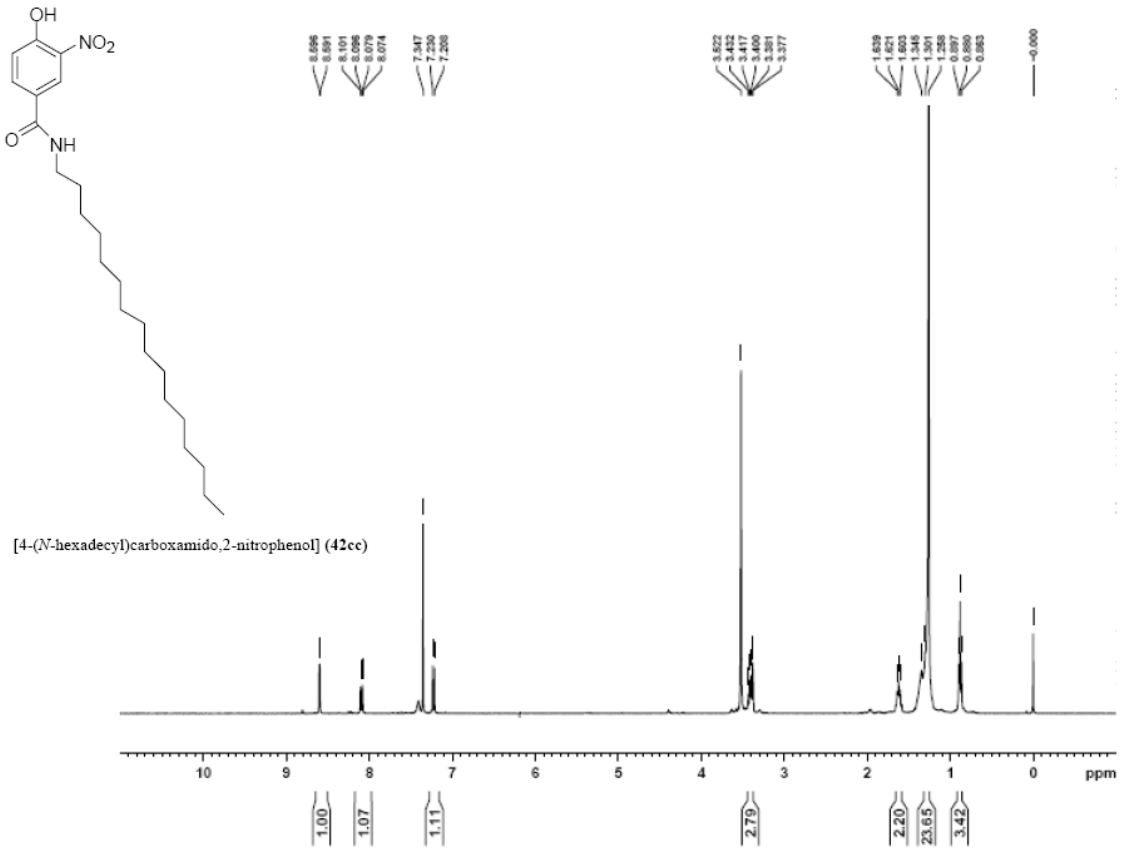

[4-(*N*-hexadecyl)carboxamido,2-nitrophenol] **(42cc)**

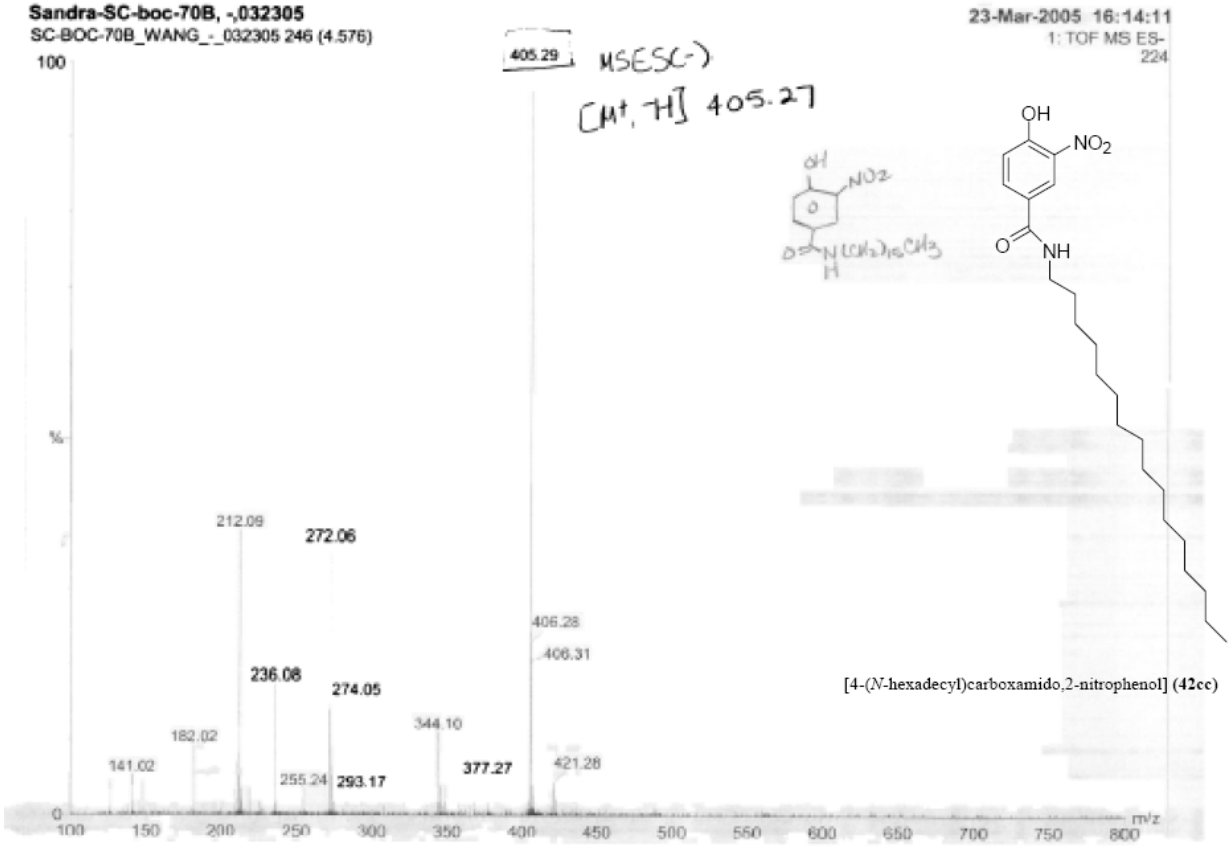
Sandra-SC-boc-70B, -,032305
SC-BOC-70B_WANG_-_032305 246 (4.576)
23-Mar-2005 16:14:11
1: TOF MS ES-
224
405.29
MSES(-)
[M+, H] 405.27
OH
NO2
O
NH
100
%
0
212.09
272.06
406.28
406.31
236.08
274.05
344.10
182.02
141.02
255.24
293.17
377.27
421.28
100
150
200
250
300
350
400
450
500
550
600
650
700
750
800
m/z
[4-(N-hexadecyl)carboxamido,2-nitrophenol] (42cc)

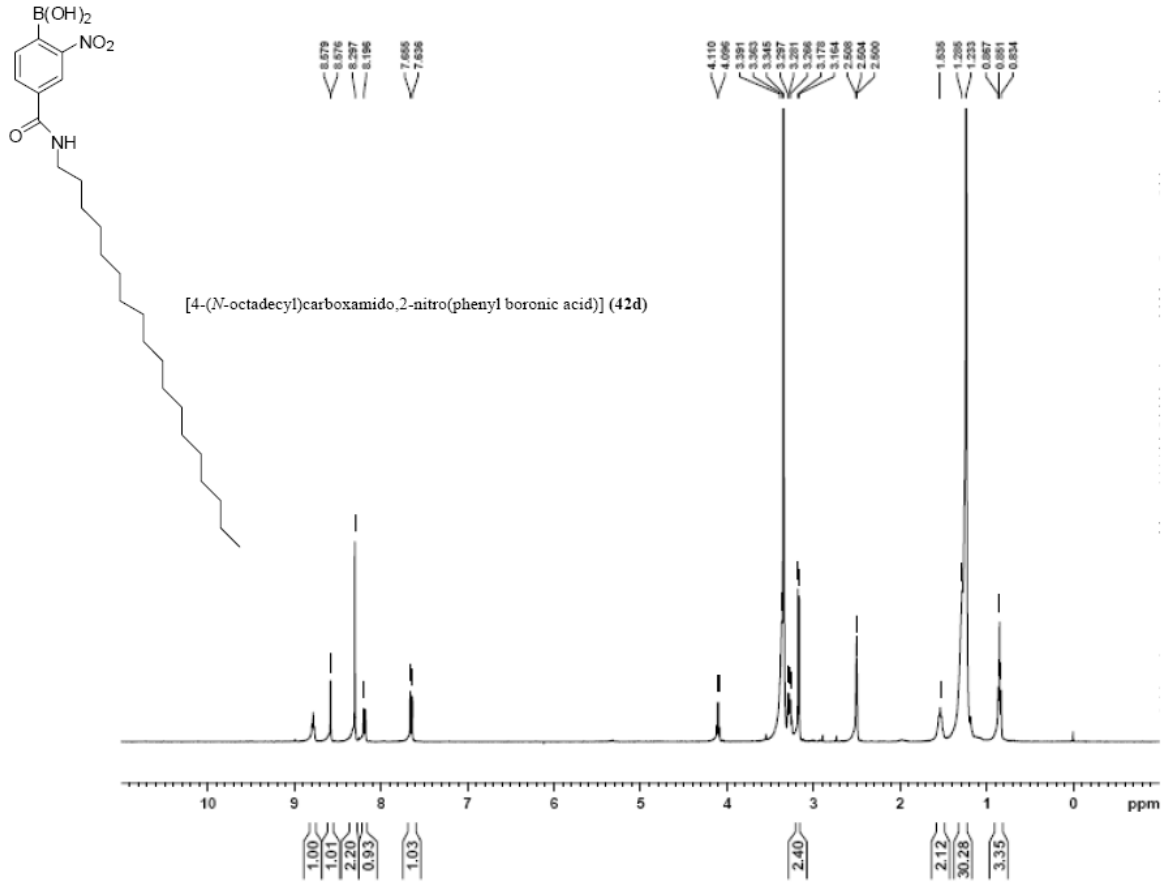
B(OH)2
NO2
O
NH
[4-(N-octadecyl)carboxamido,2-nitro(phenyl boronic acid)] (42d)
8.579
8.576
8.297
8.195
7.665
7.636
4.110
4.096
3.391
3.363
3.345
3.297
3.281
3.266
3.170
3.164
2.508
2.504
2.500
1.625
1.288
1.233
0.857
0.851
0.834
10
9
8
7
6
5
4
3
2
1
0
ppm
1.00
1.01
2.20
0.93
1.03
2.40
2.12
30.28
3.35

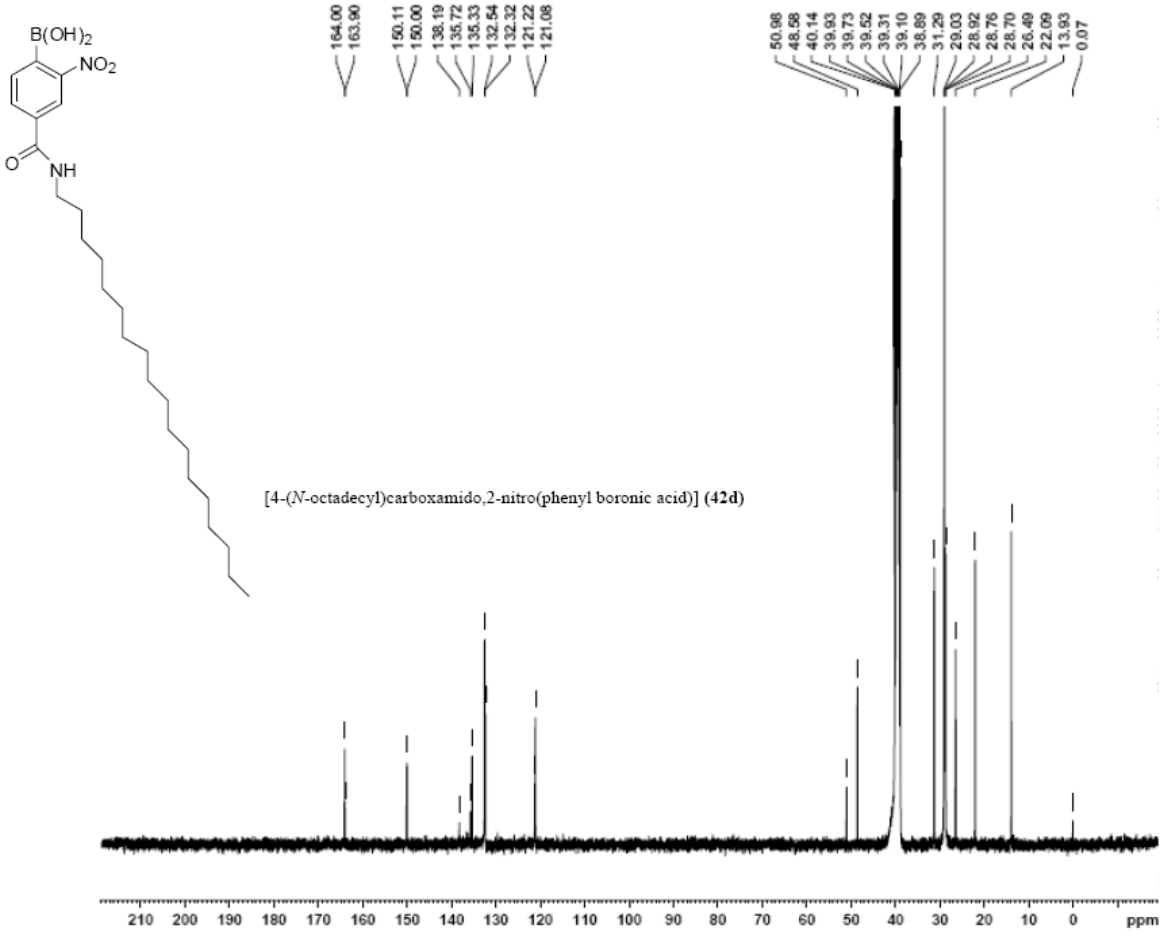
B(OH)2
NO2
O
NH
164.00
163.90
150.11
150.00
138.19
135.72
135.33
132.54
132.32
121.22
121.08
50.98
48.58
40.14
39.93
39.73
39.52
39.31
39.10
38.89
31.29
29.03
28.92
28.76
28.70
26.49
22.09
13.93
0.07
[4-(N-octadecyl)carboxamido,2-nitro(phenyl boronic acid)] (42d)
210 200 190 180 170 160 150 140 130 120 110 100 90 80 70 60 50 40 30 20 10 0 ppm

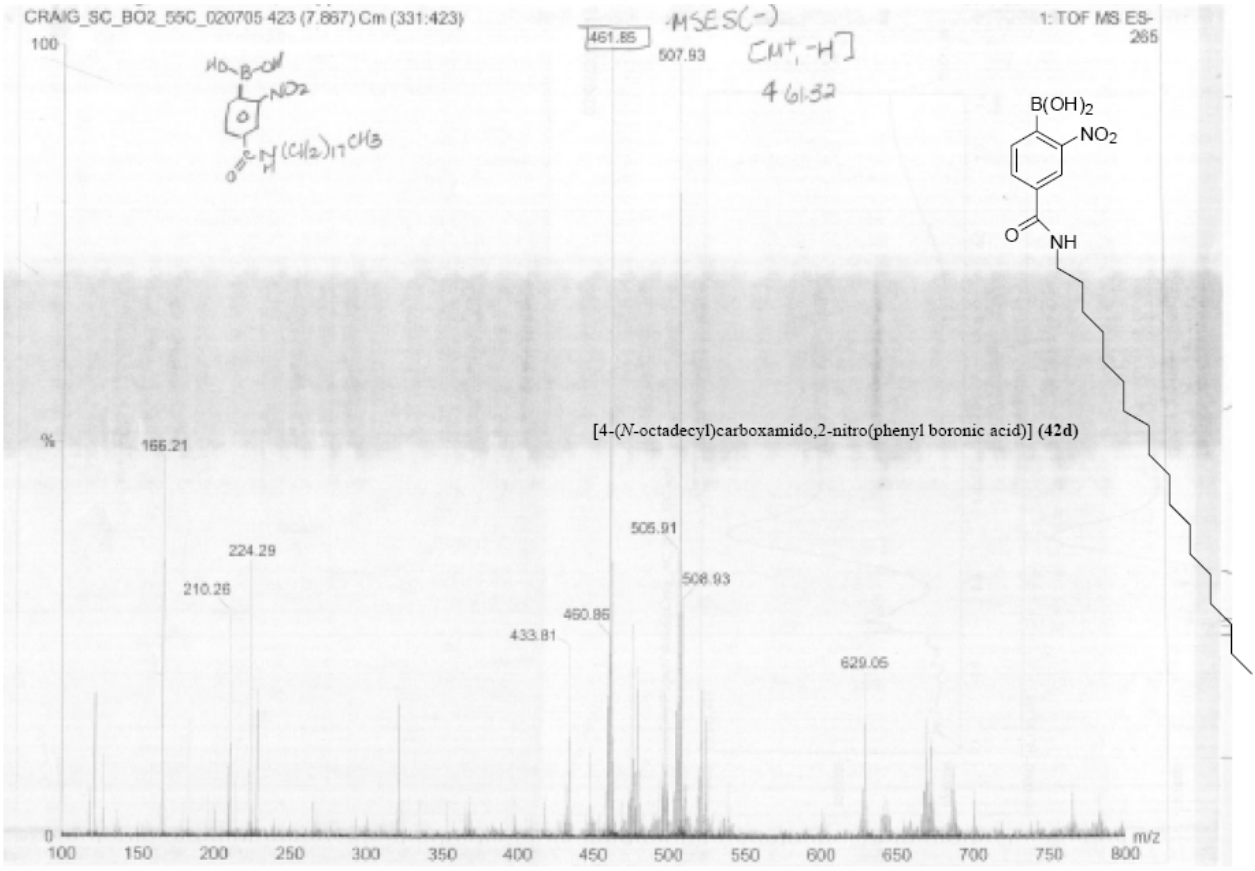

[4-(*N*-octadecyl)carboxamido,2-nitro(phenyl boronic acid)] **(42d)**

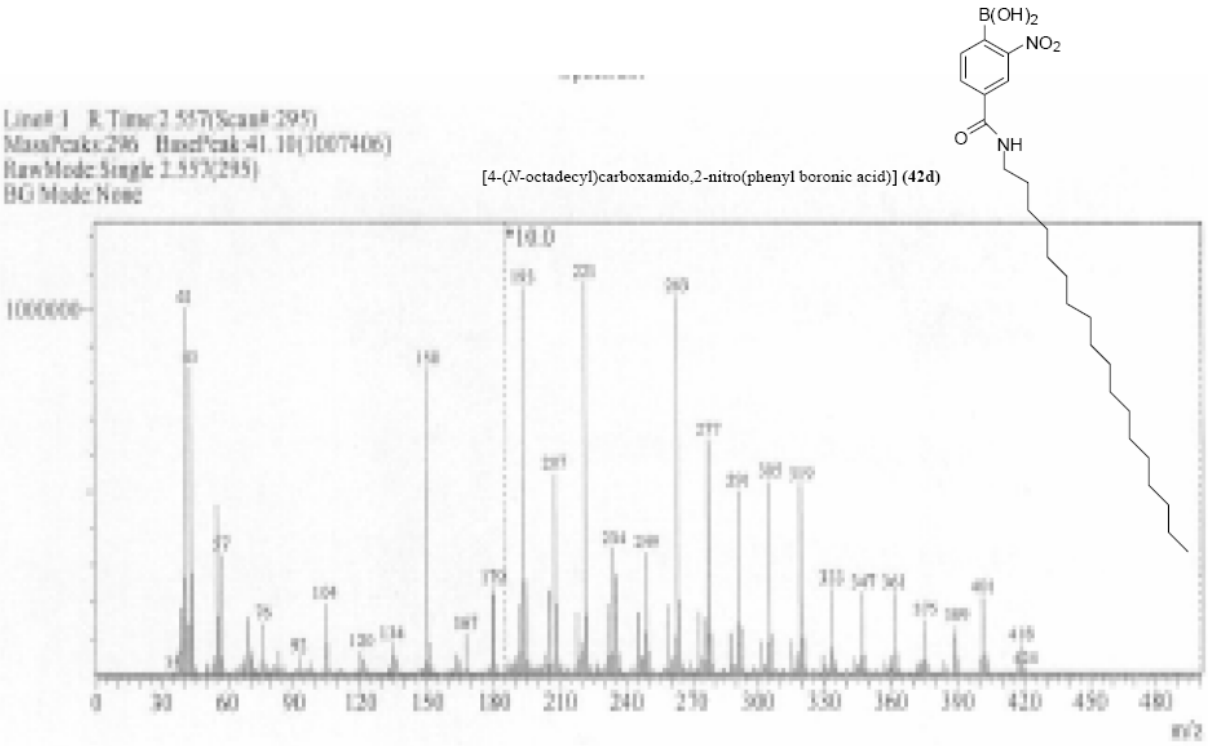
B(OH)2
NO2
O
NH
Line#:1 R.Time:2.557(Scan#:295)
Mass Peaks:296 Base Peak:41.10(1007406)
Raw Mode:Single 2.557(295)
BG Mode:None
[4-(N-octadecyl)carboxamido,2-nitro(phenyl boronic acid)] (42d)
1000000
0 30 60 90 120 150 180 210 240 270 300 330 360 390 420 450 480
m/z

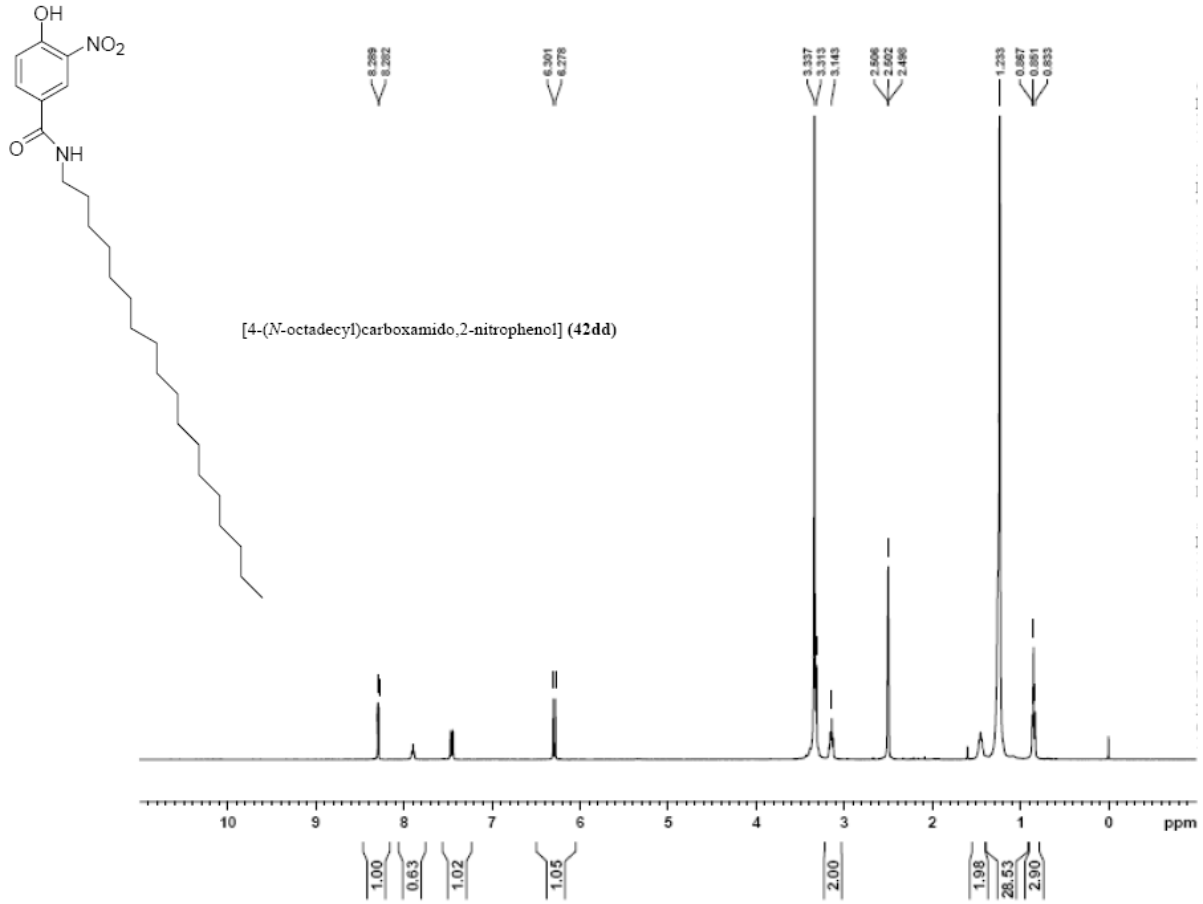
OH
NO2
O
NH
[4-(N-octadecyl)carboxamido,2-nitrophenol] (42dd)
8.299
8.282
6.301
6.278
3.337
3.313
3.148
2.506
2.502
2.498
1.233
0.867
0.851
0.833
10
9
8
7
6
5
4
3
2
1
0
ppm
1.00
0.63
1.02
1.05
2.00
1.98
28.53
2.90

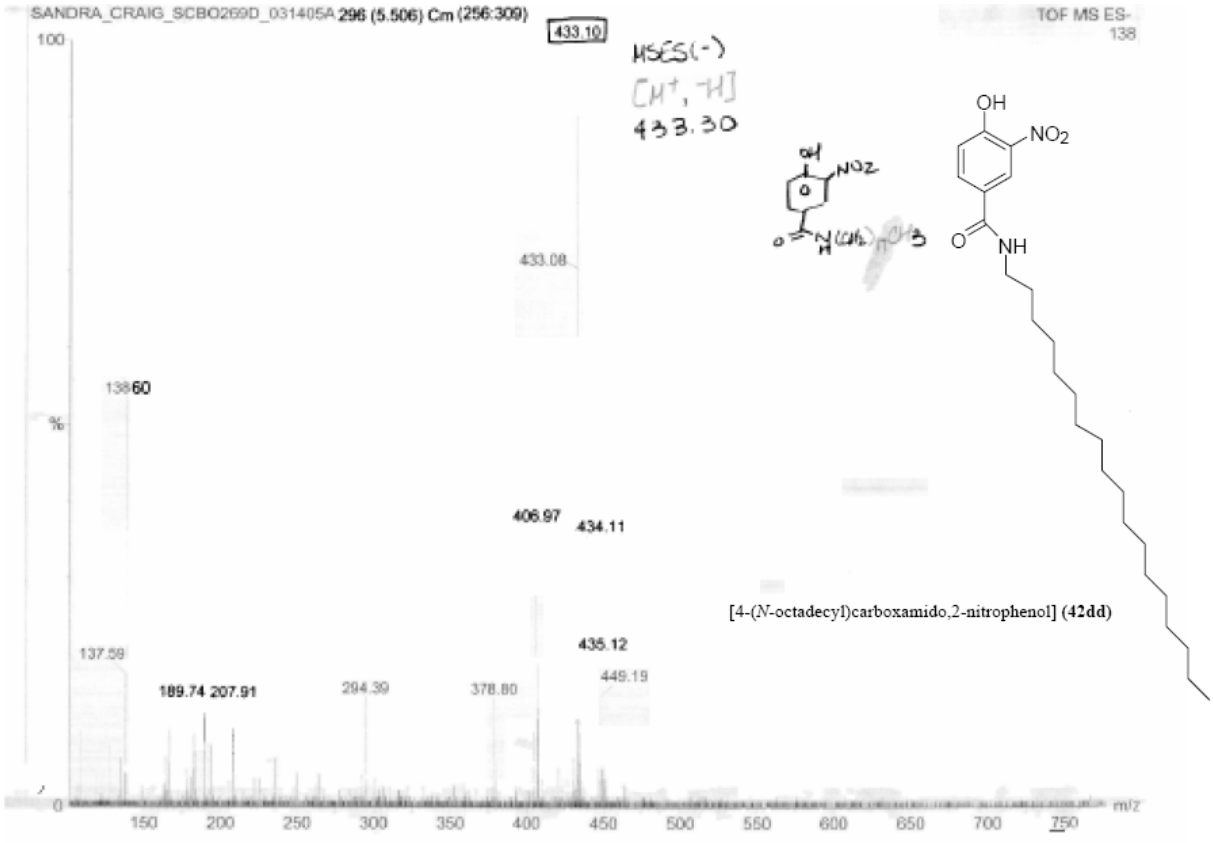
SANDRA_CRAIG_SCBO269D_031405A 296 (5.506) Cm (256:309)
433.10
TOF MS ES-
138
MSES(-)
[M+, -H]
433.30
433.08
138.60
406.97
434.11
435.12
449.19
137.59
189.74 207.91
294.39
378.80
100
%
0
150 200 250 300 350 400 450 500 550 600 650 700 750
m/z
OH
NO2
NH
O
[4-(N-octadecyl)carboxamido,2-nitrophenol] (42dd)